

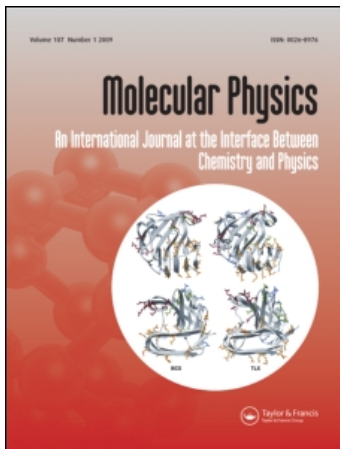
This article was downloaded by: [NEICON Consortium]

On: 9 June 2010

Access details: Access Details: [subscription number 788155938]

Publisher Taylor & Francis

Informa Ltd Registered in England and Wales Registered Number: 1072954 Registered office: Mortimer House, 37-41 Mortimer Street, London W1T 3JH, UK



## Molecular Physics

Publication details, including instructions for authors and subscription information:

<http://www.informaworld.com/smpp/title~content=t713395160>

### High resolution infrared spectroscopy and global vibrational analysis for the CH<sub>3</sub>D and CHD<sub>3</sub> isotopomers of methane

O. N. Ulenikov<sup>ab</sup>; E. S. Bekhtereva<sup>ab</sup>; S. Albert<sup>a</sup>; S. Bauerecker<sup>ac</sup>; H. Hollenstein<sup>a</sup>; M. Quack<sup>a</sup>

<sup>a</sup> Physical Chemistry, ETH-Zürich, CH-8093 Zürich, Switzerland <sup>b</sup> Laboratory of Molecular Spectroscopy, Physics Department, Tomsk State University, Tomsk, 634050, Russia <sup>c</sup> Institute of Physical and Theoretical Chemistry, Technische Universität Braunschweig, D-38106, Braunschweig, Germany

Online publication date: 27 May 2010

**To cite this Article** Ulenikov, O. N. , Bekhtereva, E. S. , Albert, S. , Bauerecker, S. , Hollenstein, H. and Quack, M.(2010) 'High resolution infrared spectroscopy and global vibrational analysis for the CH<sub>3</sub>D and CHD<sub>3</sub> isotopomers of methane', Molecular Physics, 108: 7, 1209 — 1240

**To link to this Article:** DOI: 10.1080/00268976.2010.483131

**URL:** <http://dx.doi.org/10.1080/00268976.2010.483131>

## PLEASE SCROLL DOWN FOR ARTICLE

Full terms and conditions of use: <http://www.informaworld.com/terms-and-conditions-of-access.pdf>

This article may be used for research, teaching and private study purposes. Any substantial or systematic reproduction, re-distribution, re-selling, loan or sub-licensing, systematic supply or distribution in any form to anyone is expressly forbidden.

The publisher does not give any warranty express or implied or make any representation that the contents will be complete or accurate or up to date. The accuracy of any instructions, formulae and drug doses should be independently verified with primary sources. The publisher shall not be liable for any loss, actions, claims, proceedings, demand or costs or damages whatsoever or howsoever caused arising directly or indirectly in connection with or arising out of the use of this material.

## INVITED ARTICLE

# High resolution infrared spectroscopy and global vibrational analysis for the CH<sub>3</sub>D and CHD<sub>3</sub> isotopomers of methane†

O.N. Ulenikov<sup>ab</sup>, E.S. Bekhtereva<sup>ab</sup>, S. Albert<sup>a</sup>, S. Bauerecker<sup>ac</sup>, H. Hollenstein<sup>a</sup> and M. Quack<sup>a\*</sup>

<sup>a</sup>Physical Chemistry, ETH-Zürich, CH-8093 Zürich, Switzerland; <sup>b</sup>Laboratory of Molecular Spectroscopy, Physics Department, Tomsk State University, Tomsk, 634050, Russia; <sup>c</sup>Institute of Physical and Theoretical Chemistry, Technische Universität Braunschweig, D-38106, Braunschweig, Germany

(Received 26 February 2010; final version received 5 March 2010)

We report infrared spectra of CH<sub>3</sub>D and CHD<sub>3</sub> in the range 2900 to 9000 cm<sup>-1</sup> measured with the Zürich high resolution Fourier transform infrared (FTIR) interferometer Bruker IFS 125 prototype (ZP 2001) at 80 K in a collisional-cooling cell with optical paths ranging from 5 to 10 m. In all, 57 new ro-vibrational bands of CH<sub>3</sub>D and 40 for CHD<sub>3</sub> were assigned and analysed. Using a strategy of the direct assignment of the  $J=0$  states of excited vibrational levels, precise experimental values of the band centres with uncertainties in the range of about 0.0001 to 0.0003 cm<sup>-1</sup> were obtained. Including 15 previously known band centres of CH<sub>3</sub>D and 12 previously known band centres of CHD<sub>3</sub>, these data were used as the initial information for the determination of the harmonic frequencies, anharmonic coefficients, and vibrational resonance interaction parameters in an effective hamiltonian. A joint set of 64 parameters reproduces the 124 experimental vibrational energies of both molecules up to 6500 cm<sup>-1</sup> with a root mean deviation of  $d_{\text{rms}} = 0.73 \text{ cm}^{-1}$ . The results are discussed in relation to intramolecular dynamics on a global potential hypersurface of methane, intramolecular vibrational redistribution, and the spectroscopy of the atmospheres of the earth and planetary systems.

**Keywords:** infrared spectroscopy; vibration–rotation spectra; CH<sub>3</sub>D; CHD<sub>3</sub>; overtone and combination bands; spectroscopic parameters; isotopes; methane; FTIR; intramolecular quantum dynamics; potential hypersurfaces; resonances

## 1. Introduction

Methane is the prototypical hydrocarbon with fundamental importance ranging from the theory of chemical bonding [1,2], rotational dynamics in symmetrical molecules [3], our understanding of the structure of potential hypersurfaces [4–9], unimolecular reaction rate theory [10,11], fundamental bimolecular reaction dynamics [12–15], to even the fundamental physics of chirality and parity violation [16–19]. Methane has also been studied in the context of accurate multidimensional calculations of vibrational dynamics [4,20–25]. Apart from these fundamental aspects methane plays a central role in various fields of science and technology. We might mention here combustion and environmental processes, atmospheric chemistry in the context of the greenhouse effect, planetary science and astrophysics. In all these contexts the understanding of the methane spectra is essential.

The present work is part of a large effort to unravel methane's rovibrational spectra and dynamics up to

high vibrational excitations. Our recent work on the spherical top isotopomers <sup>12</sup>CH<sub>4</sub> and <sup>13</sup>CH<sub>4</sub> provides also a guide to the extensive literature impossible to cite in completeness here [26–29]. Recently, we have provided high resolution analyses for the isotopomer CD<sub>2</sub>H<sub>2</sub> giving a rather complete picture of vibrational state dynamics covering the spectral range from low excitations to about 6500 cm<sup>-1</sup> [30–32]. This asymmetric top molecule has many advantages for such an initial study of deuterio isotopomers. Here we turn our attention to the symmetric top isotopomers CH<sub>3</sub>D and CD<sub>3</sub>H. These isotopomers are of interest for a number of reasons. CH<sub>3</sub>D is obviously the most abundant deuterio isotopomer in natural environments allowing for its detection in the Earth's atmosphere and also in an astrophysical context. CD<sub>3</sub>H has been a prototype for anharmonic intramolecular quantum dynamics arising from the strong and very selective coupling between the CH stretching and CH bending modes [33,34]. The isolated CH chromophore in this molecule

\*Corresponding author. Email: martin@quack.ch

†Dedicated to R.N. Zare on the occasion of his 70th birthday.

provides a spectroscopic window to this mode selective dynamics by allowing analyses extending to excitations exceeding 2 eV ( $18,500\text{ cm}^{-1}$ ), achieved already more than two decades ago [7,20], similar to the case of  $\text{CF}_3\text{H}$  [35,36]. However, these early results were mostly limited to the levels of the CH chromophore itself, excluding other modes. In addition, the spectra taken then were of limited resolution. Recent progress has allowed us to derive highly accurate vibrational level positions including excitation of all modes. The experimental approach involves spectra recorded at sufficiently low temperature either in supersonic jet expansions [29,37] or collisional-cooling cells [32] in such a way that a correct and precise assignment of transitions to the  $J=0$  rotational level of the excited state checked by combination differences in the lower state is possible. By adding the known rotational energy of the lower level of the transition in the vibrational ground state, one obtains a direct and precise result depending on the resolution of the spectra and the signal-to-noise level in the spectra for the excited vibrational level energies. The main advantage of this strategy is to avoid a complete global rovibrational analysis of large numbers of interacting levels. Such a complete global analysis has been done successfully for the main isotopomer  $^{12}\text{CH}_4$  only recently up to the octad region around  $4500\text{ cm}^{-1}$  consisting of 35 interacting levels [26]. We are able now to present correct and precise assignments using our direct approach for 57 newly observed vibrational levels of  $\text{CH}_3\text{D}$  in addition to 15 previously known band centres and for 37 vibrational levels of  $\text{CD}_3\text{H}$  in addition to 10 band centres previously analysed. Our new results extending to  $6500\text{ cm}^{-1}$  and beyond will provide benchmarks for the understanding of the vibrational dynamics of these isotopomers. A preliminary account of some of our results has been presented in [38,39]. A few bands of  $\text{CH}_3\text{D}$  were subsequently also analysed in [40].

## 2. Experimental

The Fourier transform infrared (FTIR) spectra of  $\text{CH}_3\text{D}$  and  $\text{CD}_3\text{H}$  have been recorded in the

wavenumber range from 2800 to  $9000\text{ cm}^{-1}$  with the Zürich FTIR spectrometer Bruker IFS 125 prototype 2001 [41–43]. The nominal instrumental resolution, defined by  $1/d_{\text{MPOD}}$  (maximum optical path difference) ranged from 0.0027 to 0.0048  $\text{cm}^{-1}$  resulting in essentially Doppler limited spectra. The Doppler widths at 80 K range from about  $0.004\text{ cm}^{-1}$  at 2800 to  $0.0096\text{ cm}^{-1}$  at  $6600\text{ cm}^{-1}$ . About 100 spectra were typically co-added in each spectral region. A multi-reflection collisional cooling cell based on White optics and embedded in a Dewar was used for recording the cold spectra [43] similar to the design described in [44–46]. Optical path lengths ranging from 5 to 10 m were used for the measurements. More details of the experimental setup and procedures can be found in [43].

Most of the  $\text{CH}_3\text{D}$  and  $\text{CD}_3\text{H}$  spectra were taken at about 80 K. The total sample pressure of a mixture of  $\text{CH}_3\text{D}/\text{CD}_3\text{H}$  and He in the cell ranged from 2.8 to 3.5 mbar in most cases. In addition, spectra with a pressure of 0.5 mbar were recorded in order to measure the strong lines without saturation. Pressure broadening can be neglected under these conditions. All spectra were self-apodised. The aperture used was 1 mm. Table 1 summarises the experimental parameters. The wavenumbers were calibrated with OCS at room temperature ( $2900$  to  $3600\text{ cm}^{-1}$ ) [47] and with  $^{12}\text{CH}_4$  from  $3000$  to  $6000\text{ cm}^{-1}$  [26,48]. The deuterated samples were purchased from Cambridge Isotope Laboratories. The identity, chemical and isotopic purity (specified to be better than 98%) was obvious from the spectra.

The absolute wavenumber accuracy of non-blended, unsaturated and not too weak lines (about 10,100 assignments) can be estimated to be better than  $10^{-4}\text{ cm}^{-1}$  in the range from 2800 to  $6600\text{ cm}^{-1}$ .

## 3. Theoretical background: symmetry and Hamiltonian model

### 3.1. Point group and molecular symmetry group for the $\text{C}_{3v}$ isotopomers of methane

$\text{CH}_3\text{D}$  is a prolate symmetric top and  $\text{CHD}_3$  is an oblate symmetric top with an equilibrium geometry

Table 1. Experimental setup for the regions  $2900$ – $6500\text{ cm}^{-1}$  of the infrared spectrum of  $\text{CH}_3\text{D}$  and  $\text{CHD}_3$ .

Region $/\text{cm}^{-1}$	Resolution $/\text{cm}^{-1}$	Windows	Source	Detector	Beamsplitter	Opt. filter $/\text{cm}^{-1}$	Aperture $/\text{mm}$	$\nu_{\text{mirror}}$ $/( \text{kHz})$	Electr. filter $/\text{cm}^{-1}$	Calib. gas
2800–3700	0.0027	KBr	Globar	InSb	$\text{CaF}_2$	3000–3600	1.0	40	2600–3700	OCS [47]
3300–4300	0.0033	KBr	Tungsten	InSb	$\text{CaF}_2$	3400–4400	1.0	40	2800–5500	
4100–6000	0.0033	KBr	Tungsten	InSb	$\text{CaF}_2$	4100–6000	1.0	40	3200–6300	$^{12}\text{CH}_4$ [26,48]
5100–6500	0.0048	KBr	Tungsten	InSb	$\text{CaF}_2$	5500–6200	1.0	40	3600–7800	

corresponding to the  $C_{3v}$  point group of order 6 (Figure 1).

This point group is isomorphous to the molecular symmetry group  $M_{S6}$ , which is a subgroup of the permutation inversion group  $S_3^*$  applicable to both isotopomers of methane if the tunnelling substructure of the levels of methane and parity are considered explicitly [49,50].

Table 2 provides the character table for  $C_{3v}$  and  $M_{S6}$  as well as the induced representation  $\Gamma_m \uparrow S_3^*$  generated by the motional species  $\Gamma_m$  in  $M_{S6}$ . This is thus the structure of sublevels of  $A_1$ ,  $A_2$ , and  $E$  in  $C_{3v}$  ( $M_{S6}$ ) including tunnelling, motional and parity assignment for  $S_3^*$  (letter symbol with exponent + for positive parity, - for negative parity providing the symmetry

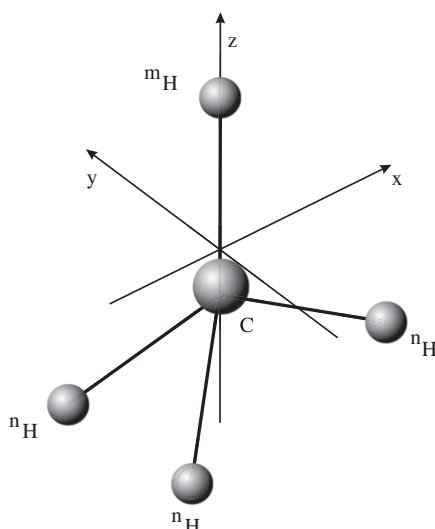


Figure 1. Equilibrium structure of the  $\text{CH}_3\text{D}$  molecule and axes definitions used in the present work ( $n=1$ ,  $m=2$  für  $\text{CH}_3\text{D}$ , a similar definition applies to  $\text{CHD}_3$  with  $n=2$ ,  $m=1$ , but a shift of the centre of mass).

Table 2. Character table for  $C_{3v}$  and the isomorphous group  $M_{S6}$  with the induced representations  $\Gamma(M_{S6}) \uparrow S_3^*$ . The point group operations  $C_3$ ,  $\sigma_v$  follow standard notation [51] and for the permutations the common cyclic notation is used [49,50,52] with a star indicating space inversion operations. For the irreducible representations the conventional point group labels are used, whereas the species in  $S_3^*$  indicate pure permutational species by the letter symbol and parity by the exponent + or - (see [49,50,52,53] for this convention).

$\Gamma(C_{3v})$	$E$	$2C_3$	$3\sigma_v$	$\Gamma_m \uparrow S_3^*$
$\Gamma(M_{S6})$	$E$	$2(123)$	$3(12)^*$	
$A_1$	1	1	1	$(A_1^+) + A_2^-$
$A_2$	1	1	-1	$A_2^+ + (A_1^-)$
$E$	2	-1	0	$E^+ + E^-$

property under the space inversion operation,  $\hat{P}$  or  $E^*$ ). At the resolution of our experiments the tunnelling substructure cannot be observed and thus one might usually label all rovibronic levels by the species  $A_1$ ,  $A_2$ ,  $E$  in  $C_{3v}$ . However, because of the generalised Pauli principle and approximate separability of rovibrational and nuclear spin wavefunctions, the total allowed symmetry species are the product of the ‘motional’ (rovibronic or rovibrational) species  $\Gamma_m$  and nuclear spin species  $\Gamma_{ns}$  with  $\Gamma_m \otimes \Gamma_{ns} = A_2^\pm$  for the protons (Fermions), say in  $\text{CH}_3\text{D}$ . The  $2^3$  nuclear spin functions for the three protons form a reducible representation  $D_R = 4A_1^+ + 2E^+$ , where the four  $A_1^+$  functions correspond to total ( $\text{H}_3$ ) nuclear spin  $I=3/2$  ( $-3/2 \leq M_I \leq +3/2$ ) and the two  $E^+$  functions to total ( $\text{H}_3$ )-nuclear spin  $I=1/2$  (with  $M_I=\pm 1/2$ ). One can write the ( $\text{H}_3$ )-nuclear spin multiplets as  ${}^4A_1$  and  ${}^2E$ . Thus the motional (rovibronic) wave functions of species  $A_2^+$  and  $A_2^-$  occur combined with nuclear spin species  $A_1^\mp$  and total ( $\text{H}_3$ )-nuclear spin ( $I=3/2$ ) and the motional species  $E^+$  and  $E^-$  occur with nuclear spin species  $E^\pm$  (and  $I=1/2$ ). The  $A_1^\pm$  motional species have no Pauli-allowed partner among the nuclear spin functions and thus are forbidden by the generalised Pauli principle in the case of  $\text{CH}_3\text{D}$ . This is indicated by the parentheses in  $\Gamma_m \uparrow S_3^*$  in Table 2. From this consideration one sees that assigning a symmetry species in  $S_3^*$  to the levels of the  $C_{3v}$  molecule,  $\text{CH}_3\text{D}$  provides actually additional information.  $A_1$  levels (in  $C_{3v}$ ) are actually pure  $A_2^-$  in  $S_3^*$ , with well-defined negative parity, and similarly  $A_2$  levels in  $C_{3v}$  result in  $A_2^+$  with pure positive parity and no tunnelling doublet structure. For levels of symmetry species  $E$  in  $C_{3v}$  one finds a non-resolved tunnelling doublet  $E^+$  and  $E^-$  with levels of different parity (and both combining with ( $\text{H}_3$ )-nuclear spin  $I=1/2$  and thus an extra degeneracy of 2 from  $M_I=\pm 1$ ). Of course, in all cases the further nuclear spin from the one deuteron in  $\text{CH}_3\text{D}$  (with  $I_D=1$ ) has to be added to the considerations.

Completely analogous considerations apply to  $\text{CHD}_3$  where the  $3^3$  nuclear spin functions of ( $\text{D}_3$ ) form a reducible representation corresponding to the ( $\text{D}_3$ )-nuclear spin multiplet notation  ${}^7A_1^+(I=3) + {}^3A_1^+(I=1) + {}^1A_2^+(I=0) + {}^5E^+(I=2) + {}^3E^+(I=1)$  [49]. These spin functions for the boson D combine with the motional functions to give Pauli-allowed overall totally symmetric symmetry species  $A_1^\pm$ . Thus all levels in  $C_{3v}$  ( $A_1$ ,  $A_2$ ,  $E$ ) result in tunnelling doublets of different parity  $A_1^\pm$ ,  $A_2^\pm$  and  $E^\pm$  in  $S_3^*$  and a more complex  $\text{D}_3$ -nuclear spin multiplet structures as given by the reducible representation indicated above. Again, the extra nuclear spin (1/2) from the single H has to be considered in addition.

Table 3. Values of the fundamental band centres of the CH<sub>3</sub>D molecule (in cm<sup>-1</sup>).

$\nu$	$\Gamma$	$\nu_0^{\text{exp.}}/\text{cm}^{-1}$	Ref.	Assignment
$\nu_1$	$A_1$	2969.512	[25]	CH <sub>3</sub> s-stretch
$\nu_2$	$A_1$	2200.041	[25]	CD stretch
$\nu_3$	$A_1$	1306.848	[54]	CH <sub>3</sub> s-deform
$\nu_4$	$E$	3016.713	[25]	CH <sub>3</sub> d-stretch
$\nu_5$	$E$	1472.022	[54]	CH <sub>3</sub> d-deform
$\nu_6$	$E$	1166.103	[54]	CH <sub>3</sub> rock

In practice in assigning symmetry species, one uses first the conventional C<sub>3v</sub> symmetry species for both CH<sub>3</sub>D and CD<sub>3</sub>H and then derives the substructure of the almost degenerate levels and the corresponding nuclear spin statistical weights from the induced representation in Table 2 and the considerations given above.

The electric dipole selection rules take a very simple form in S<sub>3</sub><sup>\*</sup>: conservation of nuclear spin symmetry and change of parity in the optical transition, thus

$$A_1^+ \leftrightarrow A_1^- \quad (\text{Ia})$$

$$A_2^+ \leftrightarrow A_2^- \quad (\text{Ib})$$

$$E^+ \leftrightarrow E^- \quad (\text{Ic})$$

with all other transitions being electric dipole forbidden with the approximation of nuclear spin symmetry conservation [49,50,52,53]. For magnetic dipole transitions one has no change of parity in the transition, but these are extremely weak in the infrared spectra and not analysed here.

### 3.2. The effective rotational-vibrational Hamiltonian

The nine vibrational normal modes  $q_\lambda$  of both molecules have the symmetry species  $A_1$  or  $E$  in C<sub>3v</sub>, three nondegenerate modes  $q_\lambda$  ( $\lambda=1, 2, 3$ )  $\in A_1$  and three doubly degenerate modes  $q_{\mu_1}$  and  $q_{\mu_2}$  ( $\mu=4, 5, 6$ )  $\in E$ . Tables 3 and 4 summarise the six vibrational fundamentals as known today for the CH<sub>3</sub>D and CHD<sub>3</sub> isotopomers.

The presence of degenerate modes in the C<sub>3v</sub> symmetric methane isotopomers leads to a more complicated picture of ro-vibrational spectra than for CH<sub>2</sub>D<sub>2</sub> [32], especially in excited overtone and combination bands largely governed by symmetry. It is therefore suitable to make use of the symmetry properties of these molecules [3], applying theorems and results of the theory of irreducible tensorial sets, [57,58], for the construction of the molecular hamiltonian, ro-vibrational eigenfunctions, and the various matrix elements as adapted to the C<sub>3v</sub> type molecules, see e.g. [58,59].

Table 4. Values of the fundamental band centres of the CHD<sub>3</sub> Molecule (in cm<sup>-1</sup>).

$\nu$	$\Gamma$	$\nu_0^{\text{exp.}}/\text{cm}^{-1}$	Ref.	Assignment
$\nu_1$	$A_1$	2992.786	[This work] <sup>a</sup>	CH stretch
$\nu_2$	$A_1$	2142.583	[56]	CD <sub>3</sub> s-stretch
$\nu_3$	$A_1$	1004.548	[55]	CD <sub>3</sub> s-deform
$\nu_4$	$E$	2250.828	[56]	CD <sub>3</sub> d-stretch
$\nu_5$	$E$	1292.500	[55]	CD <sub>3</sub> rock
$\nu_6$	$E$	1035.920	[55]	CD <sub>3</sub> d-deform

Note: <sup>a</sup>Ref. [20] gave 2992.75 cm<sup>-1</sup> with an estimated measurement (and calibration) uncertainty of 0.02 cm<sup>-1</sup>, in essential agreement with the present much more accurate result.

On the other hand, the presence of numerous and strong resonance interactions between different vibrational states of both CH<sub>3</sub>D and CHD<sub>3</sub> leads to the necessity to use even in a preliminary analysis of infrared spectroscopic data a Hamiltonian model which takes into account explicitly all strong resonance interactions. Using C<sub>3v</sub> symmetry, the Hamiltonian takes the following form [59]

$$H^{\text{v.-r.}} = \sum_{v\Gamma, v'\Gamma'} H^{v\Gamma, v'\Gamma'}, \quad (1)$$

where the summation extends over all interacting vibrational states;  $\Gamma=A_1, A_2, E$  is the symmetry species of the vibrational state. The diagonal operators  $H^{v\Gamma, v\Gamma}$  describe the rotational structures of the corresponding vibrational state and can be written in the following form:

$$H_{\text{diag.}} = \sum_v H^{vA_1, vA_1} + \sum_v H^{vA_2, vA_2} + \sum_v H^{vE, vE}. \quad (2)$$

The operators  $H^{vA_i, vA_i}$  ( $i=1, 2$ ) which describe the rotational-vibrational structures of nondegenerate vibrational states have the form:

$$\begin{aligned} & H^{vA_i, vA_i} = |vA_i\rangle \langle vA_i| \{ E^{va_i} + B^{va_i} (J_x^2 + J_y^2) + C^{va_i} J_z^2 - D_J^{va_i} J^4 \\ & - D_{JK}^{va_i} J_z^2 - D_K^{va_i} J_z^4 + H_J^{va_i} J^6 + H_{JK}^{va_i} J^4 J_z^2 \\ & + H_{KJ}^{va_i} J_z^4 + H_K^{va_i} J_z^6 + L_J^{va_i} J^8 + \dots \\ & + [(\epsilon'^{va_i} J_z + \epsilon'^{va_i} J_z J^2 + \epsilon'^{va_i} J_z^3 + \dots), (J_+^3 + J_-^3)]_+ \\ & + h'^{va_i} (J_+^6 + J_-^6) + \dots \}. \end{aligned} \quad (3)$$

Here  $B^{va_i}, C^{va_i}, D_J^{va_i}, D_{JK}^{va_i}, D_K^{va_i}, H_J^{va_i}, H_{JK}^{va_i}, H_{KJ}^{va_i}, H_K^{va_i}, L_J^{va_i}, \dots$  are the rotational constants and centrifugal distortion parameters, respectively (it should be mentioned that the notations  $B$  and  $C$  for the rotational parameters are used in the spectroscopic literature for the oblate symmetric top molecules, like CHD<sub>3</sub>; for the prolate symmetric top molecules, like CH<sub>3</sub>D, the

notation  $A$  is used instead of  $C$ ). The operators  $(J_+^3 + J_-^3)$  connect rotational states  $|JK\rangle$  and  $|JK'\rangle$  with different values of the quantum numbers  $K$ , namely  $\Delta K = K - K' = \pm 3$ . They account, in particular, for the  $A_1/A_2$  splittings of  $K=3$  levels, and the operators  $J_+$  and  $J_-$  have the form of  $J_{\pm} = J_x \mp iJ_y$ . The parameters  $\epsilon'^a$  and  $\epsilon'_K$  describe the  $J$  and  $K$  dependence of the main  $\epsilon'^a$  parameter. The expression  $[..., ...]_+$  denotes an anticommutator.

For doubly degenerate vibrational states the  $H^{vE,vE}$  operator is

$$H^{vE,vE} = H_1^{vE,vE} + H_2^{vE,vE} + H_3^{vE,vE}, \quad (4)$$

where

$$\begin{aligned} H_1^{vE,vE} &= (|vE_1\rangle\langle vE_1| + |vE_2\rangle\langle vE_2|) \{ E^{ve} + B^{ve}(J_x^2 + J_y^2) + C^{ve}J_z^2 \\ &\quad - D_J^{ve}J^4 - D_{JK}^{ve}J_z^2J_z^2 - D_K^{ve}J_z^4 + H_J^{ve}J^6 + H_{JK}^{ve}J^4J_z^2 \\ &\quad + H_{KK}^{ve}J_z^4 + H_K^{ve}J_z^6 + L_J^{ve}J^8 + \dots \\ &\quad + [(\epsilon'^{ve}J_z + \epsilon_J^{ve}J_zJ^2 + \epsilon_K^{ve}J_z^3 + \dots), (J_+^3 + J_-^3)]_+ \}, \end{aligned} \quad (5)$$

$$\begin{aligned} H_2^{vE,vE} &= (|vE_1\rangle\langle vE_2| - |vE_2\rangle\langle vE_1|) \{ 2(C\zeta)^{ve}J_z + \eta_J^{ve}J_zJ^2 \\ &\quad + \eta_K^{ve}J_z^3 + \eta_{JJ}^{ve}J_zJ^4 + \eta_{JK}^{ve}J_z^3J^2 \\ &\quad + \eta_{KK}^{ve}J_z^5 + \eta_{JJJ}^{ve}J_zJ^6 + \eta_{JKK}^{ve}J_z^3J^4 \\ &\quad + \eta_{KKK}^{ve}J_z^5J^2 + \eta_{KKK}^{ve}J_z^7 + \dots \}, \end{aligned} \quad (6)$$

and

$$\begin{aligned} H_3^{vE,vE} &= (|vE_2\rangle\langle vE_2| - |vE_1\rangle\langle vE_1|) \{ [iA^{ve}, (J_+ - J_-)]_+ \\ &\quad + [B^{ve}, (J_+ + J_-)]_+ + [C^{ve}, (J_+^2 + J_-^2)]_+ \\ &\quad + [iD^{ve}, (J_+^2 - J_-^2)]_+ + [F^{ve}, (J_+^4 + J_-^4)]_+ \\ &\quad + [iG^{ve}, (J_-^4 - J_+^4)]_+ \\ &\quad + (|vE_1\rangle\langle vE_2| + |vE_2\rangle\langle vE_1|) \{ [A^{ve}, (J_+ + J_-)]_+ \\ &\quad + [iB^{ve}, (J_- - J_+)]_+ + [iC^{ve}, (J_+^2 - J_-^2)]_+ \\ &\quad + [D^{ve}, (J_+^2 + J_-^2)]_+ + [iF^{ve}, (J_+^4 - J_-^4)]_+ \\ &\quad + [G^{ve}, (J_+^4 + J_-^4)]_+ \}, \end{aligned} \quad (7)$$

$$\begin{aligned} A^{ve} &= \frac{1}{2}\alpha^{ve} + \frac{1}{2}\alpha_J^{ve}J^2 + \alpha_K^{ve}J_z^2 + \frac{1}{2}\alpha_{JJ}^{ve}J^4 \\ &\quad + \alpha_{JK}^{ve}J_z^2 + \alpha_{KK}^{ve}J_z^4 + \dots \\ &\quad + \alpha_{JJK}^{ve}J_z^4J_z^2 + \alpha_{JKK}^{ve}J_z^2J_z^4 + \dots, \\ B^{ve} &= \beta^{ve}J_z + \beta_J^{ve}J_zJ^2 + \beta_K^{ve}J_z^3 + \beta_{JJ}^{ve}J_zJ^4 + \beta_{JK}^{ve}J_z^2J_z^3 + \dots, \\ C^{ve} &= \frac{1}{2}\gamma^{ve} + \frac{1}{2}\gamma_J^{ve}J^2 + \gamma_K^{ve}J_z^2 + \frac{1}{2}\gamma_{JJ}^{ve}J^4 + \gamma_{JK}^{ve}J_z^2J_z^2 + \dots \\ &\quad + \gamma_{JJK}^{ve}J_z^4J_z^2 + \dots, \\ D^{ve} &= \delta^{ve}J_z + \delta_J^{ve}J_zJ^2 + \delta_K^{ve}J_z^3 + \delta_{JJ}^{ve}J_zJ^4 + \delta_{JK}^{ve}J_z^2J_z^3 + \dots, \\ F^{ve} &= \frac{1}{2}\kappa^{ve} + \frac{1}{2}\kappa_J^{ve}J_z^2 + \kappa_K^{ve}J_z^2 + \frac{1}{2}\kappa_{JJ}^{ve}J^4 + \kappa_{JK}^{ve}J_z^2J_z^2 + \dots, \\ G^{ve} &= \theta^{ve}J_z + \theta_J^{ve}J_zJ^2 + \theta_K^{ve}J_z^3 + \theta_{JJ}^{ve}J_zJ^4 + \theta_{JK}^{ve}J_z^2J_z^3 + \dots. \end{aligned} \quad (8)$$

In Equation (5) the  $E^{ve}, B^{ve}, \dots, \epsilon'^{ve}$  parameters have the same meaning as the corresponding ones in Equation (3) with only one exception: although the operators  $(J_+^3 + J_-^3)$  connect rotational states  $|JK\rangle$  and  $|JK'\rangle$  with  $\Delta K = K - K' = \pm 3$ , they do not split  $A_1/A_2$  levels. The operator  $H_2^{vE,vE}$  describes the  $k-l$  splittings; other types of operators,  $(J_+^n \pm J_-^n)$ , connect rotational states  $|JK\rangle$  and  $|JK'\rangle$  where  $\Delta K = K - K' = \pm n$ . Of these, the operators with  $n=2m$  provide the  $A_1-A_2$  splittings of energy levels with  $K=m$ .

The Fermi-type resonance operators  $H^{v\Gamma,v'\Gamma}$  connect vibrational states of the same symmetries and formally have the same form as expressions (3)–(8). However, the vibrational operators  $|v\Gamma_\sigma\rangle\langle v\Gamma_{\sigma'}|$  in these formulae should be exchanged by  $|v\Gamma_\sigma\rangle\langle v'\Gamma_{\sigma'}|$ , and the parameters  $E^{va_i}, B^{va_i}, \dots, \theta_{JK}^{ve}, \dots$  in Equations (3)–(8) should be exchanged by the corresponding resonance operators  $E^{va_i,v'a_i}, B^{va_i,v'a_i}, \dots, \theta_{JK}^{ve,v'e}, \dots$

Finally, the Coriolis-type interaction operators which connect vibrational states of different symmetries, have the following form:

$$\begin{aligned} H^{vA_1,v'E} &= |vA_1\rangle\langle v'E_1| \{ [iA^{va_1,v'e}, (J_+ - J_-)]_+ \\ &\quad + [B^{va_1,v'e}, (J_+ + J_-)]_+ \\ &\quad + [C^{va_1,v'e}, (J_+^2 + J_-^2)]_+ + [iD^{va_1,v'e}, (J_-^2 - J_+^2)]_+ \\ &\quad + [F^{va_1,v'e}, (J_+^4 + J_-^4)]_+ + [iG^{va_1,v'e}, (J_-^4 - J_+^4)]_+ \\ &\quad + |vA_1\rangle\langle v'E_2| \{ [A^{va_1,v'e}, (J_+ + J_-)]_+ \\ &\quad + [iB^{va_1,v'e}, (J_- - J_+)]_+ \\ &\quad + [iC^{va_1,v'e}, (J_+^2 - J_-^2)]_+ + [D^{va_1,v'e}, (J_+^2 + J_-^2)]_+ \\ &\quad + [iF^{va_1,v'e}, (J_+^4 - J_-^4)]_+ + [G^{va_1,v'e}, (J_+^4 + J_-^4)]_+ \}. \end{aligned} \quad (9)$$

and

$$\begin{aligned} H^{vA_2,v'E} &= -|vA_2\rangle\langle v'E_2| \{ [iA^{va_2,v'e}, (J_+ - J_-)]_+ \\ &\quad + [B^{va_2,v'e}, (J_+ + J_-)]_+ \\ &\quad + [C^{va_2,v'e}, (J_+^2 + J_-^2)]_+ + [iD^{va_2,v'e}, (J_-^2 - J_+^2)]_+ \\ &\quad + [F^{va_2,v'e}, (J_+^4 + J_-^4)]_+ + [iG^{va_2,v'e}, (J_-^4 - J_+^4)]_+ \\ &\quad + |vA_2\rangle\langle v'E_1| \{ [A^{va_2,v'e}, (J_+ + J_-)]_+ \\ &\quad + [iB^{va_2,v'e}, (J_- - J_+)]_+ \\ &\quad + [iC^{va_2,v'e}, (J_+^2 - J_-^2)]_+ + [D^{va_2,v'e}, (J_+^2 + J_-^2)]_+ \\ &\quad + [iF^{va_2,v'e}, (J_+^4 - J_-^4)]_+ + [G^{va_2,v'e}, (J_+^4 + J_-^4)]_+ \}. \end{aligned} \quad (10)$$

The operators  $A^{va_i,v'e}, B^{va_i,v'e}, \dots$ , etc., can be derived from Equation (8) by replacing the parameters

Table 5. Elements of the  $G$ -reduction matrix for the  $C_{3v}$  point group.<sup>a</sup>

Element	Value
$(J)G_{NA_1}^m$	$\frac{(-i)^J}{2^{1/2}}(1 + \delta_{N,0})^{-1/2}(\delta_{m,3N} + (-1)^{(J+3N)}\delta_{m,-3N})$
$(J)G_{NA_2}^m$	$\frac{(-i)^{J+1}}{2^{1/2}}(1 - 2\delta_{N,0})(1 + \delta_{N,0})^{-1/2}(\delta_{m,3N} + (-1)^{(J+3N+1)}\delta_{m,-3N})$
$(J)G_{NE1}^m$	$\frac{(-i)^J}{2^{1/2}}(\delta_{m,3N+1} + (-1)^{(J+3N+1)}\delta_{m,-(3N+1)})$
$(J)G_{NE2}^m$	$\frac{(-i)^{J+1}}{2^{1/2}}(\delta_{m,3N+1} + (-1)^{(J+3N)}\delta_{m,-(3N+1)})$
$(J)G_{(N+1+\{(J-1)/3\})E1}^m$	$\frac{(-i)^J}{2^{1/2}}(\delta_{m,3N+2} + (-1)^{(J+3N)}\delta_{m,-(3N+2)})$
$(J)G_{(N+1+\{(J-1)/3\})E2}^m$	$\frac{(-i)^{J-1}}{2^{1/2}}(\delta_{m,3N+2} + (-1)^{(J+3N+1)}\delta_{m,-(3N+2)})$

Note: <sup>a</sup>The index  $N$  takes the following values:  $N=0, 1, \dots, \{J/3\}$  for the states of  $A_1$  and  $A_2$  symmetry;  $N=0, 1, \dots, \{(J-1)/3\}$  for the states of  $E$  symmetry. The nomenclature of the rotational states is illustrated also in Figure 2.

$\alpha, \beta, \dots$  by  $\alpha^{va_i, v'e}, \beta^{va_i, v'e}, \dots$ , etc. ( $i=1, 2$ ). The last type of Coriolis resonance interactions has the following form:

$$H^{vA_1, v'A_2}$$

$$\begin{aligned} &= |vA_1\rangle\langle v'A_2| \{2(C\xi)^{va_1, v'a_2} J_z \\ &+ \eta_J^{va_1, v'a_2} J_z J^2 + \eta_K^{va_1, v'a_2} J_z^3 + \eta_{JJ}^{va_1, v'a_2} J_z J^4 + \eta_{JK}^{va_1, v'a_2} J_z^3 J^2 \\ &+ \eta_{KK}^{va_1, v'a_2} J_z^5 + \eta_{JJJ}^{va_1, v'a_2} J_z J^6 + \eta_{JKK}^{va_1, v'a_2} J_z^3 J^4 \\ &+ \eta_{JJK}^{va_1, v'a_2} J_z^5 J^2 + \eta_{KKK}^{va_1, v'a_2} J_z^7 + \dots\}. \end{aligned} \quad (11)$$

### 3.3. Symmetrised rotational-vibrational functions

Since the  $C_{3v}$  symmetry group has three irreducible representations  $A_1$ ,  $A_2$ , and  $E$  (with the two components  $E_1$  and  $E_2$ ), every vibration-rotation wave functions should be symmetric ( $A_1$ ), antisymmetric ( $A_2$ ), or be transformed under symmetry operations according to one from two lines ( $E_1$  or  $E_2$ ) of the irreducible representation  $E$ . Thus every vibration-rotation state function should have the form [58,59]

$$|v\gamma_v, JK\gamma_r, m\gamma_s\rangle \equiv (|v\gamma_v\rangle \otimes |JK\gamma_r\rangle)_s^\gamma. \quad (12)$$

It should be mentioned that the sets of indices  $v\gamma_v$ ,  $JK\gamma_r$ , and  $m\gamma_s$  are single valued and determine every vibration-rotation state function. In Equation (12)  $\gamma_v$ ,  $\gamma_r$ , and  $\gamma$  denote symmetries of vibrational, rotational, and vibrational-rotational states, respectively;  $s$  is the line of the irreducible representation  $\gamma$ . The index  $m$  distinguishes between the vibrational-rotational states of the same symmetry;  $0 \leq K \leq J$  with total angular momentum quantum number  $J$ ; the symbol  $\otimes$  denotes a direct tensorial product.

In accordance with [58,59], the pure rotational functions  $|Jk\gamma_r\sigma\rangle$  can be written with the help of elements of the so-called  $G$ -reduction matrix (for the  $C_{3v}$  point symmetry group they are presented in Table 5) in the form

$$|Jk\gamma_r\sigma\rangle = \sum_k (J)G_{\gamma r s}^k |Jk\rangle. \quad (13)$$

Here the index  $s$  denotes the line of the ‘rotational’ irreducible representation  $\gamma_r$ ;  $|Jk\rangle$  denotes the ( $m=0$ ) part of the usual well-known rotational functions [3,60]

$$|Jkm\rangle = \exp(-ik\varphi)d_{km}^j(\vartheta)\exp(-im\psi). \quad (14)$$

In Equations (13) and (14),  $J \geq k \geq -J$ . Since for a free molecule the index  $m$  in the functions (14) is nonessential, we omitted it both in Equation (13) and further on in this paper.

For molecules belonging to the  $C_{3v}$  symmetry group, using the data from Table 5, one can write the rotational functions (13) in an explicit form as

$$2^{1/2}|JK\gamma_r\sigma\rangle = C_{JK\gamma_r\sigma}^l \{|JK\rangle + (-1)^l(-1)^{J+K}|J-K\rangle\}, \quad (15)$$

where the coefficients  $C_{JK\gamma_r\sigma}^l$  are presented in Table 6.

In order to take into account the definition of the so-called tensorial product of two irreducible tensorial values [57,61], we write

$$(A^\Gamma \otimes B^{\Gamma'})_\sigma^\gamma = ([\gamma])^{1/2} \sum_{ss'} \begin{pmatrix} \gamma & \Gamma & \Gamma' \\ \sigma & s & s' \end{pmatrix} A_s^\Gamma B_{s'}^{\Gamma'}, \quad (16)$$

and using Equation (15), the symmetrised vibrational-rotational functions (12) can be written in a more traditional form. In this case:

- (1) For the  $A_1$ - (or  $A_2$ )-type vibrational states the ro-vibrational wavefunctions have the simple form of the usual products of vibrational

Table 6. Coefficients  $C_{JK\gamma\sigma}^l$  of symmetrised rotational functions.

$\gamma_1\sigma_1$	$\gamma_2\sigma_2$	$\gamma_3\sigma_3$	Value	$\gamma_1\sigma_1$
even	0	$A_1$	0	$(-i)^J 2^{1/2}$
odd	0	$A_2$	1	$-(-i)^{J+1} 2^{1/2}$
any	3, 6, 9, ...	$A_1$	0	$(-1)^J$
		$A_2$	1	$(-1)^{J+1}$
	1, 4, 7, ...	$E_1$	0	$(-1)^J$
		$E_2$	1	$(-1)^{J+1}$
	2, 5, 8, ...	$E_1$	0	$(-1)^J$
		$E_2$	1	$(-1)^{J-1}$

Table 7. Coefficients  $A_{JKm\gamma s}^{\gamma_r \sigma}$  and  $B_{JKm\gamma s}^{\gamma_r \sigma}$  of symmetrised rotational-vibrational functions.

$J$	$K$	$m\gamma s$	$\gamma_r \sigma$	$A_{JKm\gamma s}^{\gamma_r \sigma}$	$B_{JKm\gamma s}^{\gamma_r \sigma}$
any	$k \neq 0, 3, 6, 9, \dots$	$A_1$	$E_1$	1	
			$E_2$		1
			$A_2$		-1
			$E_1$	1	
			$E_2$	-1	
		$E_1$	$E_1$		1
			$E_2$	1	
			$E_1$		1
			$E_2$	1	
			$E_1$		
any	$k = 3, 6, 9, \dots$	$1E_1$	$A_1$	1	
			$A_2$		1
			$1E_2$	1	
			$A_1$		-1
			$A_2$	1	
		$2E_1$	$A_1$	1	
			$A_2$		1
			$2E_1$	1	
			$A_2$		1
			$2E_2$	1	
even	$k = 0$	$E_1$	$A_1$	$2^{1/2}$	
		$E_1$	$A_1$		$2^{1/2}$
odd	$k = 0$	$E_2$	$A_2$		$2^{1/2}$
		$E_2$	$A_2$	$-2^{1/2}$	

functions  $|vA_1\rangle$  (or  $|vA_2\rangle$ ) and pure rotational functions (15),

$$|vA_1, JK, \gamma\sigma\rangle = |vA_1\rangle|JK\gamma\sigma\rangle, \quad (17)$$

or

$$|vA_2, JK, \gamma\sigma\rangle = |vA_2\rangle|JK\gamma\sigma'\rangle, \quad (18)$$

respectively. In Equation (18),  $\gamma_r = A_1$  when  $\gamma = A_2$  and  $\gamma_r = A_2$  when  $\gamma = A_1$ ; furthermore one has  $\gamma_r \sigma = E_1$  when  $\gamma\sigma = E_2$  and  $\gamma_r \sigma = E_2$  when  $\gamma\sigma = E_1$ .

- (2) For the  $E$ -type vibrational states ro-vibrational functions have a more complicated form,

$$2^{1/2}|vE, JK, m\gamma_r s\rangle = \sum_{\gamma_r \sigma} A_{JKm\gamma s}^{\gamma_r \sigma} |vE1\rangle|JK\gamma_r \sigma\rangle + \sum_{\gamma_r \sigma} B_{JKm\gamma s}^{\gamma_r \sigma} |vE2\rangle|JK\gamma_r \sigma\rangle, \quad (19)$$

Table 8. Non-zero  $3\Gamma$  symbols  $\begin{pmatrix} \gamma_1 & \gamma_2 & \gamma_3 \\ \sigma_1 & \sigma_2 & \sigma_3 \end{pmatrix}$  of the  $C_{3v}$  symmetry group.<sup>a</sup>

$\gamma_1\sigma_1$	$\gamma_2\sigma_2$	$\gamma_3\sigma_3$	Value	$\gamma_1\sigma_1$	$\gamma_2\sigma_2$	$\gamma_3\sigma_3$	Value
$A_1$	$A_1$	$A_1$	1	$A_2$	$E_1$	$E_2$	$1/2^{1/2}$
$A_1$	$A_2$	$A_2$	1	$E_1$	$E_1$	$E_1$	$-1/2$
$A_1$	$E_1$	$E_1$	$1/2^{1/2}$	$E_1$	$E_2$	$E_2$	$1/2$
$A_1$	$E_2$	$E_2$	$1/2^{1/2}$				

Note: <sup>a</sup>Other non-zero  $3\Gamma$  symbols are connected with the values given in the table by the relations

$$\begin{pmatrix} \gamma_1 & \gamma_2 & \gamma_3 \\ \sigma_1 & \sigma_2 & \sigma_3 \end{pmatrix} = \begin{pmatrix} \gamma_2 & \gamma_3 & \gamma_1 \\ \sigma_2 & \sigma_3 & \sigma_1 \end{pmatrix} = (-1)^{\gamma_1 + \gamma_2 + \gamma_3} \begin{pmatrix} \gamma_1 & \gamma_3 & \gamma_2 \\ \sigma_1 & \sigma_3 & \sigma_2 \end{pmatrix},$$

$$\text{where } (-1)^{A_1} = (-1)^E = +1; (-1)^{A_2} = -1.$$

where the coefficients  $A_{JKm\gamma s}^{\gamma_r \sigma}$  and  $B_{JKm\gamma s}^{\gamma_r \sigma}$  are presented in Table 7. In Equation (16) [ $\gamma$ ] denotes the dimension of the irreducible representation  $\gamma$ , namely  $[A_1] = [A_2] = 1$  and  $[E] = 2$ ;

$$\begin{pmatrix} \gamma & \Gamma & \Gamma' \\ \sigma & s & s' \end{pmatrix}$$

are  $3\Gamma$  symbols of the corresponding symmetry group. Table 8 presents non-zero  $3\Gamma$  symbols for the  $C_{3v}$  symmetry group.

#### 4. Analysis of the experimental data

The spectra of both the  $\text{CH}_3\text{D}$  and  $\text{CHD}_3$  species were measured in the region of  $2900\text{--}9000\text{ cm}^{-1}$ . The corresponding overviews of the recorded spectra are shown in Figures 3 and 4. The regions of very strong absorbance in both figures correspond to the fundamental bands. In Figure 3, the bands  $\nu_1$  and  $\nu_4$  are clearly pronounced near  $3000\text{ cm}^{-1}$ . Similarly, the fundamental band  $\nu_1$  is clearly seen in Figure 4. The weaker, but, as a rule, also well-recognised bands belong to doubly excited first overtone and combinational bands (they are marked on Figures 3 and 4). The total number of such bands as seen in absorption is 21 (27 if one takes into account the presence of both allowed subbands of symmetries  $A_1$  and  $E$  in the bands  $2\nu_4$ ,  $2\nu_5$ ,  $2\nu_6$ ,  $\nu_4 + \nu_5$ ,  $\nu_4 + \nu_6$ , and  $\nu_5 + \nu_6$ ) for any of the two symmetric top methane isotopomers. A number of weak bands, belonging to triple excitations of vibrational quanta and appearing, as a rule, by strong resonance interactions with stronger first overtone and combinational bands, also can be seen in the pictures of the overview spectra. As is well known, at higher excitations the Fermi resonance polyad system of the CH chromophore in  $\text{CHD}_3$  (involving  $\nu_1$  and  $\nu_5$ ) becomes dominant in absorption [20]. In total, we were

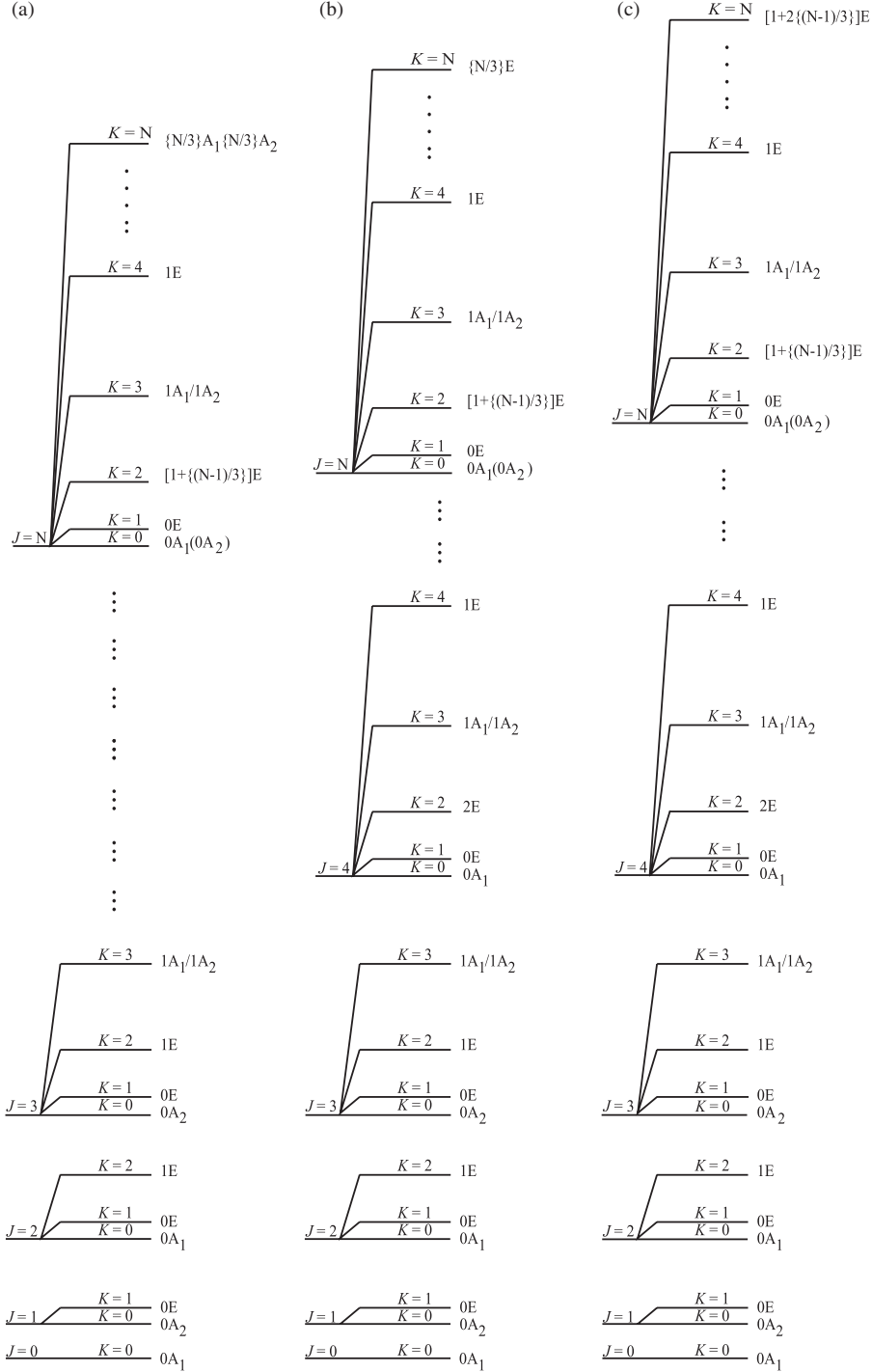


Figure 2. Nomenclature of states of different rotational symmetry species in  $C_{3v}$  for a given value of quantum number  $J$ : (a)  $J$  is divisible by 3; (b)  $J - 1$  is divisible by 3; (c)  $J + 1$  is divisible by 3. It should be noted that the indices  $n\Gamma$  determine uniquely the  $K$  index and vice versa; for  $nA$  indices  $K = 3n$  at  $0 \leq n \leq \{J/3\}$ ; for  $nE$  indices  $K = 3n + 1$  at  $0 \leq n \leq \{(J-1)/3\}$ , or  $K = 3(n - [(J-1)/3]) - 1$  at  $n \geq 1 + \{(J-1)/3\}$ . The symbol  $\{B\}$  above denotes the integer part of the number  $B$ .

able to assign ro-vibrational transitions to 57 (for  $\text{CH}_3\text{D}$ ) and 40 (for  $\text{CHD}_3$ ) previously unknown bands. Transitions with values of the quantum number  $J \leq 8$  to 12 for the strong bands and  $J \leq 5$  to 6 for the weak

bands were assigned in the spectra recorded at a temperature of about 80 K.

As in our previous analysis of the  $\text{CH}_2\text{D}_2$  low temperature ro-vibrational spectra [32], a line

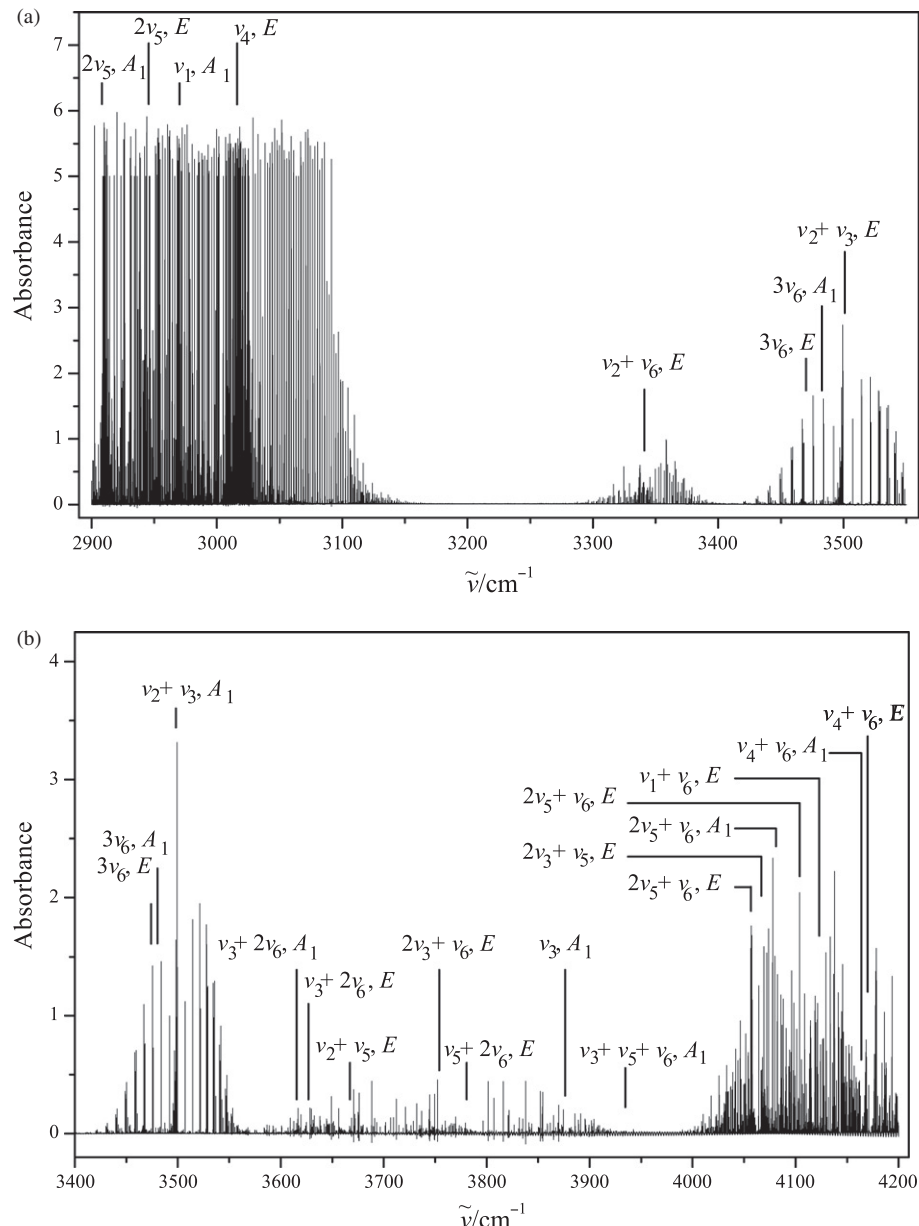


Figure 3. Survey spectrum as decadic absorbance  $\lg(I_0/I)$  of  $\text{CH}_3\text{D}$  in the region of  $2900\text{--}6500\text{ cm}^{-1}$ . Experimental conditions are presented in Table 1.

assignment in the low temperature spectra was much easier than the assignment of ‘room temperature’ spectra because of the smaller number of lines in the cold spectra. As an illustration, Figure 5 presents a small part of the spectrum of  $\text{CH}_3\text{D}$  recorded at 80 K in the region of  $4128.50$  to  $4129.75\text{ cm}^{-1}$  (upper trace). For comparison, a spectrum in the same region previously recorded with our BOMEM FTIR spectrometer at room temperature is shown in the lower trace of Figure 5. The great improvement in the new data is clearly visible. On the basis of our new experimental data, more than 5700 transitions

were assigned to 57 newly identified bands of  $\text{CH}_3\text{D}$ , and more than 4400 transitions were assigned to 40 newly identified bands of  $\text{CHD}_3$ . The rotational assignment was confirmed with the help of the Ground State Combination Differences (GSCD) method, and the ground state energies were taken from [62] for  $\text{CH}_3\text{D}$  and [63] for  $\text{CHD}_3$  (Table 9). Because of numerous and strong resonance interactions, an effective Hamiltonian of the form defined by Equations (1)–(11) was used for the calculation and preliminary prediction of line positions for both molecules.

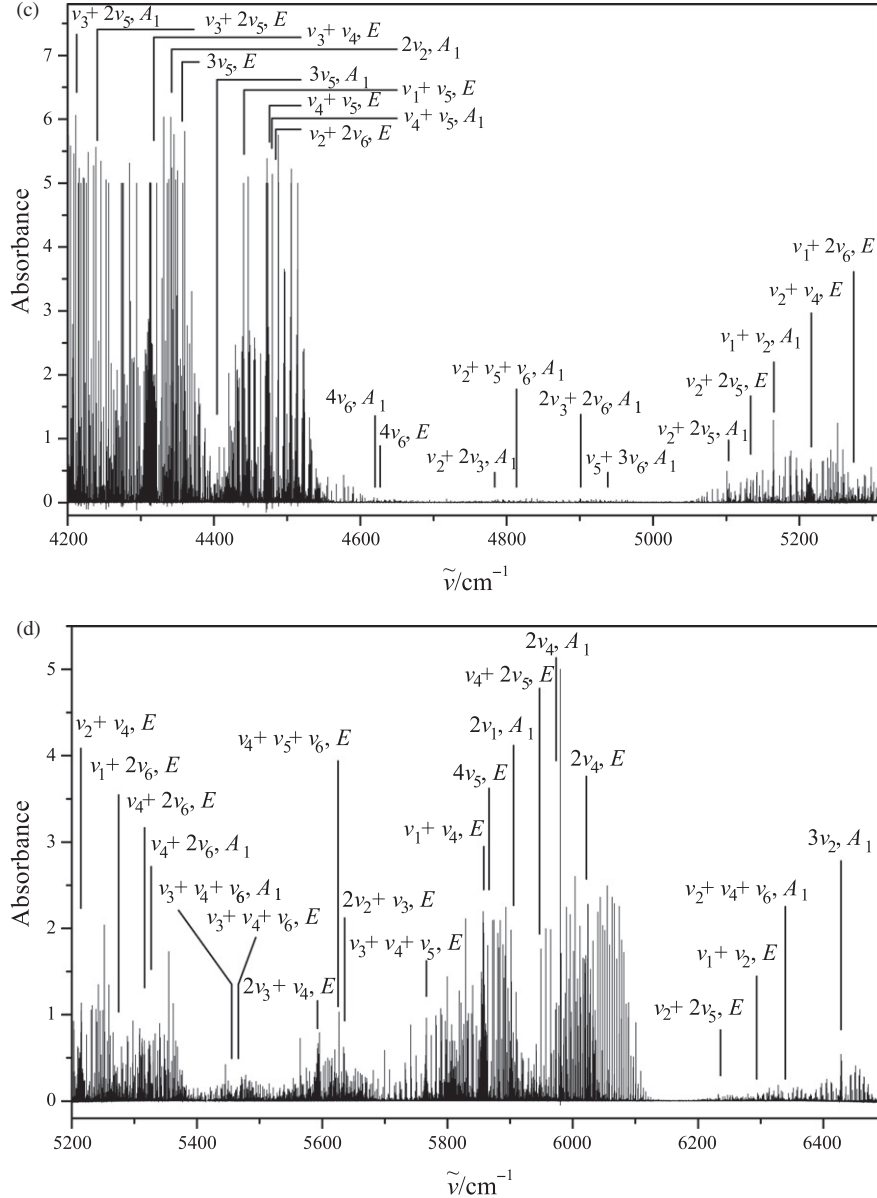


Figure 3. Continued.

To make a vibrational assignment, some additional criteria were used. Firstly, preliminary estimates of the band centres were made on the basis of the methane intramolecular potential functions determined earlier from analysis of 94 experimental band centres of CH<sub>2</sub>D<sub>2</sub> (see [32] and references cited therein). The second criterion for the vibrational symmetry assignment arose from the analysis of pronounced sets of *P* transitions in the experimental spectra. One of them is the set of transitions of the type

$$\langle v\gamma_v, J K, e | \leftarrow \langle v_{\text{ground}}, J' = J + 1 K' = 1, e |, \quad (20)$$

where notations of the upper and lower ro-vibrational states correspond to Equation (12);  $K=1$  for the  $A_1$ ,

and  $K=0$  for the *E*-type vibrational bands. In this case, if the set of transitions with  $J+1 = \dots, 6, 5, 4, \dots$ , Equation (20), is limited by the value  $J+1 = 2$ , one can expect that a corresponding set of transitions belongs to a band of the  $A_1$  symmetry. When the set of transitions is limited by the value  $J+1 = 1$ , one can be sure that a corresponding set of transitions belongs to the  $\Delta K = -1$  subband of an *E*-type vibrational band.

Similarly, if a set of transitions  $J+1 = \dots, 6, 5, 4, \dots$  with

$$\langle v\gamma_v, J K, a_2/a_1 | \leftarrow \langle v_{\text{ground}}, J' = J + 1 K' = 3, a_1/a_2 |, \quad (21)$$

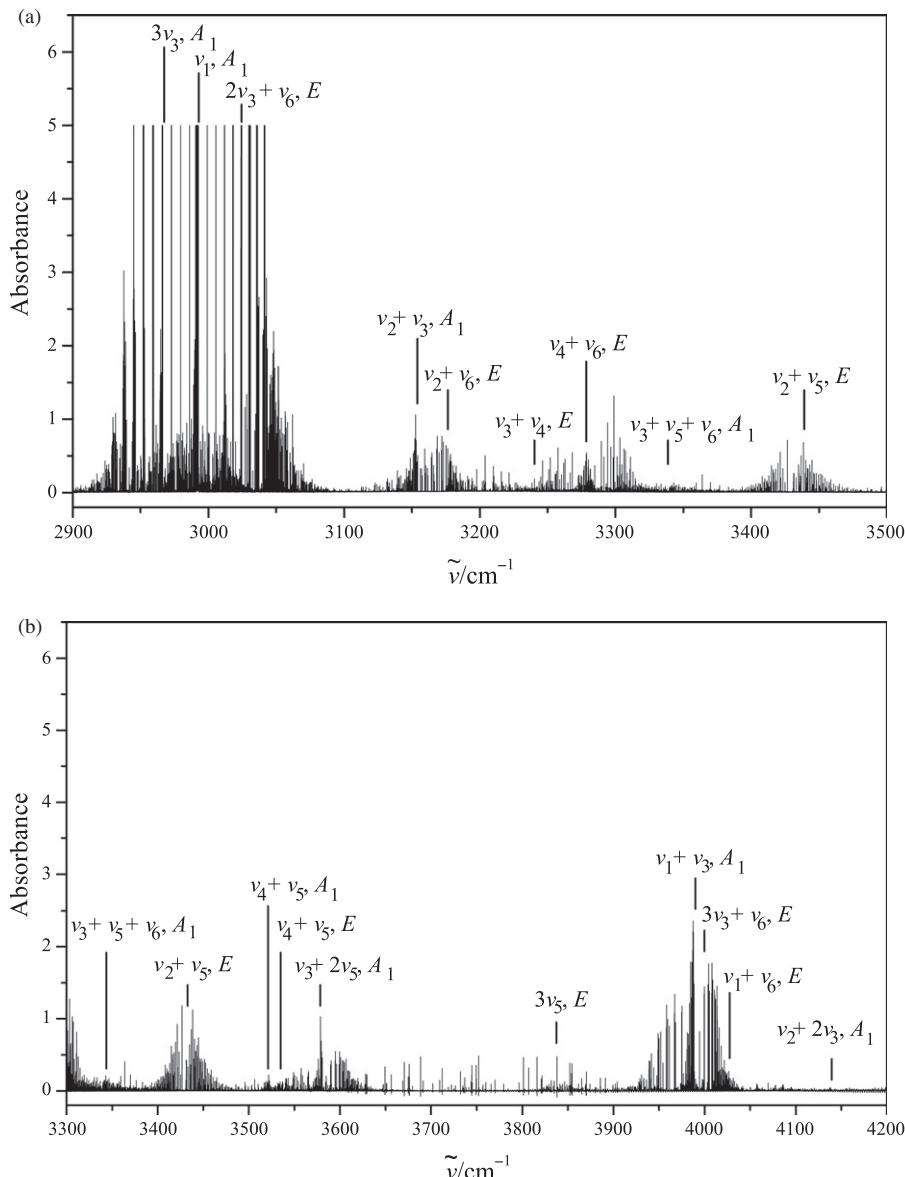


Figure 4. Survey spectrum as decadic absorbance  $\lg(I_0/I)$  of  $\text{CHD}_3$  in the region of  $2900\text{--}6500\text{ cm}^{-1}$ . Experimental conditions are presented in Table 1.

is limited by the value  $J+1=3, 4$ , or  $2$ , one can expect that a corresponding set of transitions belongs to a vibrational band of the  $A_1$  symmetry, or to a  $\Delta K=+1$ , or  $\Delta K=-1$  subband of an  $E$ -type vibrational band, respectively. As an additional criterion, the set of transitions

$$\langle v\gamma_r, J\ K, a_2/a_1 | \leftarrow \langle v_{\text{ground}}, J'=J+1\ K'=0, a_1/a_2 |, \quad (22)$$

can be used as well. This assignment procedure is illustrated by Figures 6 and 7. Tables 10 and 11 provide examples of numerical results in the procedure. It is thus important to stress that the band centres of

practically all bands were found from an experimental transition assigned in the spectrum. The total list of experimental band centres is presented in column 5 of Table 12 for  $\text{CH}_3\text{D}$ .

The same assignment procedure was used also for the analysis of the experimental spectrum of  $\text{CHD}_3$ . The list of band centres for the bands analysed is presented in column 5 of Table 13.

## 5. Results of the vibrational analysis

As a first step in the theoretical analysis of high-resolution spectra of the  $C_{3v}$  symmetric isotopomers of

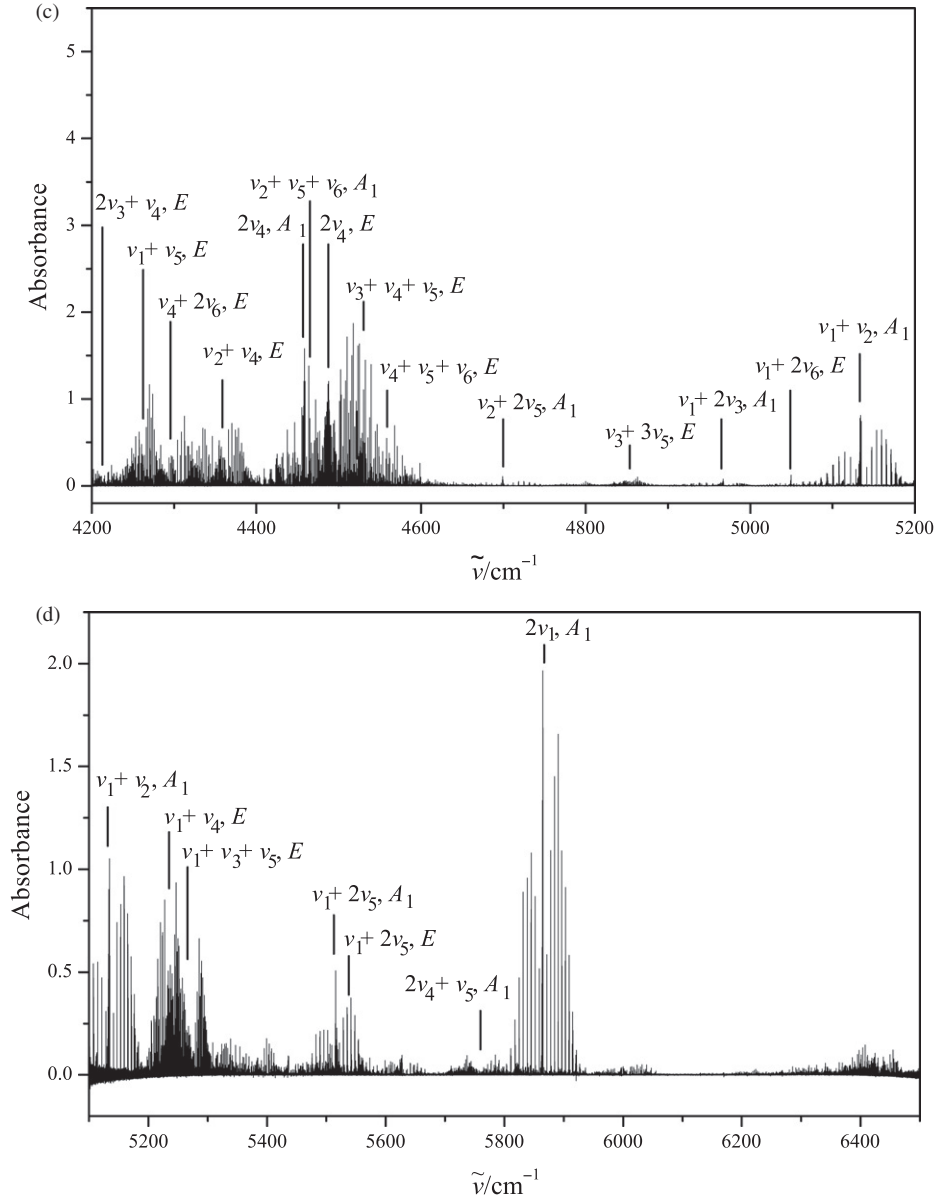


Figure 4. Continued.

methane, we present here a pure vibrational analysis of all band centres of CH<sub>3</sub>D and CHD<sub>3</sub> as known now up to about 9000 cm<sup>-1</sup>. The analysis was carried out with the Hamiltonian model of Section 3.2 which takes into account both the anharmonicity of vibrations, and some types of pure vibrational resonance interactions:

$$H^{\text{vib.}} = \sum_{vl\gamma_v, \tilde{v}\tilde{l}\tilde{\gamma}_v} |vl\gamma_v\rangle \langle \tilde{v}\tilde{l}\tilde{\gamma}_v| H_{vl\gamma_v \tilde{v}\tilde{l}\tilde{\gamma}_v}. \quad (23)$$

Here the summation includes all vibrational states studied.

As mentioned in Section 4, the use of the symmetrised wave functions is suitable in the theoretical study of symmetric top molecules. Following this strategy, we used symmetrised vibrational functions of the type

$$|v_1 v_2 v_3\rangle |[(v_4 l_4 \gamma_4) \otimes (v_5 l_5 \gamma_5)]^{\gamma_{45}} \otimes (v_6 l_6 \gamma_6)\rangle^\gamma, \quad (24)$$

in the construction of the elements  $H_{vl\gamma_v \tilde{v}\tilde{l}\tilde{\gamma}_v}$ , Equation (23) where  $\gamma_\lambda$  denotes the symmetry of the elementary vibrational functions  $|v_\lambda l_\lambda\rangle$ , and  $\gamma_{45}$  denotes a symmetry of that part of the full vibrational wave function, which depends on the doubly degenerate coordinates  $q_{4s}$  and  $q_{5s}$  ( $s = 1, 2$ ).

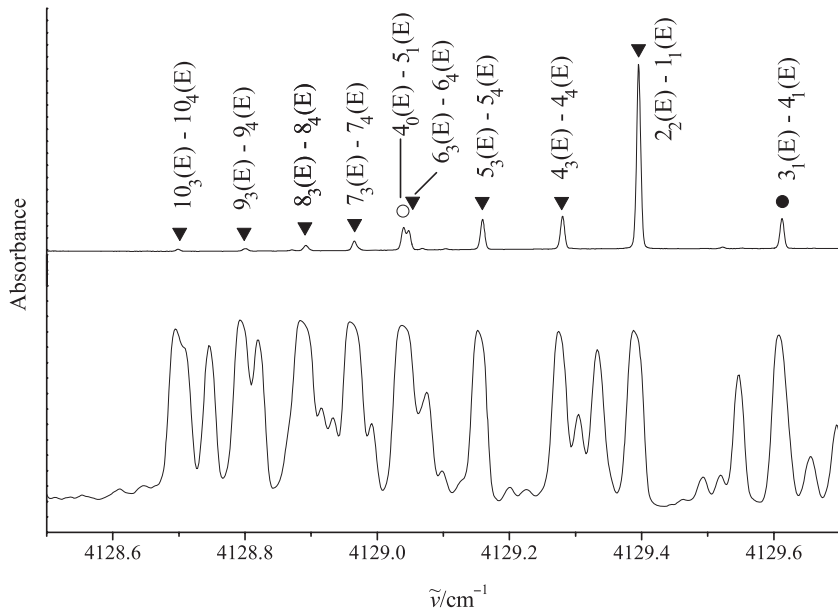


Figure 5. Small portion of the spectrum of the  $\text{CH}_3\text{D}$  molecule. Upper trace: Bruker IFS 125 Zürich prototype (ZP 2001) spectrum at 80 K. Lines belonging to the  $\nu_1 + \nu_6$ ,  $\nu_4 + \nu_6(A_1)$ , and  $\nu_4 + \nu_6(E)$  bands are marked by dark triangles, dark circles, and open circles, respectively. Lower trace: Bomem DA002 spectrum at 293 K (conditions commonly used in [20]).

Table 9. Ground state parameters of the  $\text{CH}_3\text{D}$  and  $\text{CHD}_3$  isotopomers of methane (in  $\text{cm}^{-1}$ ).<sup>a</sup>

Parameter	$\text{CH}_3\text{D}$ [62]	$\text{CHD}_3$ [63]
1	2	3
$A(C)$	3.880193378	2.6289695
$B$	5.25082109	3.2791847
$D_J/10^4$	0.5262994	0.49494
$D_{JK}/10^4$	1.264339	-0.38315
$D_K/10^4$	-0.7896593	0.13391
$H_J/10^8$	0.143479	0.2127
$H_{JK}/10^8$	1.214490	-0.3298
$H_{KJ}/10^8$	-0.67214	0.1874
$H_K/10^8$	-0.16436	-0.0178
$L_J/10^{12}$	-	-0.134
$L_{JK}/10^{12}$	-0.1836	0.171
$L_{KJ}/10^{12}$	-	-
$L_{KK}/10^{12}$	1.490	-
$L_K/10^{12}$	-	-
$\tilde{\epsilon}/10^5$	0.32	-0.289
$\tilde{h}_3/10^{10}$	0.32503	1.0191

Note: <sup>a</sup>These parameters were determined from ground state combination differences. Direct measurements of the far infrared spectrum exist as well [4] (pressure broadened).

In our present analysis we used two types of matrix elements in Equation (23):

(a) *diagonal elements*  $H_{v\gamma v\gamma v\gamma}$ . It is possible to show that all diagonal elements  $H_{v\gamma v\gamma v\gamma}$  have

the form

$$H_{v\gamma v\gamma v\gamma} = \sum_{\lambda} \omega_{\lambda} \left( v_{\lambda} + \frac{d_{\lambda}}{2} \right) + \sum_{\lambda, \mu \geq \lambda} x_{\lambda, \mu} \left( v_{\lambda} + \frac{d_{\lambda}}{2} \right) \left( v_{\mu} + \frac{d_{\mu}}{2} \right) \\ + \sum_{\lambda, \mu \geq \lambda, \nu \geq \mu} y_{\lambda, \mu, \nu} \left( v_{\lambda} + \frac{d_{\lambda}}{2} \right) \left( v_{\mu} + \frac{d_{\mu}}{2} \right) \left( v_{\nu} + \frac{d_{\nu}}{2} \right) \\ + \sum_{\lambda} g_{\lambda \lambda} l_{\lambda}^2 + \sum_{\lambda, \mu > \lambda} g_{\lambda \mu} l_{\lambda} l_{\mu}, \quad (25)$$

where  $d_{\lambda} = 1$  for the nondegenerate modes  $q_{\lambda} = 1, 2, 3$ , and  $d_{\lambda} = 2$  for the doubly degenerate vibrational modes  $q_{\lambda} = 4, 5, 6$ .

(b) ‘resonance interaction’ elements of the type  $H_{v\gamma \tilde{v}\gamma}$  ( $v\gamma \neq \tilde{v}\gamma$ ). Because of numerous perturbations even in ‘pure vibrational’ spectra of both molecules, a correct analysis has to take into account resonance interactions between the corresponding interacting vibrational states. In order to decide which type of vibrational states should be connected by resonance interactions, we firstly made calculations of the absolute values of ratios

$$\frac{\langle v\gamma | k_{\lambda \mu \nu} \{(q_{\lambda} \otimes q_{\mu}) \otimes q_{\nu}\} | v'\gamma \rangle}{(E_v - E_{v'})} \quad (26)$$

and

$$\frac{\langle v\gamma | k_{\lambda \mu \nu \xi} \{(q_{\lambda} \otimes q_{\mu}) \otimes (q_{\nu} \otimes q_{\xi})\} | v'\gamma \rangle}{(E_v - E_{v'})} \quad (27)$$

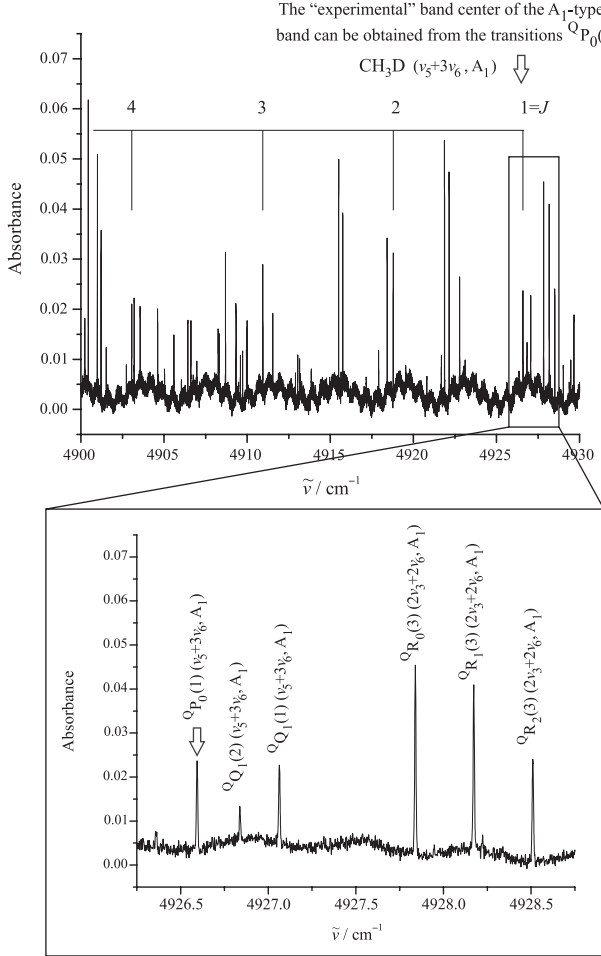


Figure 6. Set of transitions,  ${}^Q P_0(J)$ , for the  $A_1$ -type band,  $v_5 + 3v_6$ , of the  $\text{CH}_3\text{D}$  isotopomer. The first line of the progression, which corresponds to the transition  ${}^Q P_0(1)$  with  $J^{\text{upper}} = 0$ , can be recognised beyond doubt. The lower part of the Figure 6 shows in more detail the section of the spectrum close to the transition  ${}^Q P_0(1)$ . Assigned lines of some other bands also indicated. See also Figure 8.

The latter have been calculated with the methane potential function estimated on the basis of highly accurate experimental  $\text{CH}_2\text{D}_2$  data in [32].

Both the harmonic frequencies  $\omega_\lambda$ , and the parameters  $k_{\lambda \dots v}$  (effective anharmonic coupling constants in normal mode notations) are quite different for  $\text{CH}_3\text{D}$  and  $\text{CHD}_3$ . Therefore the vibrational resonance interactions are also quite different for these molecules. As the analysis shows, for our present investigation the resonance interactions are important, as follows:

$$(1) \quad H_{v\gamma, \tilde{v}\gamma} = \frac{k_{\lambda\lambda}}{2(2^{1/2})} \left\{ \frac{2v_i \pm 1 + 1}{4} \right\}^{1/2} (q_\lambda^+ q_\lambda^- + q_\lambda^- q_\lambda^+), \quad (28)$$

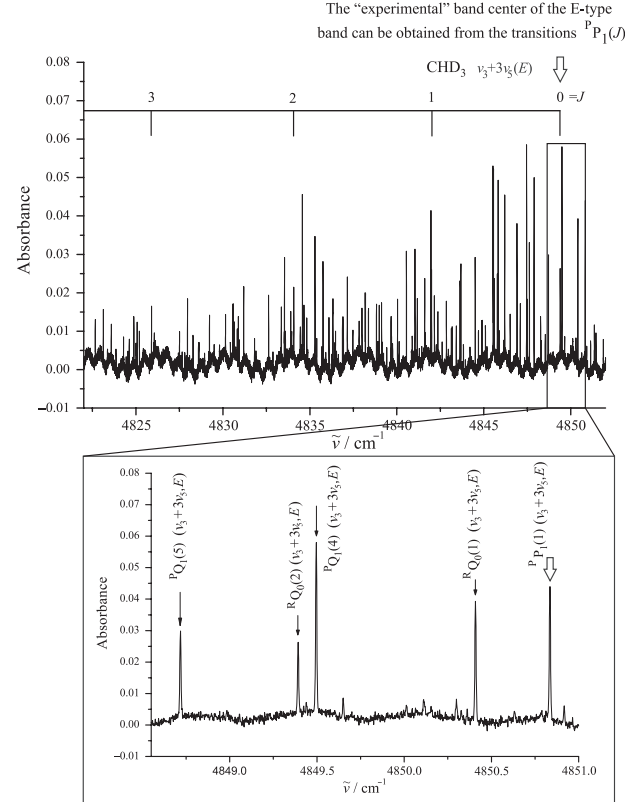


Figure 7. Analogous set of transitions,  ${}^Q P_0(J)$ , for the  $E$ -type band,  $v_3 + 3v_5$  of the  $\text{CHD}_3$  isotopomer. The first line of the progression, which corresponds to the transition  ${}^P P_1(1)$  with  $J^{\text{upper}} = 0$ , again can be recognised beyond doubt (see also the lower part of the Figure 7 and caption to Figure 6). See also Figure 9.

if  $|v\gamma\rangle = (\dots, v_i, \dots, v_\lambda l_\lambda \gamma_\lambda, \dots)$  and  $|\tilde{v}\tilde{l}\tilde{\gamma}\rangle = (\dots, v_i \pm 1, \dots, v_\lambda \mp 2l_\lambda \gamma_\lambda, \dots)$ . In this case, we took into account  $v_i = v_1$  and  $v_\lambda = v_5$  for  $\text{CH}_3\text{D}$  and  $\text{CHD}_3$ .

$$(2) \quad H_{v\gamma, \tilde{v}\gamma} = \frac{F_{ii, \lambda\lambda}}{2^{1/2}} \left\{ \frac{v_i \pm 1 + 1}{2} \right\}^{1/2} \left\{ \frac{v_i \pm 1}{2} \right\}^{1/2} \times (q_\lambda^+ q_\lambda^- + q_\lambda^- q_\lambda^+), \quad (29)$$

if  $|v\gamma\rangle = (\dots, v_i, \dots, v_\lambda l_\lambda \gamma_\lambda, \dots)$  and  $|\tilde{v}\tilde{l}\tilde{\gamma}\rangle = (\dots, v_i \pm 2, \dots, v_\lambda \mp 2l_\lambda \gamma_\lambda, \dots)$ . For  $\text{CH}_3\text{D}$  one should take  $v_i = v_1$  and  $v_\lambda = v_4$ ; and for  $\text{CHD}_3$  one should take  $v_i = v_3$  and  $v_\lambda = v_6$ . For the  $\text{CHD}_3$  isotopomer one has:

$$(3) \quad H_{v\gamma, \tilde{v}\gamma} = H_{\tilde{v}\gamma, v\gamma} = \frac{k_{345}}{4} (v_3 + 1)^{1/2} (q_4^+ q_5^- + q_4^- q_5^+). \quad (30)$$

Here  $\tilde{v}_1 = v_1$ ,  $\tilde{v}_2 = v_2$ ,  $\tilde{v}_3 = v_3 + 1$ ,  $\tilde{v}_4 = v_4 - 1$ ,  $\tilde{v}_5 = v_5 + 1$ ,  $\tilde{v}_6 = v_6$ .

For the  $\text{CH}_3\text{D}$  isotopomer one has:

$$(4) \quad H_{v\gamma, \tilde{v}\gamma} = H_{\tilde{v}\gamma, v\gamma} = \frac{F_{3356}}{4(2^{1/2})} \{v_3(v_3 - 1)\}^{1/2} \times (q_5^+ q_6^- + q_5^- q_6^+) \quad (31)$$

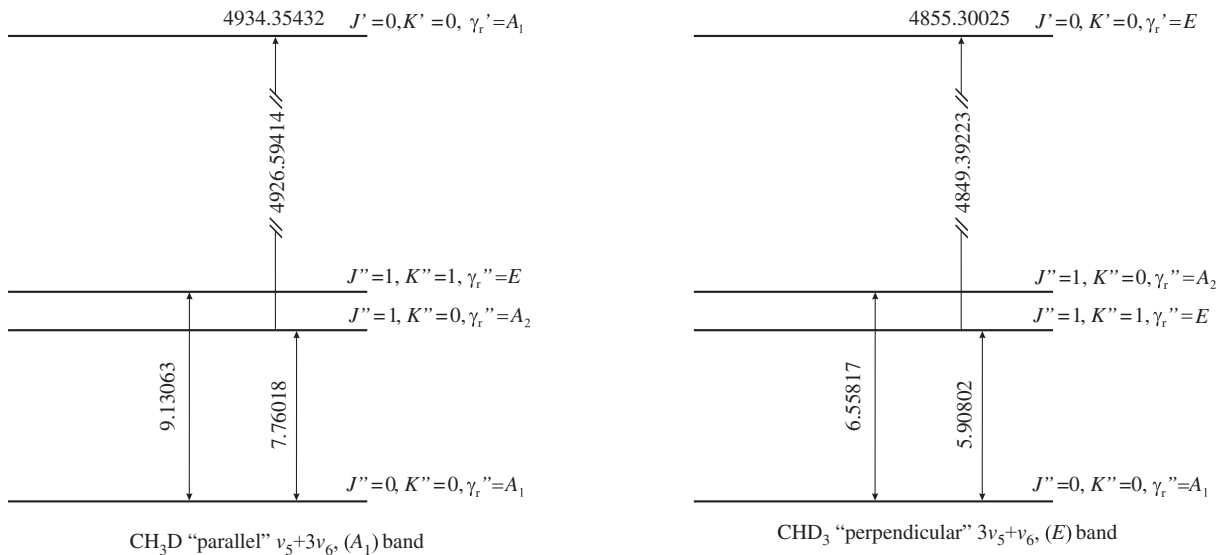


Figure 8. Level scheme relating to Figure 6.

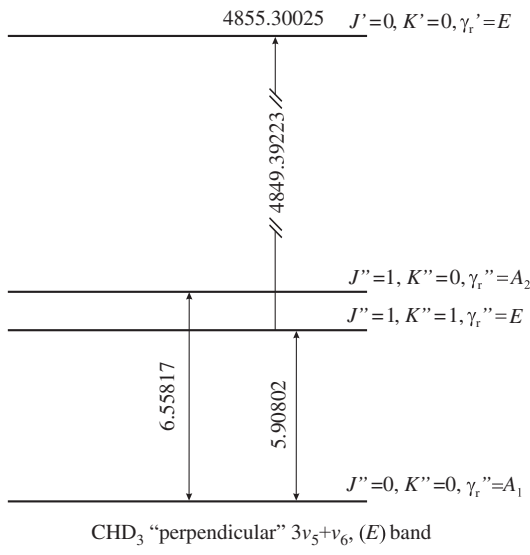


Figure 9. Level scheme relating to Figure 7.

Table 10. Line positions and levels for the transitions  $[J=0](upper\ vibr.\ st.) \leftarrow [J''=1](gr.\ vibr.\ st.)$  for some absorption bands of  $\text{CH}_3\text{D}$  ( $\text{cm}^{-1}$ ).

Band	Transition	$J''\ K''\ \gamma_r''$	$E''_{\text{rot.}}/\text{hc}$	$E'_{\text{vib.}}/\text{hc}$
$v_3 + v_3 + v_3$	( $A_1$ )	3927.4877	7.7602	3935.2479
$2v_5 + v_6$	( $1E$ )	4049.5611	9.1306	4058.6917
$2v_3 + v_5$	( $E$ )	4058.7280	9.1306	4067.8586
$2v_5 + v_6$	( $A_1$ )	4073.1815	7.7602	4080.9417
$2v_5 + v_6$	( $2E$ )	4093.3113	9.1306	4102.4419
$v_1 + v_6$	( $E$ )	4113.4594	9.1306	4122.5901
$v_4 + v_6$	( $A_1$ )	4155.7331	7.7602	4163.4933
$v_4 + v_6$	( $E$ )	4161.2319	9.1306	4170.3625
$v_3 + 2v_5$	( $A_1$ )	4207.5285	7.7602	4215.2887
$v_3 + 2v_5$	( $E$ )	4232.6136	9.1306	4241.7442

Table 11. Line positions and levels for the transitions  $[J=0](upper\ vibr.\ st.) \leftarrow [J''=1](gr.\ vibr.\ st.)$  for some absorption bands of  $\text{CHD}_3$  ( $\text{cm}^{-1}$ ).

Band	Transition	$J''\ K''\ \gamma_r''$	$E''_{\text{rot.}}/\text{hc}$	$E'_{\text{vib.}}/\text{hc}$
$2v_3 + v_4$	( $E$ )	4206.4244	5.9080	4212.3324
$v_1 + v_5$	( $E$ )	4255.7536	5.9080	4261.6616
$v_2 + v_4$	( $E$ )	4350.6155	5.9080	4356.5235
$2v_4$	( $A_1$ )	4451.2228	6.5582	4457.7810
$v_2 + v_5 + v_6$	( $A_1$ )	4456.4283	6.5582	4462.9865
$2v_4$	( $E$ )	4480.4003	5.9080	4486.3083
$v_3 + v_4 + v_5$	( $E$ )	4523.1538	5.9080	4529.0618
$v_4 + v_5 + v_6$	( $1E$ )	4552.0213	5.9080	4557.9293
$v_2 + 2v_5$	( $A_1$ )	4692.3241	6.5582	4698.8823
$v_3 + 3v_5$	( $E$ )	4849.3922	5.9080	4855.3003

Table 12. Values of the experimental band centres of CH<sub>3</sub>D (in cm<sup>-1</sup>).<sup>a</sup>

Band	Centre [64]	Centre calc., I	Centre calc., II	Centre exp.	Ref.	Band	Centre [64]	Centre calc., I	Centre calc., II	Centre exp.	Ref.
1	2	3	4	5	6	1	2	3	4	5	6
$v_6, E$	1163.29	1160.89	1160.74	1161.103	[54]	$v_2 + v_3 + v_6, E$	4637.57	4639.30	4639.33		
$v_3, A_1$	1309.77	1307.34	1307.48	1306.848	[54]	$4v_6, 2E$	4664.03	4643.18	4643.49		
$v_5, E$	1471.99	1472.14	1472.16	1472.022	[54]	$v_3 + 3v_6, E$	4796.64	4769.91	4769.92		
$v_2, A_1$	2194.60	2199.34	2199.08	2200.041	[25]	$v_3 + 3v_6, A_1$	4787.06	4781.90	4782.04	4781.529	tw
$2v_6, A_1$	2325.81	2316.62	2316.37	2316.273	[25]	$v_2 + 2v_3, A_1$	4801.80	4782.83	4782.83		
$2v_6, E$	2328.39	2322.61	2322.44	2323.289	[25]	$v_2 + v_5 + v_6, E$	4795.16	4801.06	4801.10		
$v_3 + v_6, E$	2471.97	2465.14	2465.14	2465.458	[25]	$v_2 + v_5 + v_6, A_1$	4805.27	4811.54	4811.54	4811.172	tw
$2v_3, A_1$	2605.94	2598.43	2598.57	2597.681	[25]	$2v_3 + 2v_6, A_1$	4927.39	4901.65	4901.65	4901.422	tw
$v_5 + v_6, E$	2626.16	2623.17	2623.13	2623.433	[25]	$2v_3 + 2v_6, E$	4929.97	4907.66	4907.72		
$v_5 + v_6, A_1$	2636.27	2633.43	2633.37	2633.155	[25]	$v_5 + 3v_6, 1E$	4939.93	4924.69	4924.76		
$v_3 + v_5, E$	2779.73	2776.61	2776.73	2776.287	[25]	$v_5 + 3v_6, 2E$	4944.88	4926.39	4926.63		
$2v_5, A_1$	2938.18	2910.14	2910.01	2910.120	[25]	$v_5 + 3v_6, A_1$	4954.99	4935.08	4935.11	4934.354	tw
$2v_5, E$	2941.01	2940.22	2940.25	2940.098	[25]	$v_5 + 3v_6, 3E$	4970.26	4955.49	4955.70		
$v_1, A_1$	2939.47	2969.61	2969.49	2969.512	[25]	$v_2 + v_3 + v_5, E$	4964.26	4964.94	4964.98		
$v_4, E$	3012.02	3015.80	3015.90	3016.713	[25]	$3v_3 + v_6, E$	5048.52	5027.63	5027.40		
$v_2 + v_6, E$	3335.62	3342.42	3342.24	3342.573	tw	$v_3 + v_5 + 2v_6, A_1$	5087.69	5073.33	5073.48		
$3v_6, E$	3490.14	3471.84	3471.66	3471.465	tw	$v_3 + v_5 + 2v_6, 1E$	5095.23	5077.52	5077.57		
$3v_6, A_1$	3495.30	3483.83	3483.79	3482.240	tw	$v_3 + v_5 + 2v_6, 2E$	5107.92	5093.52	5093.61		
$v_2 + v_3, A_1$	3497.63	3499.31	3499.25	3499.718	tw	$v_2 + 2v_5, A_1$	5127.41	5103.61	5103.53	5103.572	tw
$v_3 + 2v_6, A_1$	3633.40	3617.78	3617.71	3616.793	tw	$v_2 + 2v_5, E$	5128.94	5132.28	5132.29	5132.103	tw
$v_3 + 2v_6, E$	3635.98	3623.78	3623.77	3625.011	tw	$4v_3, A_1$	5157.46	5135.13	5134.70		
$v_2 + v_5, E$	3663.26	3667.83	3667.72	3668.078	tw	$v_1 + v_2, A_1$	5130.90	5164.61	5164.53	5165.046	tw
$2v_3 + v_6, E$	3767.05	3752.70	3752.74	3753.889	tw	$2v_5 + 2v_6, 1A_1$	5249.01	5206.46	5206.55		
$v_5 + 2v_6, A_1$	3782.14	3775.03	3775.05		tw	$2v_3 + v_5 + v_6, E$	5225.85	5206.50	5206.68		
$v_5 + 2v_6, 1E$	3789.67	3778.97	3778.91	3779.769	tw	$v_2 + v_4, E$	5232.90	5207.26	5207.25		
$v_5 + 2v_6, 2E$	3802.36	3794.54	3794.53		tw	$2v_5 + 2v_6, 1E$	5208.26	5216.66	5216.66	5215.206	tw
$3v_3, A_1$	3888.50	3874.44	3874.39	3874.741	tw	$2v_3 + v_5 + v_6, A_1$	5235.96	5221.92	5221.83		
$v_3 + v_5 + v_6, E$	3932.81	3924.55	3924.62			$2v_5 + 2v_6, 2E$	5250.55	5223.41	5223.60		
$v_3 + v_5 + v_6, A_1$	3942.92	3935.47	3935.48	3935.248	tw	$2v_5 + 2v_6, 3E$	5251.59	5237.32	5237.40		
$2v_5 + v_6, 1E$	4094.62	4059.64	4059.68	4058.692	tw	$2v_5 + 2v_6, 2A_1$	5273.35	5262.33	5262.47		
$2v_3 + v_5, E$	4073.87	4066.77	4066.73	4067.859	tw	$v_1 + 2v_6, A_1$	5252.76	5269.72	5269.69		
$2v_5 + v_6, A_1$	4086.05	4081.40	4081.44	4080.942	tw	$v_1 + 2v_6, E$	5255.34	5275.64	5275.68	5276.520	tw
$2v_5 + v_6, 2E$	4106.27	4101.00	4101.02	4102.442	tw	$v_4 + 2v_6, 1E$	5322.46	5313.31	5313.41		
$v_1 + v_6, E$	4095.86	4122.20	4122.10	4122.590	tw	$v_4 + 2v_6, 2E$	5325.50	5313.66	5313.67	5314.220	tw
$v_4 + v_6, A_1$	4167.85	4164.13	4164.18	4163.493	tw	$v_4 + 2v_6, A_1$	5324.58	5325.99	5326.05	5325.677	tw
$v_4 + v_6, E$	4167.39	4170.47	4170.50	4170.363	tw	$3v_3 + v_5, E$	5354.40	5336.62	5336.54		
$v_3 + 2v_5, A_1$	4245.18	4215.16	4214.98	4215.289	tw	$v_3 + 2v_5 + v_6, 1E$	5399.24	5364.60	5364.43		
$v_3 + 2v_5, E$	4246.71	4241.83	4241.92	4241.744	tw	$v_3 + 2v_5 + v_6, A_1$	5390.66	5379.92	5380.03		
$v_1 + v_3, A_1$	4246.97	4279.17	4278.54			$v_3 + 2v_5 + v_6, 2E$	5410.89	5400.18	5400.24		
$v_3 + v_4, E$	4312.35	4312.78	4312.86	4313.422	tw	$v_1 + v_3 + v_6, E$	5403.56	5428.93	5428.32		
$2v_2, A_1$	4326.87	4342.50	4342.27	4344.123	tw	$v_3 + v_4 + v_6, A_1$	5467.09	5458.03	5458.07	5456.630	tw
$3v_5, E$	4403.97	4356.14	4356.27	4356.890	tw	$v_3 + v_4 + v_6, E$	5466.63	5464.37	5464.39	5464.627	tw
$3v_5, A_1$	4407.04	4404.27	4404.27	4404.366	tw	$2v_2 + v_6, E$	5445.62	5467.76	5467.84		
$v_1 + v_5, E$	4391.15	4440.42	4440.71	4439.733	tw	$3v_5 + v_6, 1E$	5542.96	5497.43	5497.71		
$v_4 + v_5, E$	4467.68	4472.68	4472.63	4472.657	tw	$2v_3 + 2v_5, A_1$	5537.28	5498.22	5498.28		
$v_2 + 2v_6, A_1$	4475.88	4480.34	4480.28			$3v_5 + v_6, A_1$	5560.11	5512.94	5512.82		
$v_2 + 2v_6, E$	4478.46	4486.33	4486.34	4486.893	tw	$2v_3 + 2v_5, E$	5538.82	5527.10	5527.11		
$v_4 + v_5, A_1$	4471.12	4486.84	4486.76	4484.820	tw	$3v_5 + v_6, 2E$	5549.99	5535.59	5535.69		
$4v_6, A_1$	4653.71	4619.20	4619.24	4618.447	tw	$3v_5 + v_6, 3E$	5573.29	5564.92	5564.85		
$4v_6, 1E$	4656.29	4625.20	4625.31	4626.909	tw	$v_1 + v_5 + v_6, E$	5539.71	5583.15	5583.55		
$v_1 + 2v_3, A_1$	5542.16	5572.34	5571.13			$v_3 + v_5 + 3v_6, 2E$	6249.40	6221.60	6221.98		
$2v_3 + v_4, E$	5599.08	5593.53	5593.45	5593.699	tw	$v_3 + v_5 + 3v_6, A_1$	6259.52	6231.56	6231.65		
$v_1 + v_5 + v_6, A_1$	5549.82	5594.30	5594.51			$v_2 + 2v_5 + v_6, 1E$	6260.30	6236.08	6236.32	6236.184	tw
$v_4 + v_5 + v_6, A_1$	5613.93	5617.51	5617.45			$v_2 + 2v_3 + v_5, E$	6251.80	6246.67	6246.70		
$v_2 + 3v_6, E$	5617.95	5617.74	5617.98			$v_3 + v_5 + 3v_6, 3E$	6274.79	6251.66	6251.96		

(continued)

Table 12. Continued.

Band	Centre [64]	Centre calc., I	Centre calc., II	Centre exp.	Ref.	Band	Centre [64]	Centre calc., I	Centre calc., II	Centre exp.	Ref.
1	2	3	4	5	6	1	2	3	4	5	6
$v_4 + v_5 + v_6, 1E$	5617.83	5621.09	5621.04			$v_2 + 2v_5 + v_6, A_1$	6251.81	6255.65	6255.90		
$v_4 + v_5 + v_6, 2E$	5624.50	5625.33	5625.26	5627.609	tw	$v_2 + 2v_5 + v_6, 2E$	6272.03	6275.45	6275.65		
$v_2 + 3v_6, A_1$	5623.11	5629.73	5630.11			$4v_3 + v_6, E$	6316.52	6282.61	6282.14		
$2v_2 + v_3, A_1$	5623.16	5635.10	5635.13	5635.975	tw	$v_1 + v_2 + v_6, E$	6266.31	6299.47	6299.64	6298.488	tw
$v_4 + v_5 + v_6, 3E$	5627.48	5641.37	5641.27			$v_2 + v_4 + v_6, A_1$	6341.83	6337.79	6337.95	6337.064	tw
$v_3 + 3v_5, E$	5707.64	5658.39	5658.40			$v_2 + v_4 + v_6, E$	6341.47	6344.13	6344.26		
$v_3 + 3v_5, A_1$	5710.71	5703.00	5703.03			$2v_3 + v_5 + 2v_6, 1E$	6387.26	6346.99	6347.41		
$v_1 + v_3 + v_5, E$	5697.91	5747.02	5746.79			$2v_3 + v_5 + 2v_6, A_1$	6379.73	6352.08	6352.39		
$5v_6, 1E$	5819.09	5763.38	5763.88			$2v_5 + 3v_6, 1E$	6381.60	6364.91	6365.40		
$v_3 + v_4 + v_5, E$	5765.98	5766.80	5766.68	5767.069	tw	$2v_5 + 3v_6, 2E$	6405.24	6365.90	6365.83		
$v_2 + v_3 + 2v_6, A_1$	5776.73	5774.13	5774.30			$2v_5 + 3v_6, 1A_1$	6396.67	6367.40	6367.76		
$5v_6, A_1$	5824.25	5775.37	5776.00			$2v_5 + 3v_6, 2A_1$	6410.40	6373.88	6374.11		
$4v_5, A_1$	5863.95	5775.85	5775.10			$2v_3 + v_5 + 2v_6, 2E$	6399.95	6375.02	6375.12		
$v_2 + v_3 + 2v_6, E$	5779.31	5780.12	5780.36			$5v_3, A_1$	6412.97	6380.48	6379.50		
$v_3 + v_4 + v_5, A_1$	5769.42	5780.96	5780.81			$2v_5 + 3v_6, 3E$	6416.89	6390.36	6390.74		
$5v_6, 2E$	5834.57	5799.35	5800.26			$v_2 + v_3 + 2v_5, A_1$	6424.49	6400.94	6400.88		
$4v_5, 1E$	5841.15	5800.65	5801.04			$v_1 + 3v_6, E$	6411.55	6417.14	6417.34		
$2v_2 + v_5, E$	5792.20	5807.34	5807.39			$2v_5 + 3v_6, 4E$	6442.28	6423.10	6423.52		
$v_1 + 2v_5, A_1$	5839.62	5829.74	5822.83			$v_2 + v_3 + 2v_5, 2E$	6428.03	6426.52	6426.64		
$v_1 + v_4, E$	5877.43	5855.01	5854.93	5855.063	tw	$v_1 + 3v_6, A_1$	6416.71	6428.61	6428.96		
$v_1 + 2v_5, E$	5865.48	5864.26	5864.22	5864.066	tw	$3v_2, A_1$	6396.80	6429.44	6429.58	6428.364	tw
$2v_1, A_1$	5841.96	5903.96	5903.74	5904.157	tw	$v_4 + 3v_6, A_1$	6479.38	6456.32	6456.49		
$4v_5, 2E$	5870.09	5904.62	5905.27			$v_4 + 3v_6, 1E$	6478.92	6461.98	6462.30		
$v_3 + 4v_6, A_1$	5959.12	5914.19	5914.43			$v_4 + 3v_6, 2E$	6483.62	6462.67	6462.81		
$v_2 + 2v_3 + v_6, E$	5925.90	5919.16	5919.30			$v_1 + v_2 + v_3, A_1$	6433.09	6467.13	6467.58		
$v_3 + 4v_6, 1E$	5961.70	5920.19	5920.49			$3v_3 + v_5 + v_6, E$	6505.40	6477.36	6477.31		
$v_4 + 2v_5, A_1$	5920.36	5925.52	5925.28			$v_4 + 3v_6, 3E$	6485.00	6481.00	6481.26		
$v_2 + v_5 + 2v_6, A_1$	5928.87	5935.11	5935.44			$3v_3 + v_5 + v_6, A_1$	6515.51	6487.03	6486.98		
$v_3 + 4v_6, 2E$	5969.44	5938.17	5938.68			$v_2 + v_3 + v_4, E$	6501.98	6496.87	6496.90		
$v_2 + v_5 + 2v_6, 1E$	5936.40	5939.23	5939.46			$v_3 + 2v_5 + 2v_6, 1A_1$	6552.60	6509.74	6509.58		
$v_4 + 2v_5, 1E$	5922.27	5940.46	5940.61	5940.240	tw	$v_3 + 2v_5 + 2v_6, 1E$	6536.49	6514.18	6514.18		
$v_4 + 2v_5, 2E$	5927.25	5953.85	5953.54			$v_3 + 2v_5 + 2v_6, 2E$	6554.13	6518.84	6519.11		
$v_2 + v_5 + 2v_6, 2E$	5949.10	5954.77	5955.06			$v_3 + 2v_5 + 2v_6, 3E$	6555.18	6533.45	6533.56		
$2v_4, A_1$	5935.55	5980.41	5980.42	5980.416	tw	$v_2 + 3v_5, E$	6588.67	6545.98	6546.27		
$2v_4, E$	5986.09	6022.14	6022.08	6022.214	tw	$v_3 + 2v_5 + 2v_6, 2A_1$	6576.94	6559.06	6559.21		
$2v_3 + 3v_6, E$	6089.62	6047.35	6047.62			$v_1 + v_3 + 2v_6, A_1$	6559.46	6573.62	6573.10		
$v_2 + 3v_3, A_1$	6063.04	6051.50	6051.36			$v_1 + v_3 + 2v_6, E$	6562.04	6579.53	6579.08		
$2v_3 + 3v_6, A_1$	6094.78	6061.00	6061.35			$2v_2 + 2v_6, A_1$	6563.76	6587.87	6588.30		
$v_5 + 4v_6, 1A_1$	6101.93	6069.67	6069.99			$v_2 + 3v_5, A_1$	6591.74	6592.69	6592.79		
$v_5 + 4v_6, 1E$	6099.56	6075.89	6076.09			$2v_2 + 2v_6, E$	6566.34	6593.86	6593.76		
$v_5 + 4v_6, 2E$	6109.47	6075.94	6076.56			$4v_3 + v_5, E$	6621.46	6594.24	6594.36		
$v_5 + 4v_6, 3E$	6122.16	6085.99	6086.48			$v_3 + v_4 + 2v_6, 1E$	6620.68	6604.12	6604.23		
$v_2 + v_3 + v_5 + v_6, E$	6095.18	6095.08	6095.28			$v_3 + v_4 + 2v_6, 2E$	6623.72	6604.47	6604.48		
$v_2 + v_3 + v_5 + v_6, A_1$	6105.30	6106.19	6106.32			$v_3 + v_4 + 2v_6, A_1$	6622.80	6616.80	6616.86		
$v_5 + 4v_6, 2A_1$	6140.01	6114.58	6115.21			$v_1 + v_2 + v_5, E$	6580.67	6631.77	6632.23		
$3v_3 + 2v_6, A_1$	6207.88	6170.88	6170.75			$2v_3 + 2v_5 + v_6, 1E$	6690.34	6636.08	6636.49		
$3v_3 + 2v_6, E$	6210.46	6177.08	6177.01			$2v_3 + 2v_5 + v_6, A_1$	6681.76	6636.80	6637.41		
$v_3 + v_5 + 3v_6, 1E$	6244.45	6220.01	6220.21			$3v_5 + 2v_6, 1E$	6680.73	6650.99	6651.19		
$v_2 + v_4 + v_5, E$	6660.69	6660.50	6660.46			$4v_5 + v_6, 3E$	7022.66	6985.72	6985.86		
$3v_5 + 2v_6, 1A_1$	6697.88	6664.24	6664.26			$v_1 + v_4 + v_6, A_1$	7027.73	6995.48	6995.56		
$3v_5 + 2v_6, 2E$	6705.41	6665.11	6665.18			$v_1 + v_4 + v_6, E$	7027.27	7001.80	7001.86		
$3v_5 + 2v_6, 3E$	6718.10	6667.74	6667.76			$4v_5 + v_6, 2A_1$	7037.38	7024.77	7024.85		
$v_2 + v_4 + v_5, A_1$	6664.13	6674.67	6674.59			$v_1 + 2v_3 + v_5, E$	6991.18	7032.76	7032.24		
$2v_3 + 2v_5 + v_6, 2E$	6701.99	6681.82	6681.84			$v_1 + 2v_5 + v_6, A_1$	6980.65	7037.53	7038.38		
$3v_5 + 2v_6, 2A_1$	6708.48	6691.49	6691.69			$2v_3 + v_4 + v_5, E$	7050.77	7041.40	7041.23		

(continued)

Table 12. Continued.

Band	Centre [64]	Centre calc., I	Centre calc., II	Centre exp.	Ref.	Band	Centre [64]	Centre calc., I	Centre calc., II	Centre exp.	Ref.
1	2	3	4	5	6	1	2	3	4	5	6
$v_1 + 2v_3 + v_6, E$	6697.76	6715.55	6714.73			$v_1 + 2v_5 + v_6, 1E$	6989.23	7047.67	7047.65		
$3v_5 + 2v_6, 4E$	6741.40	6726.03	6726.30			$v_2 + 2v_3 + 2v_6, A_1$	7064.12	7050.15	7050.49		
$v_1 + v_5 + 2v_6, A_1$	6690.14	6727.18	6727.79			$v_3 + 5v_6, 1E$	7123.47	7055.28	7055.99		
$v_1 + v_5 + 2v_6, 1E$	6697.67	6732.00	6732.41			$v_2 + 2v_3 + 2v_6, E$	7066.70	7055.93	7056.36		
$2v_3 + v_4 + v_6, A_1$	6752.83	6732.82	6732.84			$2v_3 + v_4 + v_5, A_1$	7054.22	7056.74	7056.48		
$2v_3 + v_4 + v_6, E$	6752.37	6739.97	6739.93			$v_4 + 2v_5 + v_6, 1E$	7057.54	7060.49	7060.33		
$v_2 + 4v_6, A_1$	6759.34	6747.30	6747.98			$v_1 + 2v_5 + v_6, 2E$	7000.87	7061.02	7061.35		
$v_1 + v_5 + 2v_6, 2E$	6710.36	6749.24	6749.49			$v_3 + 5v_6, A_1$	7128.63	7067.27	7068.12		
$v_2 + 4v_6, 1E$	6761.92	6753.30	6754.04			$v_2 + v_5 + 3v_6, 1E$	7064.49	7067.50	7068.05		
$2v_2 + v_3 + v_6, E$	6741.00	6757.28	6757.62			$v_2 + v_5 + 3v_6, 2E$	7069.44	7068.66	7069.43		
$v_4 + v_5 + 2v_6, 1E$	6762.04	6760.91	6760.90			$v_4 + 2v_5 + v_6, 2E$	7064.88	7076.66	7076.38		
$v_4 + v_5 + 2v_6, 2E$	6766.40	6763.16	6763.23			$v_3 + 4v_5, A_1$	7144.43	7077.40	7076.66		
$v_4 + v_5 + 2v_6, 3E$	6770.03	6764.65	6764.72			$v_2 + v_5 + 3v_6, A_1$	7079.56	7077.84	7078.35		
$v_2 + 4v_6, 2E$	6769.66	6771.28	6772.23			$v_4 + 2v_5 + v_6, 1A_1$	7070.02	7079.38	7079.61		
$v_4 + v_5 + 2v_6, 1A_1$	6773.48	6772.12	6772.12			$v_4 + 2v_5 + v_6, 3E$	7069.56	7082.48	7082.26		
$3v_3 + 2v_5, A_1$	6815.89	6772.21	6771.88			$v_4 + 2v_5 + v_6, 4E$	7078.22	7085.60	7085.81		
$v_4 + v_5 + 2v_6, 2A_1$	6783.19	6775.21	6775.14			$v_3 + 5v_6, 2E$	7138.95	7091.25	7092.37		
$3v_3 + 2v_5, E$	6817.42	6791.00	6791.11			$2v_2 + v_3 + v_5, E$	7086.63	7097.09	7097.34		
$v_4 + v_5 + 2v_6, 4E$	6785.71	6798.30	6798.24			$v_2 + v_5 + 3v_6, 3E$	7094.83	7097.93	7097.53		
$v_3 + 3v_5 + v_6, 1E$	6845.60	6802.44	6802.25			$v_3 + 4v_5, 1E$	7167.19	7099.99	7100.20		
$v_3 + 3v_5 + v_6, A_1$	6862.76	6810.87	6810.74			$v_4 + 2v_5 + v_6, 2A_1$	7084.65	7110.02	7109.69		
$v_3 + 3v_5 + v_6, 2E$	6852.64	6831.24	6831.37			$2v_4 + v_6, 1E$	7083.52	7124.34	7124.51		
$v_1 + 3v_3, A_1$	6823.88	6852.03	6849.83			$v_3 + 2v_4, A_1$	7149.89	7132.12	7131.50		
$3v_3 + v_4, E$	6872.33	6859.21	6858.78			$v_1 + v_3 + v_4, 1E$	7176.88	7156.01	7155.27		
$v_3 + 3v_5 + v_6, 3E$	6875.94	6861.54	6861.59			$2v_4 + v_6, 2E$	7134.53	7157.93	7157.89		
$v_1 + v_3 + v_5 + v_6, E$	6845.47	6886.88	6886.76			$v_3 + 4v_5, 2E$	7171.80	7160.13	7160.06		
$6v_6, 1A_1$	6983.74	6897.01	6898.21			$2v_4 + v_6, A_1$	7133.61	7170.61	7170.53		
$v_1 + v_3 + v_5 + v_6, A_1$	6855.58	6898.60	6898.30			$v_2 + 3v_3 + v_6, E$	7200.80	7184.50	7184.52		
$6v_6, 1E$	6986.32	6903.10	6904.28			$2v_3 + 4v_6, A_1$	7251.01	7190.03	7190.52		
$v_2 + v_3 + 3v_6, E$	6917.82	6908.46	6908.93			$2v_3 + 4v_6, 1E$	7253.59	7195.16	7195.80		
$v_3 + v_4 + v_5 + v_6, A_1$	6911.21	6908.53	6908.43			$5v_5, 1E$	7321.00	7199.91	7199.88		
$2v_2 + 2v_3, A_1$	6906.04	6910.91	6911.09			$v_1 + v_3 + 2v_5, A_1$	7165.66	7204.53	7204.06		
$v_3 + v_4 + v_5 + v_6, 1E$	6915.11	6912.41	6912.30			$v_1 + v_3 + 2v_5, E$	7145.97	7208.40	7208.51		
$4v_5 + v_6, 1E$	6996.93	6915.22	6915.09			$v_5 + 5v_6, 1E$	7260.77	7206.11	7207.19		
$v_3 + v_4 + v_5 + v_6, 2E$	6921.78	6916.36	6916.24			$v_5 + 5v_6, 2E$	7265.73	7207.94	7208.69		
$v_2 + v_3 + 3v_6, A_1$	6922.98	6920.45	6921.06			$v_3 + v_4 + 2v_5, A_1$	7216.71	7216.77	7216.43		
$6v_6, 2E$	6994.06	6920.99	6922.46			$2v_3 + 4v_6, 2E$	7261.33	7217.83	7218.35		
$2v_2 + v_5 + v_6, E$	6901.98	6922.76	6923.19			$v_5 + 5v_6, 1A_1$	7260.98	7218.13	7218.85		
$4v_5 + v_6, 1A_1$	7002.43	6932.22	6932.82			$v_5 + 5v_6, 2A_1$	7275.84	7222.20	7223.55		
$v_3 + v_4 + v_5 + v_6, 3E$	6924.77	6932.72	6932.56			$v_2 + v_3 + v_5 + 2v_6, A_1$	7227.81	7226.05	7226.55		
$2v_2 + v_5 + v_6, A_1$	6912.09	6933.58	6933.93			$v_2 + v_3 + v_5 + 2v_6, 1E$	7235.34	7230.34	7230.74		
$2v_3 + 3v_5, E$	6997.80	6940.78	6940.64			$v_3 + v_4 + 2v_5, 1E$	7218.61	7233.30	7233.25		
$6v_6, 2A_1$	7006.96	6950.97	6952.78			$v_5 + 5v_6, 3E$	7291.11	7237.35	7238.36		
$4v_5 + v_6, 2E$	7011.01	6956.58	6956.46			$2v_2 + 2v_5, A_1$	7253.16	7240.76	7241.03		
$2v_1 + v_6, E$	6994.12	6973.88	6967.38			$5v_5, A_1$	7324.07	7242.41	7243.04		
$2v_3 + 3v_5, A_1$	7000.87	6984.90	6984.83			$v_3 + v_4 + 2v_5, 2E$	7223.59	7245.10	7244.68		
$v_2 + v_3 + v_5 + 2v_6, 2E$	7248.03	7246.40	7246.83			$2v_3 + v_5 + 3v_6, 3E$	7565.68	7530.35	7530.67		
$2v_2 + 2v_5, E$	7254.70	7268.16	7268.44			$v_2 + v_3 + 2v_5 + v_6, 1E$	7558.29	7532.84	7532.97		
$v_5 + 5v_6, 4E$	7311.54	7270.48	7271.78			$2v_5 + 4v_6, 3A_1$	7585.02	7545.40	7546.08		
$2v_1 + v_5, E$	7276.02	7278.79	7272.77			$v_2 + v_3 + 2v_5 + v_6, A_1$	7549.72	7546.80	7547.17		
$2v_1 + v_3, A_1$	7226.52	7284.26	7283.59			$v_1 + 4v_6, A_1$	7569.51	7556.01	7556.61		
$v_1 + v_4 + v_5, E$	7314.15	7292.20	7292.25			$v_1 + 4v_6, 1E$	7572.09	7561.89	7562.57		
$v_1 + 2v_2, A_1$	7261.46	7303.55	7303.82			$v_2 + v_3 + 2v_5 + v_6, 2E$	7569.94	7567.26	7567.55		
$v_2 + 4v_3, A_1$	7325.30	7304.82	7304.36			$v_1 + 4v_6, 2E$	7579.83	7579.77	7580.65		
$v_1 + v_4 + v_5, A_1$	7317.59	7306.37	7306.37			$2v_5 + 4v_6, 5E$	7612.98	7581.91	7582.83		

(continued)

Table 12. Continued.

Band	Centre [64]	Centre calc., I	Centre calc., II	Centre exp.	Ref.	Band	Centre [64]	Centre calc., I	Centre calc., II	Centre exp.	Ref.
1	2	3	4	5	6	1	2	3	4	5	6
$v_3 + 2v_4, E$	7277.07	7308.76	7308.52			$v_4 + 4v_6, 1E$	7635.04	7597.14	7597.67		
$3v_3 + 3v_6, E$	7368.94	7315.85	7315.90			$v_4 + 4v_6, 2E$	7638.08	7597.49	7597.93		
$5v_5, 2E$	7330.21	7320.21	7320.09			$v_1 + v_2 + v_3 + v_6, E$	7567.42	7599.14	7598.85		
$3v_3 + 3v_6, A_1$	7374.10	7330.45	7330.51			$v_4 + 4v_6, 1A_1$	7637.16	7608.79	7609.54		
$2v_2 + v_4, E$	7342.32	7342.53	7342.72			$v_4 + 4v_6, 2A_1$	7646.28	7609.82	7610.31		
$v_1 + 3v_5, E$	7285.17	7359.80	7359.05			$6v_3, A_1$	7654.76	7610.51	7608.78		
$v_3 + v_5 + 4v_6, 1A_1$	7405.34	7360.99	7361.52			$3v_3 + v_5 + 2v_6, A_1$	7658.11	7618.98	7619.10		
$v_1 + 3v_5, A_1$	7288.24	7363.48	7364.47			$3v_3 + v_5 + 2v_6, 1E$	7665.64	7622.82	7622.85		
$v_3 + v_5 + 4v_6, 1E$	7402.97	7364.46	7364.94			$v_2 + v_3 + v_4 + v_6, A_1$	7634.46	7624.32	7624.52		
$v_2 + 2v_5 + 2v_6, 1A_1$	7416.85	7364.49	7365.05			$v_2 + v_3 + v_4 + v_6, E$	7633.99	7630.66	7630.84		
$v_2 + 2v_3 + v_5 + v_6, E$	7381.52	7367.24	7367.79			$v_4 + 4v_6, 3E$	7644.44	7634.15	7634.82		
$v_3 + v_5 + 4v_6, 2E$	7412.87	7368.02	7368.84			$3v_3 + v_5 + 2v_6, 2E$	7678.34	7638.54	7638.64		
$v_4 + 3v_5, 1E$	7370.12	7374.31	7373.87			$v_3 + 2v_5 + 3v_6, 1E$	7684.07	7654.03	7654.04		
$v_2 + 2v_5 + 2v_6, 1E$	7376.40	7376.39	7376.72			$v_3 + 2v_5 + 3v_6, 2E$	7707.71	7657.25	7657.84		
$v_2 + 2v_5 + 2v_6, 2E$	7394.05	7379.85	7380.46			$v_3 + 2v_5 + 3v_6, 1A_1$	7699.13	7662.02	7662.44		
$v_3 + v_5 + 4v_6, 3E$	7425.56	7380.62	7381.11			$v_3 + 2v_5 + 3v_6, 2A_1$	7712.86	7667.36	7667.59		
$v_2 + 2v_3 + v_5 + v_6, A_1$	7391.63	7384.62	7383.32			$v_2 + 3v_5 + v_6, 1E$	7705.40	7669.44	7670.09		
$v_4 + 3v_5, 2E$	7370.48	7389.54	7389.90			$v_2 + 2v_3 + 2v_5, A_1$	7711.89	7673.24	7673.73		
$v_2 + 2v_5 + 2v_6, 3E$	7395.09	7394.15	7394.61			$v_3 + 2v_5 + 3v_6, 3E$	7719.36	7686.00	7686.29		
$v_4 + 3v_5, A_1$	7373.93	7403.71	7404.02			$v_2 + 3v_5 + v_6, A_1$	7722.55	7688.05	7688.05		
$v_3 + v_5 + 4v_6, 2A_1$	7443.42	7405.46	7406.31			$v_2 + 2v_3 + 2v_5, E$	7713.42	7704.12	7704.24		
$v_4 + 3v_5, 3E$	7380.44	7416.81	7416.24			$v_2 + 3v_5 + v_6, 2E$	7712.44	7706.20	7706.62		
$v_2 + 2v_5 + 2v_6, 2A_1$	7392.51	7419.07	7419.61			$v_3 + 2v_5 + 3v_6, 4E$	7744.74	7716.73	7718.28		
$4v_3 + 2v_6, A_1$	7474.69	7424.74	7424.30			$v_1 + v_3 + 3v_6, E$	7717.10	7718.26	7716.86		
$v_1 + v_2 + 2v_6, A_1$	7401.08	7429.26	7429.73			$v_1 + v_3 + 3v_6, A_1$	7722.26	7729.64	7729.50		
$4v_3 + 2v_6, E$	7477.27	7431.00	7430.62			$4v_3 + v_5 + v_6, E$	7771.27	7731.58	7731.17		
$v_1 + v_2 + 2v_6, E$	7403.66	7435.18	7435.72			$v_2 + 3v_5 + v_6, 3E$	7735.73	7735.80	7736.16		
$2v_4 + v_5, 1E$	7378.38	7441.28	7441.74			$4v_3 + v_5 + v_6, A_1$	7781.38	7741.91	7741.47		
$2v_4 + v_5, A_1$	7425.48	7463.77	7463.37			$v_3 + v_4 + 3v_6, A_1$	7776.47	7744.04	7744.23		
$v_2 + v_4 + 2v_6, 1E$	7474.27	7469.15	7469.59			$v_3 + v_4 + 3v_6, 1E$	7776.01	7749.70	7750.04		
$v_2 + v_4 + 2v_6, 2E$	7477.31	7469.50	7469.84			$v_3 + v_4 + 3v_6, 2E$	7780.71	7750.38	7750.55		
$v_2 + v_4 + 2v_6, A_1$	7476.39	7481.83	7482.23			$v_1 + v_2 + 2v_3, A_1$	7721.57	7752.36	7751.48		
$2v_5 + 4v_6, 1A_1$	7532.09	7489.43	7490.18			$v_1 + v_2 + v_5 + v_6, E$	7706.96	7756.75	7757.54		
$2v_3 + v_5 + 3v_6, 1E$	7535.35	7491.82	7492.48			$v_3 + v_4 + 3v_6, 3E$	7782.09	7768.72	7768.99		
$2v_4 + v_5, 2E$	7432.37	7492.10	7491.62			$v_1 + v_2 + v_5 + v_6, A_1$	7717.07	7768.73	7769.15		
$2v_3 + v_5 + 3v_6, 2E$	7540.30	7495.73	7496.41			$v_2 + 2v_3 + v_4, E$	7782.00	7770.02	7769.96		
$2v_5 + 4v_6, 1E$	7544.57	7502.12	7502.60			$2v_3 + 2v_5 + 2v_6, 1E$	7826.44	7777.67	7778.47		
$2v_5 + 4v_6, 2A_1$	7560.68	7504.56	7505.56			$3v_5 + 3v_6, 1E$	7845.45	7780.20	7781.15		
$2v_5 + 4v_6, 2E$	7562.21	7507.77	7508.49			$2v_3 + 2v_5 + 2v_6, 1A_1$	7842.55	7780.54	7781.05		
$v_2 + 3v_3 + v_5, E$	7525.62	7509.70	7509.69			$v_2 + v_4 + v_5 + v_6, A_1$	7784.68	7787.52	7787.70		
$2v_3 + v_5 + 3v_6, A_1$	7550.41	7511.62	7511.75			$v_2 + v_4 + v_5 + v_6, 1E$	7788.58	7791.28	7791.44		
$2v_5 + 4v_6, 3E$	7563.26	7518.46	7519.20			$3v_5 + 3v_6, 2E$	7847.54	7793.47	7793.72		
$2v_5 + 4v_6, 4E$	7571.00	7521.02	7521.59			$v_2 + v_4 + v_5 + v_6, 2E$	7795.25	7795.34	7795.50		
$5v_3 + v_6, E$	7570.82	7524.58	7523.59			$2v_3 + 2v_5 + 2v_6, 2E$	7844.08	7798.12	7798.43		
$3v_5 + 3v_6, 1A_1$	7820.28	7799.38	7800.09			$v_3 + v_4 + v_5 + 2v_6, 1E$	8058.19	8049.14	8049.09		
$3v_5 + 3v_6, 2A_1$	7862.60	7799.82	7799.84			$v_3 + v_4 + v_5 + 2v_6, 2E$	8062.55	8051.11	8051.14		
$v_2 + v_4 + v_5 + v_6, 3E$	7798.24	7811.05	7811.19			$v_3 + v_4 + v_5 + 2v_6, 3E$	8066.18	8052.59	8052.62		
$2v_3 + 2v_5 + 2v_6, 3E$	7845.13	7811.55	7811.79			$4v_5 + 2v_6, 1A_1$	8125.54	8054.29	8054.33		
$3v_5 + 3v_6, 3E$	7852.49	7815.13	7815.58			$4v_5 + 2v_6, E$	8082.35	8054.63	8053.79		
$3v_5 + 3v_6, 4E$	7875.79	7817.99	7818.44			$v_3 + v_4 + v_5 + 2v_6, 1A_1$	8069.62	8058.46	8058.48		
$5v_3 + v_5, E$	7874.82	7836.54	7835.47			$4v_5 + 2v_6, 1E$	8141.16	8060.28	8060.39		
$2v_3 + 2v_5 + 2v_6, 2A_1$	7866.89	7837.79	7837.91			$v_3 + v_4 + v_5 + 2v_6, 2A_1$	8079.33	8063.26	8063.15		
$v_2 + v_3 + 3v_5, E$	7885.63	7840.63	7840.85			$4v_5 + 2v_6, 2E$	8158.80	8064.97	8065.90		
$3v_5 + 3v_6, 5E$	7877.88	7846.36	7846.82			$4v_5 + 2v_6, 3E$	8159.85	8077.70	8078.58		
$v_1 + 2v_3 + 2v_6, A_1$	7852.50	7858.66	7857.90			$v_3 + v_4 + v_5 + 2v_6, 4E$	8081.86	8085.18	8085.13		

(continued)

Table 12. Continued.

Band	Centre [64]	Centre calc., I	Centre calc., II	Centre exp.	Ref.	Band	Centre [64]	Centre calc., I	Centre calc., II	Centre exp.	Ref.
1	2	3	4	5	6	1	2	3	4	5	6
$v_1 + v_5 + 3v_6, 1E$	7842.32	7862.88	7862.75			$v_1 + v_2 + 2v_5, A_1$	8025.80	8090.96	8091.01		
$v_1 + v_5 + 3v_6, 2E$	7847.28	7869.80	7870.83			$v_1 + v_2 + 2v_5, E$	8027.34	8092.37	8093.31		
$v_1 + 2v_3 + 2v_6, E$	7855.08	7871.22	7871.24			$2v_3 + 3v_5 + v_6, 1E$	8134.61	8101.25	8101.86		
$2v_3 + v_4 + 2v_6, 1E$	7905.26	7878.40	7878.40			$4v_5 + 2v_6, 2A_1$	8157.27	8102.42	8103.38		
$2v_3 + v_4 + 2v_6, 2E$	7908.30	7878.63	7878.55			$4v_5 + 2v_6, 3A_1$	8181.61	8108.02	8108.46		
$v_1 + v_5 + 3v_6, A_1$	7857.39	7880.58	7881.01			$4v_3 + v_4, E$	8131.88	8109.55	8108.59		
$v_2 + v_3 + 3v_5, A_1$	7888.71	7884.06	7884.22			$v_2 + v_4 + 2v_5, A_1$	8110.05	8109.70	8109.60		
$3v_5 + 3v_6, 3A_1$	7911.28	7886.61	7887.23			$2v_3 + 3v_5 + v_6, A_1$	8151.77	8110.61	8111.22		
$2v_3 + v_4 + 2v_6, A_1$	7907.38	7889.88	7889.91			$2v_3 + 3v_5 + v_6, 2E$	8141.65	8111.55	8111.53		
$v_1 + v_5 + 3v_6, 3E$	7872.66	7899.55	7900.43			$2v_1 + 2v_6, A_1$	8145.43	8111.67	8104.82		
$v_4 + v_5 + 3v_6, 1A_1$	7917.33	7900.95	7901.09			$2v_1 + 2v_6, E$	8148.01	8117.67	8110.87		
$v_4 + v_5 + 3v_6, 2A_1$	7945.70	7903.46	7903.83			$v_1 + 4v_3, A_1$	8091.89	8119.83	8116.26		
$v_4 + v_5 + 3v_6, 1E$	7911.92	7903.66	7903.86			$v_2 + v_4 + 2v_5, 1E$	8111.96	8125.21	8125.50		
$v_4 + v_5 + 3v_6, 2E$	7921.24	7907.17	7907.39			$v_1 + v_4 + 2v_6, 1E$	8176.73	8136.78	8137.11		
$v_4 + v_5 + 3v_6, 3E$	7927.91	7908.31	7908.66			$v_1 + v_4 + 2v_6, 2E$	8179.77	8137.13	8137.38		
$3v_3 + 2v_5 + v_6, 1E$	7967.78	7913.41	7913.21			$v_2 + v_4 + 2v_5, 2E$	8116.93	8138.03	8137.84		
$v_4 + v_5 + 3v_6, 4E$	7930.89	7918.56	7918.93			$4v_5 + 2v_6, 4E$	8163.41	8139.47	8139.87		
$v_4 + v_5 + 3v_6, 5E$	7943.64	7922.87	7923.08			$2v_3 + 3v_5 + v_6, 3E$	8164.95	8139.64	8139.64		
$3v_3 + 2v_5 + v_6, A_1$	7959.20	7923.05	7923.24			$v_1 + v_4 + 2v_6, A_1$	8178.84	8149.41	8149.70		
$v_1 + v_2 + v_3 + v_5, E$	7880.72	7931.24	7931.23			$v_1 + 2v_3 + v_5 + v_6, E$	8137.56	8154.27	8152.73		
$3v_3 + 2v_5 + v_6, 2E$	7979.42	7938.34	7938.60			$v_1 + 2v_3 + v_5 + v_6, A_1$	8147.67	8163.63	8162.10		
$v_3 + 3v_5 + 2v_6, 1A_1$	7999.40	7941.01	7941.10			$v_2 + 2v_4, A_1$	8133.54	8168.88	8169.24		
$v_2 + v_3 + v_4 + v_5, E$	7952.29	7947.25	7947.20			$v_1 + 2v_5 + 2v_6, 1E$	8121.90	8171.09	8172.27		
$v_4 + v_5 + 3v_6, 3A_1$	7916.74	7951.35	7951.64			$2v_3 + v_4 + v_5 + v_6, A_1$	8194.85	8182.30	8182.08		
$v_3 + 3v_5 + 2v_6, 1E$	7982.25	7951.41	7951.23			$4v_5 + 2v_6, 5E$	8206.44	8182.91	8183.41		
$v_3 + 3v_5 + 2v_6, 2E$	8006.93	7959.44	7959.53			$v_1 + 2v_5 + 2v_6, 1A_1$	8138.01	8183.12	8183.24		
$v_3 + 3v_5 + 2v_6, 3E$	8019.63	7960.30	7960.67			$v_1 + 2v_5 + 2v_6, 2E$	8139.54	8183.82	8184.94		
$v_2 + v_3 + v_4 + v_5, A_1$	7955.72	7961.42	7961.33			$2v_3 + v_4 + v_5 + v_6, 1E$	8198.75	8186.31	8186.06		
$v_2 + 4v_5, A_1$	8045.33	7963.00	7962.72			$v_1 + 2v_5 + 2v_6, 3E$	8140.59	8189.11	8189.30		
$v_3 + 3v_5 + 2v_6, 2A_1$	8010.01	7985.00	7985.19			$2v_3 + v_4 + v_5 + v_6, 2E$	8205.42	8190.41	8190.16		
$v_2 + 4v_5, 1E$	8046.86	7986.82	7987.48			$v_4 + 2v_5 + 2v_6, 1E$	8196.48	8196.29	8196.34		
$v_1 + 3v_3 + v_6, E$	7978.29	7994.80	7992.76			$v_4 + 2v_5 + 2v_6, 1A_1$	8204.29	8204.16	8204.10		
$3v_3 + v_4 + v_6, A_1$	8024.89	7997.54	7997.13			$3v_3 + 3v_5, E$	8274.30	8205.33	8205.24		
$3v_3 + v_4 + v_6, E$	8024.43	8003.95	8003.51			$v_2 + 2v_4, E$	8184.09	8205.72	8205.70		
$2v_1 + v_2, A_1$	8032.96	8018.11	8011.18			$2v_3 + v_4 + v_5 + v_6, 3E$	8208.40	8206.53	8206.27		
$v_3 + 3v_5 + 2v_6, 4E$	8042.92	8020.46	8020.66			$v_1 + 2v_5 + 2v_6, 2A_1$	8162.35	8208.54	8209.74		
$v_1 + v_3 + v_5 + 2v_6, A_1$	7994.75	8027.56	8027.69			$v_4 + 2v_5 + 2v_6, 2A_1$	8214.59	8211.94	8211.95		
$v_1 + v_3 + v_5 + 2v_6, 1E$	8002.28	8032.18	8032.15			$v_4 + 2v_5 + 2v_6, 2E$	8216.49	8218.94	8219.38		
$4v_3 + 2v_5, A_1$	8080.81	8034.21	8033.11			$v_4 + 2v_5 + 2v_6, 3E$	8219.53	8219.65	8219.94		
$v_1 + v_2 + v_4, E$	8071.93	8042.95	8043.14			$v_3 + 4v_5 + v_6, 1E$	8297.51	8221.82	8221.14		
$v_1 + v_3 + v_5 + 2v_6, 2E$	8014.97	8048.38	8048.34			$v_4 + 2v_5 + 2v_6, 4E$	8221.47	8223.04	8223.06		
$v_2 + 4v_5, 2E$	8051.47	8049.04	8049.21			$v_3 + 4v_5 + v_6, 1A_1$	8303.01	8227.19	8227.65		
$v_4 + 2v_5 + 2v_6, 3A_1$	8218.61	8231.30	8231.72			$v_4 + 3v_5 + v_6, 1E$	8498.13	8499.42	8499.15		
$v_4 + 2v_5 + 2v_6, 5E$	8237.85	8231.82	8231.72			$v_1 + 3v_5 + v_6, A_1$	8435.71	8502.45	8501.81		
$v_3 + 4v_5 + v_6, 2E$	8311.59	8250.95	8251.09			$2v_3 + v_4 + 2v_5, 1E$	8501.30	8509.12	8508.80		
$3v_3 + 3v_5, A_1$	8277.37	8252.78	8252.41			$v_1 + 3v_5 + v_6, 3E$	8448.89	8517.14	8518.12		
$2v_4 + 2v_6, 1A_1$	8230.68	8263.10	8263.50			$2v_3 + v_4 + 2v_5, 2E$	8506.28	8519.24	8519.68		
$v_4 + 2v_5 + 2v_6, 6E$	8243.82	8263.20	8263.14			$v_4 + 3v_5 + v_6, 1A_1$	8508.61	8522.48	8522.23		
$2v_4 + 2v_6, 1E$	8233.26	8269.10	8269.56			$v_4 + 3v_5 + v_6, 2A_1$	8508.91	8525.22	8525.66		
$v_3 + 2v_4 + v_6, 1E$	8373.36	8272.50	8264.39			$v_4 + 3v_5 + v_6, 2E$	8512.51	8529.09	8529.53		
$v_3 + 4v_5 + v_6, 3E$	8323.24	8278.51	8278.63			$v_4 + 3v_5 + v_6, 3E$	8519.18	8533.36	8533.77		
$v_1 + v_3 + v_4 + v_6, A_1$	8326.02	8293.08	8292.51			$v_4 + 3v_5 + v_6, 3A_1$	8528.92	8535.58	8535.20		
$2v_4 + 2v_6, 2A_1$	8284.72	8294.56	8294.66			$v_3 + 5v_5, A_1$	8623.71	8538.81	8539.21		
$v_1 + v_3 + v_4 + v_6, E$	8325.56	8298.75	8298.18			$v_4 + 3v_5 + v_6, 4E$	8522.16	8548.93	8549.38		
$2v_4 + 2v_6, 2E$	8281.22	8301.24	8301.24			$v_4 + 3v_5 + v_6, 5E$	8538.79	8570.93	8570.51		

(continued)

Table 12. Continued.

Band	Centre [64]	Centre calc., I	Centre calc., II	Centre exp.	Ref.	Band	Centre [64]	Centre calc., I	Centre calc., II	Centre exp.	Ref.
1	2	3	4	5	6	1	2	3	4	5	6
$3\nu_3 + \nu_4 + \nu_5, E$	8321.90	8307.69	8306.98			$2\nu_1 + 2\nu_3, A_1$	8444.13	8571.84	8570.30		
$\nu_1 + 3\nu_3 + \nu_5, E$	8270.76	8312.25	8310.50			$2\nu_4 + \nu_5 + \nu_6, 1E$	8517.18	8575.41	8576.13		
$\nu_3 + 4\nu_5 + \nu_6, 2A_1$	8337.96	8315.95	8316.11			$\nu_3 + 2\nu_4 + \nu_5, 1E$	8667.27	8578.98	8571.51		
$2\nu_4 + 2\nu_6, 3E$	8282.88	8319.92	8319.94			$2\nu_3 + 2\nu_4, E$	8554.39	8579.03	8578.48		
$3\nu_3 + \nu_4 + \nu_5, A_1$	8325.34	8321.40	8320.67			$6\nu_5, 1A_1$	8728.28	8585.24	8573.74		
$5\nu_5 + \nu_6, 1E$	8451.85	8331.50	8331.90			$2\nu_4 + \nu_5 + \nu_6, 1A_1$	8527.29	8587.22	8587.50		
$\nu_1 + \nu_3 + 2\nu_5 + \nu_6, A_1$	8284.32	8338.41	8338.72			$\nu_1 + \nu_3 + \nu_4 + \nu_5, E$	8611.50	8589.29	8588.68		
$5\nu_5 + \nu_6, 1A_1$	8447.89	8340.97	8341.33			$2\nu_4 + \nu_5 + \nu_6, 2E$	8563.82	8599.83	8598.78		
$\nu_1 + \nu_3 + 2\nu_5 + \nu_6, 1E$	8292.89	8344.87	8344.53			$2\nu_4 + \nu_5 + \nu_6, 3E$	8574.86	8602.39	8602.05		
$\nu_3 + \nu_4 + 2\nu_5 + \nu_6, 1E$	8352.75	8348.65	8348.41			$\nu_1 + \nu_3 + \nu_4 + \nu_5, A_1$	8614.94	8603.46	8602.80		
$\nu_1 + \nu_3 + 2\nu_5 + \nu_6, 2E$	8304.54	8359.49	8359.59			$\nu_1 + 2\nu_4, A_1$	8773.49	8609.67	8608.92		
$\nu_3 + \nu_4 + 2\nu_5 + \nu_6, 2E$	8630.09	8362.67	8362.38			$\nu_3 + 5\nu_5, 2E$	8629.85	8613.22	8613.03		
$5\nu_5 + \nu_6, 2E$	8458.90	8364.15	8365.07			$2\nu_4 + \nu_5 + \nu_6, 2A_1$	8571.63	8618.04	8617.66		
$\nu_3 + \nu_4 + 2\nu_5 + \nu_6, 1A_1$	8365.22	8369.45	8369.48			$6\nu_5, 1E$	8775.03	8622.95	8623.57		
$\nu_3 + \nu_4 + 2\nu_5 + \nu_6, 3E$	8364.76	8370.64	8370.34			$2\nu_1 + \nu_4, E$	8708.56	8634.08	8624.00		
$\nu_3 + \nu_4 + 2\nu_5 + \nu_6, 4E$	8373.43	8375.66	8375.67			$2\nu_4 + \nu_5 + \nu_6, 4E$	8580.82	8640.34	8639.91		
$2\nu_3 + 4\nu_5, 1E$	8455.26	8379.42	8379.66			$\nu_1 + \nu_3 + 3\nu_5, E$	8587.89	8655.44	8654.55		
$5\nu_5 + \nu_6, 3E$	8482.19	8396.70	8397.20			$\nu_3 + \nu_4 + 3\nu_5, 1E$	8664.38	8662.69	8662.11		
$\nu_3 + \nu_4 + 2\nu_5 + \nu_6, 2A_1$	8379.85	8396.98	8396.61			$\nu_1 + \nu_3 + 3\nu_5, A_1$	8590.96	8664.47	8664.87		
$2\nu_3 + 4\nu_5, A_1$	8453.72	8401.33	8402.30			$\nu_3 + \nu_4 + 3\nu_5, 2E$	8664.75	8680.59	8680.64		
$2\nu_3 + 2\nu_4, A_1$	8503.84	8405.58	8396.48			$6\nu_5, 2E$	8779.63	8680.93	8681.77		
$2\nu_1 + \nu_5 + \nu_6, E$	8418.97	8412.50	8406.73			$\nu_3 + \nu_4 + 3\nu_5, A_1$	8668.19	8694.75	8694.76		
$2\nu_1 + \nu_5 + \nu_6, A_1$	8429.08	8423.09	8416.92			$\nu_3 + \nu_4 + 3\nu_5, 3E$	8674.71	8705.19	8704.48		
$2\nu_1 + \nu_3 + \nu_6, E$	8300.87	8425.50	8425.00			$2\nu_1 + 2\nu_5, A_1$	8705.47	8714.27	8710.43		
$\nu_1 + \nu_4 + \nu_5 + \nu_6, A_1$	8454.80	8428.90	8429.14			$2\nu_1 + 2\nu_5, E$	8707.01	8722.82	8717.73		
$\nu_1 + \nu_4 + \nu_5 + \nu_6, 1E$	8458.70	8430.18	8430.23			$\nu_1 + \nu_4 + 2\nu_5, A_1$	8747.83	8725.70	8725.82		
$5\nu_5 + \nu_6, 2A_1$	8469.01	8431.82	8431.96			$\nu_1 + \nu_4 + 2\nu_5, 1E$	8749.73	8729.92	8728.78		
$\nu_1 + \nu_4 + \nu_5 + \nu_6, 2E$	8465.37	8436.74	8436.96			$2\nu_1 + \nu_3 + \nu_5, E$	8581.83	8743.35	8743.13		
$2\nu_3 + 4\nu_5, 2E$	8459.87	8438.78	8438.60			$\nu_3 + 2\nu_4 + \nu_5, A_1$	8714.37	8747.53	8746.91		
$\nu_3 + 2\nu_4 + \nu_6, 2E$	8424.36	8441.47	8441.26			$\nu_1 + \nu_4 + 2\nu_5, 2E$	8754.71	8754.03	8754.07		
$\nu_1 + 2\nu_3 + \nu_4, E$	8462.66	8441.50	8440.42			$\nu_1 + 2\nu_4, E$	8778.82	8767.16	8767.51		
$\nu_1 + \nu_4 + \nu_5 + \nu_6, 3E$	8468.35	8454.00	8453.97			$6\nu_5, 2A_1$	8787.31	8772.11	8771.89		
$\nu_3 + 2\nu_4 + \nu_6, A_1$	8423.44	8454.15	8453.90			$\nu_3 + 2\nu_4 + \nu_5, 2E$	8721.26	8775.86	8775.16		
$\nu_1 + 2\nu_3 + 2\nu_5, A_1$	8435.59	8462.07	8459.48			$\nu_1 + 4\nu_5, A_1$	8726.14	8805.58	8803.34		
$5\nu_5 + \nu_6, 4E$	8498.45	8480.52	8480.61			$\nu_1 + 4\nu_5, 1E$	8727.68	8810.43	8809.10		
$\nu_1 + 3\nu_5 + \nu_6, 1E$	8418.55	8486.59	8487.84			$\nu_1 + 4\nu_5, 2E$	8732.29	8817.49	8818.78		
$\nu_1 + 3\nu_5 + \nu_6, 2E$	8425.59	8489.73	8489.20			$\nu_4 + 4\nu_5, 1E$	8817.59	8819.06	8818.38		
$2\nu_3 + \nu_4 + 2\nu_5, A_1$	8499.40	8490.85	8490.34			$\nu_4 + 4\nu_5, 1A_1$	8815.68	8834.26	8834.79		
$\nu_1 + 2\nu_3 + 2\nu_5, E$	8437.12	8497.13	8496.72			$\nu_4 + 4\nu_5, 2E$	8816.85	8841.59	8841.04		
$\nu_3 + 5\nu_5, 1E$	8620.63	8498.89	8498.70			$3\nu_1, A_1$	8711.48	8857.31	8857.17		
$\nu_4 + 4\nu_5, 3E$	8822.57	8862.59	8863.04			$2\nu_4 + 2\nu_5, 3E$	8867.19	8925.06	8924.61		
$3\nu_4, E$	8821.20	8872.55	8870.97			$2\nu_4 + 2\nu_5, 1A_1$	8816.65	8929.69	8929.86		
$\nu_4 + 4\nu_5, 2A_1$	8830.62	8875.72	8874.88			$2\nu_4 + 2\nu_5, 2A_1$	8875.61	8958.02	8957.09		
$2\nu_4 + 2\nu_5, 1E$	8818.18	8897.20	8898.13			$3\nu_4, A_1$	8922.29	9019.01	9018.53		
$2\nu_4 + 2\nu_5, 2E$	8861.84	8901.36	8900.60								

Note: <sup>a</sup>Values presented in column 2 were calculated with the parameters from Tables I (cc-pVQZ) and VI of [64]. Band centres presented in columns 3 and 4 were calculated with the parameters from Tables 14 and 15 of the present paper. Experimental values of the band centres are given in column 5.

if  $\tilde{\nu}_1 = \nu_1$ ,  $\tilde{\nu}_2 = \nu_2$ ,  $\tilde{\nu}_3 = \nu_3 - 2$ ,  $\tilde{\nu}_4 = \nu_4$ ,  $\tilde{\nu}_5 = \nu_5 + 1$ ,  $\tilde{\nu}_6 = \nu_6 + 1$  (for CHD<sub>3</sub>).

For the CHD<sub>3</sub> isotopomer one has:

$$(5) H_{v\gamma, \tilde{v}\gamma} = H_{\tilde{v}\gamma, v\gamma} = \frac{F_{1333}}{4} \{ \nu_1(\nu_3 + 1)(\nu_3 + 2)(\nu_3 + 3) \}^{1/2}$$

(32)

if  $\tilde{\nu}_1 = \nu_1 - 1$ ,  $\tilde{\nu}_2 = \nu_2$ ,  $\tilde{\nu}_3 = \nu_3 + 3$ ,  $\tilde{\nu}_4 = \nu_4$ ,  $\tilde{\nu}_5 = \nu_5$ ,  $\tilde{\nu}_6 = \nu_6 + 1$ . In Equations (28)–(31)  $q_\lambda^+ = (q_{\lambda 1} + iq_{\lambda 2})$  and  $q_\lambda^- = (q_{\lambda 1} - iq_{\lambda 2})$  are the ‘creation’ and ‘annihilation’ operators for doubly degenerate vibrational modes  $q_\lambda$ , which increase and decrease the value of the quantum

Table 13. Values of the experimental band centres of CHD<sub>3</sub> (in cm<sup>-1</sup>).<sup>a</sup>

Band	Centre [64]	Centre calc., I	Centre calc., II	Centre exp.	Ref.	Band	Centre [64]	Centre calc., I	Centre calc., II	Centre exp.	Ref.
1	2	3	4	5	6	1	2	3	4	5	6
$v_3, A_1$	1006.10	1004.39	1004.42	1004.548	[55]	$v_2 + 2v_3, A_1$	4172.90	4140.72	4140.70	4139.233	tw
$v_6, E$	1036.91	1035.45	1035.52	1035.920	[55]	$v_2 + v_3 + v_6, E$	4208.76	4188.41	4187.84		
$v_5, E$	1292.77	1292.12	1292.26	1292.500	[55]	$v_2 + 2v_6, A_1$	4209.37	4200.37	4199.83		
$2v_3, A_1$	1997.74	1991.23	1991.47	1991.084	[56]	$v_2 + 2v_6, E$	4222.38	4205.82	4205.43		
$v_3 + v_6, E$	2044.64	2043.41	2043.20	2041.441	[56]	$2v_3 + v_4, E$	4232.88	4212.28	4212.28	4212.332	tw
$2v_6, A_1$	2056.31	2059.87	2059.77	2058.9	[56]	$v_1 + v_5, E$	4258.52	4261.91	4262.35	4261.662	tw
$2v_6, E$	2069.31	2066.28	2066.32	2066.3	[56]	$v_3 + v_4 + v_6, A_1$	4280.56	4269.94	4269.87		
$v_2, A_1$	2143.71	2144.30	2144.41	2142.583	[56]	$v_3 + v_4 + v_6, E$	4279.11	4274.10	4274.37		
$v_4, E$	2252.04	2251.58	2251.30	2250.828	[56]	$3v_3 + v_5, E$	4264.60	4274.37	4275.11		
$v_3 + v_5, E$	2297.84	2301.02	2301.08	2301.165	[56]	$2v_2, A_1$	4269.78	4290.38	4291.79		
$v_5 + v_6, A_1$	2328.81	2326.71	2327.12			$v_4 + 2v_6, 1E$	4291.55	4293.48	4293.54	4294.337	tw
$v_5 + v_6, E$	2330.65	2338.40	2338.27			$v_4 + 2v_6, 2E$	4306.01	4296.01	4295.51		
$2v_5, A_1$	2565.53	2564.63	2564.72	2564.676	[83]	$v_4 + 2v_6, A_1$	4303.09	4301.56	4301.78		
$2v_5, E$	2587.14	2585.58	2585.60	2586.043	[83]	$2v_3 + v_5 + v_6, A_1$	4327.77	4324.90	4325.27		
$3v_3, A_1$	2974.91	2965.28	2965.65	2966.055	tw	$2v_3 + v_5 + v_6, E$	4329.61	4334.84	4334.68		
$v_1, A_1$	2986.85	2992.73	2992.85	2992.786	tw	$v_2 + v_4, E$	4358.41	4356.34	4356.39	4356.524	tw
$2v_3 + v_6, E$	3037.92	3024.37	3024.47	3025.400	tw	$v_3 + v_5 + 2v_6, 1E$	4365.07	4369.43	4369.10		
$3v_6, E$	3071.21	3069.31	3069.39			$v_3 + v_5 + 2v_6, 2E$	4357.54	4378.37	4377.24		
$v_3 + 2v_6, A_1$	3065.68	3076.09	3075.25			$v_5 + 3v_6, 1E$	4363.23	4382.03	4382.66		
$v_3 + 2v_6, E$	3078.69	3077.80	3077.24			$v_5 + 3v_6, A_1$	4368.70	4383.07	4382.67		
$3v_6, A_1$	3097.22	3092.49	3092.38			$v_3 + v_5 + 2v_6, A_1$	4372.38	4392.26	4390.86		
$v_2 + v_3, A_1$	3165.54	3151.77	3151.71	3154.341	tw	$v_5 + 3v_6, 2E$	4392.92	4394.66	4393.72		
$v_2 + v_6, E$	3185.29	3177.37	3177.28	3178.224	tw	$v_5 + 3v_6, 3E$	4387.40	4417.11	4416.09		
$v_3 + v_4, E$	3249.69	3240.48	3240.56	3239.943	tw	$v_2 + v_3 + v_5, E$	4453.27	4439.72	4439.34		
$v_4 + v_6, A_1$	3281.28	3276.44	3276.12			$2v_4, A_1$	4450.38	4457.55	4457.63	4457.781	tw
$v_4 + v_6, E$	3279.82	3279.50	3279.53	3279.044	tw	$v_2 + v_5 + v_6, A_1$	4473.18	4463.45	4463.54	4462.987	tw
$2v_3 + v_5, E$	3288.45	3294.01	3294.60			$v_2 + v_5 + v_6, E$	4475.03	4475.14	4474.69		
$v_3 + v_5 + v_6, A_1$	3335.52	3337.39	3337.29	3338.729	tw	$2v_4, E$	4483.39	4486.02	4486.30	4486.308	tw
$v_3 + v_5 + v_6, E$	3337.36	3348.33	3347.70			$v_3 + v_4 + v_5, A_1$	4534.30	4511.81	4511.14		
$v_5 + 2v_6, 1E$	3349.19	3356.52	3356.91			$v_3 + v_4 + v_5, E$	4534.18	4529.92	4529.86	4529.062	tw
$v_5 + 2v_6, 2E$	3360.35	3361.30	3361.20			$v_4 + v_5 + v_6, 1E$	4565.93	4555.42	4555.81		
$v_5 + 2v_6, A_1$	3364.04	3380.07	3379.55			$v_4 + v_5 + v_6, 2E$	4564.59	4558.56	4558.60	4557.929	tw
$v_2 + v_5, E$	3432.47	3431.23	3431.33	3430.959	tw	$v_4 + v_5 + v_6, 3E$	4567.89	4569.51	4570.22		
$v_4 + v_5, A_1$	3537.68	3523.29	3523.09	3523.509	tw	$v_4 + v_5 + v_6, A_1$	4566.31	4573.71	4573.54		
$v_4 + v_5, E$	3537.56	3533.86	3533.63	3533.031	tw	$2v_3 + 2v_5, A_1$	4559.15	4576.98	4577.94		
$v_3 + 2v_5, A_1$	3569.57	3578.83	3579.08	3578.927	tw	$2v_3 + 2v_5, E$	4580.76	4592.93	4593.39		
$v_3 + 2v_5, E$	3591.18	3596.56	3596.41			$v_3 + 2v_5 + v_6, 1E$	4608.22	4623.53	4623.09		
$2v_5 + v_6, 1E$	3602.55	3610.05	3610.07			$v_3 + 2v_5 + v_6, 2E$	4627.99	4631.36	4631.17		
$2v_5 + v_6, 2E$	3622.32	3619.31	3619.80			$2v_5 + 2v_6, 1A_1$	4622.06	4643.27	4642.97		
$2v_5 + v_6, A_1$	3626.00	3642.70	3642.09			$2v_5 + 2v_6, 2A_1$	4652.66	4648.42	4649.27		
$3v_5, E$	3839.89	3838.48	3838.26	3838.040	tw	$2v_5 + 2v_6, 1E$	4635.06	4650.86	4650.69		
$3v_5, A_1$	3883.11	3880.39	3880.01			$v_3 + 2v_5 + v_6, A_1$	4631.68	4653.61	4652.32		
$4v_3, A_1$	3937.63	3926.37	3926.84			$2v_5 + 2v_6, 2E$	4643.67	4664.16	4663.78		
$v_1 + v_3, A_1$	3983.22	3988.59	3988.56	3988.646	tw	$2v_5 + 2v_6, 3E$	4660.36	4695.20	4693.85		
$3v_3 + v_6, E$	4016.73	3998.34	3998.31	3997.988	tw	$v_2 + 2v_5, A_1$	4701.21	4698.56	4698.45	4698.882	tw
$v_1 + v_6, E$	4023.45	4027.14	4027.06	4027.331	tw	$v_2 + 2v_5, E$	4722.82	4719.51	4719.33		
$2v_3 + 2v_6, A_1$	4060.60	4039.58	4039.58			$v_4 + 2v_5, 1E$	4803.18	4788.90	4788.49		
$2v_3 + 2v_6, E$	4073.60	4046.71	4046.76			$v_4 + 2v_5, 2E$	4824.92	4816.35	4817.85		
$v_3 + 3v_6, E$	4082.23	4107.55	4105.88			$v_4 + 2v_5, A_1$	4824.68	4818.58	4818.14		
$v_3 + 3v_6, A_1$	4108.23	4107.57	4106.55			$v_3 + 3v_5, E$	4842.90	4855.65	4855.79	4855.300	tw
$4v_6, A_1$	4068.62	4109.06	4107.39			$5v_3, A_1$	4855.89	4874.60	4875.15		
$4v_6, 1E$	4081.62	4109.53	4108.20			$3v_5 + v_6, A_1$	4876.04	4883.04	4882.94		
$4v_6, 2E$	4120.63	4114.07	4113.72			$v_3 + 3v_5, A_1$	4886.12	4892.33	4891.71		
$3v_5 + v_6, 1E$	4877.88	4894.74	4894.09			$2v_3 + v_5 + 2v_6, 2E$	5351.42	5370.98	5369.95		
$3v_5 + v_6, 2E$	4917.42	4913.25	4913.55			$v_2 + v_4 + v_6, A_1$	5392.31	5377.64	5377.32		

(continued)

Table 13. Continued.

Band	Centre [64]	Centre calc., I	Centre calc., II	Centre exp.	Ref.	Band	Centre [64]	Centre calc., I	Centre calc., II	Centre exp.	Ref.
1	2	3	4	5	6	1	2	3	4	5	6
$3\nu_5 + \nu_6, 3E$	4922.95	4948.34	4946.98			$\nu_5 + 4\nu_6, 1E$	5372.77	5379.68	5379.99		
$4\nu_3 + \nu_6, E$	4981.09	4956.30	4956.32			$\nu_2 + \nu_4 + \nu_6, E$	5390.85	5380.24	5380.28		
$\nu_1 + 2\nu_3, A_1$	4965.13	4968.23	4968.15	4968.171	tw	$\nu_3 + \nu_5 + 3\nu_6, 1E$	5375.06	5394.41	5392.64		
$3\nu_3 + 2\nu_6, A_1$	5041.05	5019.48	5018.80			$\nu_3 + \nu_5 + 3\nu_6, 2E$	5402.91	5397.93	5397.30		
$3\nu_3 + 2\nu_6, E$	5054.06	5023.31	5022.82			$\nu_5 + 4\nu_6, 1A_1$	5376.46	5402.75	5403.33		
$\nu_1 + \nu_3 + \nu_6, E$	5021.46	5025.59	5025.15			$\nu_3 + \nu_5 + 3\nu_6, A_1$	5373.21	5407.19	5405.35		
$5\nu_6, 1E$	5061.52	5045.67	5045.28			$\nu_5 + 4\nu_6, 2E$	5417.31	5415.30	5413.33		
$\nu_1 + 2\nu_6, A_1$	5042.55	5049.64	5049.15			$\nu_5 + 4\nu_6, 2A_1$	5409.94	5428.65	5426.52		
$\nu_1 + 2\nu_6, E$	5055.55	5056.88	5056.49			$\nu_2 + 2\nu_3 + \nu_5, E$	5459.60	5431.31	5430.88		
$5\nu_6, A_1$	5087.53	5059.04	5058.93			$\nu_3 + \nu_5 + 3\nu_6, 3E$	5397.38	5432.10	5429.83		
$4\nu_5, A_1$	5094.23	5092.73	5092.00			$\nu_3 + 2\nu_4, A_1$	5439.58	5435.12	5436.24		
$4\nu_5, 1E$	5115.84	5113.68	5112.87			$\nu_5 + 4\nu_6, 3E$	5361.61	5449.54	5447.91		
$\nu_2 + 3\nu_3, A_1$	5160.81	5117.20	5117.16			$\nu_3 + 2\nu_4, E$	5472.59	5458.73	5459.38		
$5\nu_6, 2E$	5139.55	5131.04	5130.32			$2\nu_4 + \nu_6, 1E$	5470.48	5473.10	5473.29		
$\nu_3 + 4\nu_6, 1E$	5133.28	5132.72	5131.14			$\nu_2 + \nu_3 + \nu_5 + \nu_6, A_1$	5495.62	5474.89	5474.15		
$\nu_1 + \nu_2, A_1$	5128.37	5135.02	5134.96	5135.054	tw	$\nu_2 + \nu_3 + \nu_5 + \nu_6, E$	5497.46	5486.29	5485.01		
$2\nu_3 + 3\nu_6, A_1$	5104.79	5135.91	5133.71			$3\nu_3 + 2\nu_5, A_1$	5534.27	5486.88	5486.53		
$\nu_3 + 4\nu_6, 2E$	5094.27	5137.93	5135.25			$\nu_2 + \nu_5 + 2\nu_6, 1E$	5498.24	5491.04	5491.03		
$2\nu_3 + 3\nu_6, E$	5078.78	5139.44	5136.50			$\nu_2 + \nu_5 + 2\nu_6, 2E$	5509.40	5496.29	5495.58		
$\nu_3 + 4\nu_6, A_1$	5081.27	5139.82	5136.77			$2\nu_4 + \nu_6, A_1$	5502.03	5507.24	5508.19		
$\nu_2 + 2\nu_3 + \nu_6, E$	5217.76	5169.36	5168.96			$2\nu_3 + \nu_4 + \nu_5, E$	5516.34	5510.37	5511.18		
$3\nu_3 + \nu_4, E$	5201.61	5171.24	5171.49			$2\nu_4 + \nu_6, 2E$	5504.95	5512.50	5513.48		
$4\nu_5, 2E$	5180.68	5176.53	5175.49			$\nu_2 + \nu_5 + 2\nu_6, A_1$	5513.08	5514.43	5513.32		
$\nu_2 + \nu_3 + 2\nu_6, A_1$	5234.47	5219.78	5218.32			$\nu_1 + 2\nu_5, A_1$	5510.16	5514.98	5515.04	5515.603	tw
$\nu_2 + \nu_3 + 2\nu_6, E$	5247.48	5220.42	5219.24			$\nu_1 + 2\nu_5, E$	5531.78	5535.82	5535.84	5535.919	tw
$\nu_2 + 3\nu_6, E$	5228.95	5224.17	5222.86			$\nu_3 + \nu_4 + \nu_5 + \nu_6, 1E$	5562.85	5548.17	5547.73		
$\nu_2 + 3\nu_6, A_1$	5254.96	5229.65	5228.85			$2\nu_3 + \nu_4 + \nu_5, A_1$	5516.46	5560.22	5561.73		
$\nu_1 + \nu_4, E$	5241.08	5235.78	5235.59	5237.638	tw	$\nu_3 + \nu_4 + \nu_5 + \nu_6, 2E$	5564.19	5566.44	5567.60		
$2\nu_3 + \nu_4 + \nu_6, A_1$	5265.39	5237.99	5238.24			$\nu_3 + \nu_4 + \nu_5 + \nu_6, 3E$	5566.15	5566.69	5567.90		
$4\nu_3 + \nu_5, E$	5226.29	5241.08	5241.99			$\nu_3 + \nu_4 + \nu_5 + \nu_6, A_1$	5564.57	5570.77	5570.44		
$2\nu_3 + \nu_4 + \nu_6, E$	5263.93	5246.81	5247.83			$2\nu_2 + \nu_5, E$	5554.52	5572.13	5573.37		
$\nu_1 + \nu_3 + \nu_5, E$	5253.85	5273.96	5273.74	5273.275	tw	$3\nu_3 + 2\nu_5, E$	5555.88	5574.67	5575.52		
$3\nu_3 + \nu_5 + \nu_6, A_1$	5305.55	5292.60	5292.59			$\nu_4 + \nu_5 + 2\nu_6, A_1$	5577.30	5577.89	5578.02		
$\nu_3 + \nu_4 + 2\nu_6, 1E$	5292.47	5295.66	5295.30			$\nu_4 + \nu_5 + 2\nu_6, 2A_1$	5589.80	5578.31	5578.62		
$\nu_3 + \nu_4 + 2\nu_6, 2E$	5306.94	5296.03	5295.84			$\nu_4 + \nu_5 + 2\nu_6, 1E$	5577.18	5578.53	5579.67		
$\nu_1 + \nu_5 + \nu_6, A_1$	5294.25	5299.48	5299.20			$\nu_4 + \nu_5 + 2\nu_6, 2E$	5593.60	5587.97	5588.34		
$2\nu_2 + \nu_3, A_1$	5307.33	5300.93	5301.98			$\nu_4 + \nu_5 + 2\nu_6, 3E$	5587.00	5598.19	5598.08		
$\nu_3 + \nu_4 + 2\nu_6, A_1$	5304.02	5301.16	5301.45			$\nu_4 + \nu_5 + 2\nu_6, 4E$	5590.56	5601.38	5600.65		
$\nu_4 + 3\nu_6, 1E$	5326.25	5301.60	5300.90			$2\nu_3 + 2\nu_5 + \nu_6, 1E$	5599.44	5601.98	5600.17		
$\nu_1 + \nu_5 + \nu_6, E$	5296.09	5309.02	5308.67			$2\nu_3 + 2\nu_5 + \nu_6, 2E$	5619.36	5616.02	5616.21		
$\nu_4 + 3\nu_6, 2E$	5297.32	5310.63	5309.83			$\nu_2 + \nu_4 + \nu_5, A_1$	5640.28	5626.53	5626.87		
$\nu_4 + 3\nu_6, A_1$	5298.78	5311.96	5312.36			$\nu_2 + \nu_4 + \nu_5, E$	5640.16	5635.09	5635.23		
$\nu_4 + 3\nu_6, 3E$	5321.87	5318.47	5318.74			$2\nu_3 + 2\nu_5 + \nu_6, A_1$	5623.04	5643.60	5642.76		
$2\nu_2 + \nu_6, E$	5316.03	5321.07	5322.02			$\nu_3 + 2\nu_5 + 2\nu_6, 1A_1$	5629.57	5661.76	5660.33		
$3\nu_3 + \nu_5 + \nu_6, E$	5307.40	5337.07	5336.46			$\nu_3 + 2\nu_5 + 2\nu_6, 2A_1$	5660.50	5662.30	5662.00		
$2\nu_3 + \nu_5 + 2\nu_6, 1E$	5362.58	5350.49	5350.40			$\nu_3 + 2\nu_5 + 2\nu_6, 1E$	5642.57	5665.30	5664.14		
$\nu_2 + \nu_3 + \nu_4, E$	5371.78	5352.16	5352.79			$2\nu_5 + 3\nu_6, 1E$	5637.31	5672.90	5674.01		
$2\nu_3 + \nu_5 + 2\nu_6, A_1$	5366.27	5367.75	5367.03			$2\nu_5 + 3\nu_6, 2E$	5657.09	5674.65	5673.73		
$\nu_3 + 2\nu_5 + 2\nu_6, 2E$	5651.18	5681.43	5679.76			$\nu_2 + 4\nu_3, A_1$	6144.39	6081.26	6081.12		
$2\nu_5 + 3\nu_6, 3E$	5679.41	5682.34	5681.89			$\nu_1 + 3\nu_6, A_1$	6042.31	6082.04	6081.24		
$2\nu_5 + 3\nu_6, 1A_1$	5660.77	5687.04	5686.57			$\nu_4 + 3\nu_5, 2E$	6113.62	6096.94	6098.44		
$2\nu_5 + 3\nu_6, 2A_1$	5663.32	5707.04	5705.49			$\nu_4 + 3\nu_5, 3E$	6113.98	6105.31	6104.39		
$\nu_2 + \nu_3 + 2\nu_5, A_1$	5721.18	5708.68	5707.97			$\nu_3 + 4\nu_5, A_1$	6096.39	6113.21	6113.16		
$\nu_3 + 2\nu_5 + 2\nu_6, 3E$	5667.87	5712.28	5710.19			$4\nu_3 + \nu_4, E$	6155.99	6116.92	6117.03		
$2\nu_4 + \nu_5, 1E$	5728.99	5725.11	5725.55			$\nu_3 + 4\nu_5, 1E$	6118.00	6133.03	6132.89		

(continued)

Table 13. Continued.

Band	Centre [64]	Centre calc., I	Centre calc., II	Centre exp.	Ref.	Band	Centre [64]	Centre calc., I	Centre calc., II	Centre exp.	Ref.
1	2	3	4	5	6	1	2	3	4	5	6
$v_2 + v_3 + 2v_5, E$	5742.79	5728.41	5727.48			$v_1 + v_2 + v_3, A_1$	6140.59	6133.64	6133.28		
$v_2 + 2v_5 + v_6, 1E$	5743.15	5741.61	5741.15			$6v_6, 2A_1$	6037.24	6143.39	6142.19		
$2v_5 + 3v_6, 4E$	5690.46	5743.08	5740.88			$v_2 + 3v_3 + v_6, E$	6212.48	6146.68	6145.95		
$v_2 + 2v_5 + v_6, 2E$	5762.92	5750.86	5750.88			$4v_5 + v_6, 1E$	6131.58	6148.13	6147.17		
$2v_4 + v_5, 2E$	5762.13	5755.03	5756.65			$v_3 + 5v_6, 1E$	6076.07	6153.25	6150.99		
$2v_4 + v_5, A_1$	5761.77	5758.66	5758.85	5759.766	tw	$4v_5 + v_6, 2E$	6151.35	6157.38	6156.89		
$v_2 + 2v_5 + v_6, A_1$	5766.61	5774.25	5773.17			$2v_3 + 4v_6, 1E$	6092.68	6160.77	6157.64		
$2v_3 + 3v_5, E$	5831.59	5785.21	5784.81			$v_3 + 5v_6, A_1$	6102.08	6166.74	6162.92		
$6v_3, A_1$	6037.24	5809.93	5810.54			$v_1 + v_2 + v_6, E$	6169.81	6166.81	6166.31		
$v_3 + v_4 + 2v_5, 1E$	5798.96	5813.36	5815.51			$2v_3 + 4v_6, 2E$	6131.69	6170.88	6166.57		
$v_3 + v_4 + 2v_5, A_1$	5820.45	5817.23	5816.81			$v_3 + 5v_6, 2E$	6154.10	6173.42	6168.82		
$v_4 + 2v_5 + v_6, 1A_1$	5832.76	5824.59	5824.45			$2v_3 + 4v_6, A_1$	6079.67	6174.23	6169.52		
$v_4 + 2v_5 + v_6, 1E$	5831.30	5830.47	5830.58			$v_2 + 4v_6, A_1$	6231.35	6179.48	6178.64		
$v_4 + 2v_5 + v_6, 2A_1$	5851.19	5842.59	5844.59			$4v_5 + v_6, 1A_1$	6155.03	6180.77	6179.18		
$v_4 + 2v_5 + v_6, 2E$	5852.41	5842.79	5842.89			$v_2 + 4v_6, 1E$	6244.35	6186.69	6185.92		
$v_3 + v_4 + 2v_5, 2E$	5820.69	5857.15	5858.10			$v_3 + 4v_5, 2E$	6182.84	6188.79	6187.41		
$v_4 + 2v_5 + v_6, 3E$	5854.64	5860.31	5860.95			$5v_3 + v_5, E$	6173.59	6192.40	6195.34		
$2v_1, A_1$	5855.27	5865.64	5865.81	5865.004	tw	$3v_3 + v_4 + v_6, A_1$	6235.92	6197.14	6197.28		
$v_4 + 2v_5 + v_6, 4E$	5856.33	5869.87	5869.24			$3v_3 + v_4 + v_6, E$	6234.46	6202.61	6203.16		
$2v_3 + 3v_5, A_1$	5874.81	5890.57	5890.57			$4v_5 + v_6, 2A_1$	6214.34	6208.54	6208.37		
$v_3 + 3v_5 + v_6, A_1$	5880.87	5898.56	5898.05			$v_1 + 2v_3 + v_5, E$	6234.80	6214.22	6212.82		
$5v_3 + v_6, E$	5931.06	5902.55	5902.47			$v_2 + v_3 + 3v_6, A_1$	6281.97	6247.81	6245.90		
$v_3 + 3v_5 + v_6, 1E$	5922.25	5910.04	5909.01			$v_2 + 4v_6, 2E$	6283.36	6248.86	6247.54		
$3v_5 + 2v_6, 1E$	5907.92	5922.99	5922.90			$v_4 + 4v_6, 1E$	6287.36	6248.94	6249.40		
$v_3 + 3v_5 + v_6, 2E$	5927.78	5925.91	5925.35			$v_2 + 2v_3 + 2v_6, E$	6258.34	6250.04	6247.74		
$3v_5 + 2v_6, 2E$	5947.46	5926.62	5925.86			$v_2 + v_3 + 3v_6, E$	6255.96	6250.32	6247.75		
$v_1 + 3v_3, A_1$	5932.60	5935.89	5935.64			$v_2 + 2v_3 + 2v_6, A_1$	6245.34	6251.14	6248.51		
$3v_5 + 2v_6, 3E$	5958.51	5941.50	5942.36			$v_4 + 4v_6, 2E$	6301.82	6251.94	6252.00		
$3v_5 + 2v_6, 1A_1$	5911.61	5946.38	5945.19			$4v_5 + v_6, 3E$	6221.71	6255.32	6252.95		
$v_3 + 3v_5 + v_6, 3E$	5882.71	5959.61	5957.40			$v_4 + 4v_6, 1A_1$	6298.90	6258.94	6259.77		
$3v_5 + 2v_6, 2A_1$	5939.98	5968.44	5969.02			$4v_3 + v_5 + v_6, A_1$	6268.99	6262.97	6265.88		
$v_2 + 3v_5, E$	5971.79	5967.23	5967.38			$v_1 + v_3 + v_4, E$	6229.12	6264.07	6264.36		
$6v_6, 1A_1$	6154.27	5968.93	5968.55			$v_1 + v_4 + v_6, A_1$	6270.17	6266.37	6262.72		
$6v_6, 1E$	6050.24	5974.63	5974.34			$v_1 + v_4 + v_6, E$	6268.71	6269.20	6267.96		
$v_1 + 2v_3 + v_6, E$	6005.08	6001.50	6000.98			$4v_3 + v_5 + v_6, E$	6270.84	6273.09	6273.21		
$v_2 + 3v_5, A_1$	6015.02	6009.12	6008.40			$2v_2 + 2v_3, A_1$	6330.66	6291.62	6292.53		
$3v_5 + 2v_6, 4E$	5896.76	6011.67	6009.23			$v_1 + v_3 + v_5 + v_6, A_1$	6291.34	6305.18	6304.62		
$3v_3 + 3v_6, E$	6005.69	6035.15	6033.64			$3v_3 + v_5 + 2v_6, 1E$	6331.01	6309.09	6307.77		
$4v_3 + 2v_6, A_1$	6007.17	6039.98	6038.92			$3v_3 + v_5 + 2v_6, 2E$	6342.17	6311.85	6310.25		
$v_4 + 3v_5, A_1$	6070.63	6040.50	6039.41			$v_3 + v_4 + 3v_6, 1E$	6300.14	6312.49	6311.58		
$3v_3 + 3v_6, A_1$	6087.05	6040.55	6039.53			$v_1 + v_3 + v_5 + v_6, E$	6293.18	6314.70	6313.75		
$4v_3 + 2v_6, E$	6020.17	6045.02	6044.16			$v_3 + v_4 + 3v_6, 2E$	6324.69	6315.08	6314.60		
$v_4 + 3v_5, 1E$	6070.51	6054.83	6053.98			$v_3 + v_4 + 3v_6, A_1$	6301.60	6315.72	6314.88		
$v_1 + v_3 + 2v_6, A_1$	6083.32	6058.84	6057.29			$v_3 + v_4 + 3v_6, 3E$	6329.07	6319.68	6319.19		
$v_1 + v_3 + 2v_6, E$	6055.32	6061.40	6060.12			$2v_3 + v_4 + 2v_6, A_1$	6290.69	6319.95	6318.93		
$6v_6, 2E$	6089.25	6063.64	6063.21			$v_4 + 4v_6, 2A_1$	6342.29	6320.40	6319.16		
$v_1 + 3v_6, E$	6057.31	6070.59	6069.44			$v_1 + v_5 + 2v_6, 1E$	6314.48	6325.72	6325.78		
$v_2 + 2v_3 + v_4, E$	6370.92	6329.10	6330.15			$3v_3 + v_4 + v_5, E$	6484.19	6509.62	6510.48		
$v_1 + v_5 + 2v_6, 2E$	6325.64	6329.46	6329.01			$v_2 + v_5 + 3v_6, 1E$	6519.10	6514.00	6513.79		
$v_4 + 4v_6, 3E$	6336.46	6332.80	6333.21			$v_2 + v_3 + v_5 + 2v_6, 2E$	6533.73	6515.30	6513.26		
$2v_3 + v_4 + 2v_6, 1E$	6279.14	6333.29	6333.31			$v_2 + 2v_4, A_1$	6519.70	6519.92	6520.35		
$2v_2 + v_3 + v_6, E$	6355.50	6335.18	6335.46			$2v_4 + 2v_6, 2E$	6506.38	6520.67	6522.07		
$2v_3 + v_4 + 2v_6, 2E$	6293.61	6339.14	6338.82			$v_1 + v_4 + v_5, A_1$	6505.76	6526.55	6528.44		
$2v_2 + 2v_6, A_1$	6345.11	6343.03	6343.24			$v_2 + v_3 + v_5 + 2v_6, A_1$	6537.42	6528.57	6526.28		
$3v_3 + v_5 + 2v_6, A_1$	6345.85	6345.48	6344.89			$v_2 + v_5 + 3v_6, 2E$	6541.42	6528.71	6526.83		

(continued)

Table 13. Continued.

Band	Centre [64]	Centre calc., I	Centre calc., II	Centre exp.	Ref.	Band	Centre [64]	Centre calc., I	Centre calc., II	Centre exp.	Ref.
1	2	3	4	5	6	1	2	3	4	5	6
$2\nu_2 + 2\nu_6, E$	6358.11	6347.14	6347.52			$2\nu_3 + \nu_4 + \nu_5 + \nu_6, 1E$	6546.84	6537.26	6539.59		
$5\nu_5, 1E$	6350.39	6348.32	6346.81			$\nu_1 + \nu_4 + \nu_5, E$	6505.64	6540.93	6542.52		
$\nu_1 + \nu_5 + 2\nu_6, A_1$	6329.32	6352.33	6351.20			$\nu_2 + \nu_5 + 3\nu_6, 3E$	6546.95	6549.09	6547.22		
$\nu_5 + 5\nu_6, 1A_1$	6353.95	6356.73	6356.60			$2\nu_3 + \nu_4 + \nu_5 + \nu_6, 2E$	6548.18	6551.01	6553.16		
$\nu_5 + 5\nu_6, 1E$	6355.79	6358.96	6359.34			$\nu_2 + 2\nu_4, E$	6552.70	6552.20	6553.19		
$\nu_5 + 5\nu_6, 2E$	6378.12	6367.16	6366.50			$2\nu_4 + 2\nu_6, 3E$	6516.47	6554.45	6555.17		
$\nu_2 + \nu_3 + \nu_4 + \nu_6, E$	6406.13	6380.54	6380.96			$2\nu_3 + \nu_4 + \nu_5 + \nu_6, 3E$	6550.15	6555.31	6557.81		
$\nu_5 + 5\nu_6, 3E$	6383.64	6381.79	6381.27			$\nu_1 + 2\nu_5 + \nu_6, 1E$	6547.02	6558.10	6557.61		
$\nu_2 + \nu_3 + \nu_4 + \nu_6, A_1$	6407.59	6384.90	6385.57			$\nu_1 + 2\nu_5 + \nu_6, 2E$	6566.79	6567.36	6567.34		
$5\nu_5, A_1$	6393.61	6390.22	6388.55			$2\nu_3 + \nu_4 + \nu_5 + \nu_6, A_1$	6548.57	6567.47	6569.92		
$\nu_2 + \nu_4 + 2\nu_6, 1E$	6407.57	6390.37	6389.82			$\nu_3 + \nu_4 + \nu_5 + 2\nu_6, 1E$	6577.32	6576.79	6576.93		
$\nu_2 + \nu_4 + 2\nu_6, 2E$	6422.03	6394.16	6393.36			$\nu_3 + \nu_4 + \nu_5 + 2\nu_6, 1A_1$	6577.44	6577.53	6577.19		
$2\nu_3 + 2\nu_4, A_1$	6414.52	6394.17	6395.50			$\nu_3 + \nu_4 + \nu_5 + 2\nu_6, 2A_1$	6589.94	6577.60	6576.73		
$\nu_1 + \nu_2 + \nu_5, E$	6396.18	6398.53	6398.58			$3\nu_3 + 2\nu_5 + \nu_6, 1E$	6576.35	6580.58	6576.73		
$\nu_2 + \nu_4 + 2\nu_6, A_1$	6419.12	6399.19	6399.11			$2\nu_2 + \nu_3 + \nu_5, E$	6591.31	6582.38	6582.87		
$\nu_2 + 3\nu_3 + \nu_5, E$	6451.65	6413.39	6412.95			$3\nu_3 + 2\nu_5 + \nu_6, 2E$	6596.12	6589.84	6586.00		
$2\nu_3 + 2\nu_4, E$	6447.53	6415.16	6415.76			$\nu_3 + \nu_4 + \nu_5 + 2\nu_6, 2E$	6587.14	6590.36	6589.82		
$\nu_5 + 5\nu_6, 4E$	6428.29	6418.86	6419.28			$\nu_1 + 2\nu_5 + \nu_6, A_1$	6570.48	6590.74	6589.63		
$\nu_3 + \nu_5 + 4\nu_6, 1A_1$	6388.33	6421.66	6420.63			$\nu_4 + \nu_5 + 3\nu_6, 1E$	6582.50	6592.12	6592.20		
$2\nu_3 + \nu_5 + 3\nu_6, 1E$	6370.79	6429.08	6425.03			$\nu_4 + \nu_5 + 3\nu_6, 1A_1$	6584.22	6595.20	6596.78		
$\nu_3 + \nu_5 + 4\nu_6, 1E$	6373.49	6434.87	6432.14			$\nu_4 + \nu_5 + 3\nu_6, 2E$	6583.84	6595.85	6596.65		
$3\nu_2, A_1$	6378.53	6438.24	6442.15			$\nu_3 + \nu_4 + \nu_5 + 2\nu_6, 3E$	6590.71	6597.42	6597.51		
$2\nu_3 + \nu_5 + 3\nu_6, A_1$	6368.94	6441.57	6438.33			$\nu_4 + \nu_5 + 3\nu_6, 3E$	6585.80	6600.72	6601.07		
$\nu_3 + \nu_5 + 4\nu_6, 2E$	6384.65	6447.02	6443.35			$2\nu_2 + \nu_5 + \nu_6, A_1$	6600.22	6601.96	6602.94		
$2\nu_4 + 2\nu_6, 1A_1$	6473.38	6448.45	6448.71			$\nu_4 + \nu_5 + 3\nu_6, 4E$	6609.46	6605.42	6605.48		
$2\nu_3 + \nu_5 + 3\nu_6, 2E$	6393.11	6452.93	6449.15			$\nu_3 + \nu_4 + \nu_5 + 2\nu_6, 4E$	6593.74	6607.53	6606.87		
$\nu_3 + \nu_5 + 4\nu_6, 2A_1$	6421.82	6457.61	6453.77			$3\nu_3 + 2\nu_5 + \nu_6, A_1$	6599.81	6613.23	6608.29		
$\nu_3 + 2\nu_4 + \nu_6, 1E$	6461.57	6459.96	6461.88			$2\nu_2 + \nu_5 + \nu_6, E$	6602.06	6613.65	6614.09		
$2\nu_2 + \nu_4, E$	6447.44	6460.69	6462.15			$\nu_4 + \nu_5 + 3\nu_6, 2A_1$	6605.21	6614.84	6614.95		
$\nu_2 + 2\nu_3 + \nu_5 + \nu_6, A_1$	6503.81	6467.31	6465.24			$\nu_2 + \nu_3 + \nu_4 + \nu_5, A_1$	6652.63	6620.41	6620.45		
$\nu_3 + \nu_5 + 4\nu_6, 3E$	6429.19	6467.58	6464.36			$\nu_4 + \nu_5 + 3\nu_6, 3A_1$	6615.11	6623.16	6622.25		
$\nu_2 + 2\nu_3 + \nu_5 + \nu_6, E$	6505.65	6471.18	6469.93			$\nu_2 + \nu_3 + \nu_4 + \nu_5, E$	6652.51	6632.11	6632.31		
$5\nu_5, 2E$	6480.06	6474.02	6472.04			$\nu_4 + \nu_5 + 3\nu_6, 5E$	6610.61	6635.70	6635.21		
$4\nu_3 + 2\nu_5, E$	6516.65	6474.62	6476.08			$2\nu_3 + 2\nu_5 + 2\nu_6, 1A_1$	6622.43	6641.53	6641.29		
$\nu_5 + 5\nu_6, 2A_1$	6437.50	6477.37	6475.00			$2\nu_3 + 2\nu_5 + 2\nu_6, 2A_1$	6653.36	6644.61	6644.96		
$4\nu_3 + 2\nu_5, A_1$	6495.04	6477.59	6477.96			$3\nu_4, E$	6628.31	6646.47	6647.83		
$2\nu_3 + \nu_5 + 3\nu_6, 3E$	6398.64	6479.76	6476.10			$2\nu_3 + 2\nu_5 + 2\nu_6, 1E$	6635.43	6648.12	6647.75		
$2\nu_4 + 2\nu_6, 1E$	6486.38	6482.95	6483.10			$\nu_2 + \nu_4 + \nu_5 + \nu_6, 1E$	6671.91	6652.77	6653.41		
$3\nu_3 + \nu_4 + \nu_5, A_1$	6484.31	6484.05	6487.37			$\nu_2 + \nu_4 + \nu_5 + \nu_6, 2E$	6673.25	6655.95	6655.98		
$\nu_1 + \nu_3 + 2\nu_5, A_1$	6504.58	6484.55	6483.04			$2\nu_3 + 2\nu_5 + 2\nu_6, 2E$	6644.04	6659.81	6659.16		
$\nu_3 + 2\nu_4 + \nu_6, 2E$	6496.03	6485.51	6487.36			$\nu_2 + \nu_4 + \nu_5 + \nu_6, 3E$	6675.21	6664.08	6664.39		
$\nu_3 + 2\nu_4 + \nu_6, A_1$	6493.12	6492.43	6494.91			$\nu_2 + \nu_4 + \nu_5 + \nu_6, A_1$	6673.63	6666.53	6666.83		
$\nu_1 + \nu_3 + 2\nu_5, E$	6526.19	6498.94	6497.35			$\nu_3 + 2\nu_5 + 3\nu_6, 1E$	6646.28	6680.43	6678.75		
$\nu_2 + \nu_5 + 3\nu_6, A_1$	6517.26	6502.52	6501.94			$2\nu_3 + 2\nu_5 + 2\nu_6, 3E$	6660.73	6687.95	6686.06		
$\nu_2 + \nu_3 + \nu_5 + 2\nu_6, 1E$	6522.57	6505.59	6504.41			$\nu_3 + 2\nu_5 + 3\nu_6, 2E$	6666.05	6689.00	6687.66		
$2\nu_4 + 2\nu_6, 2A_1$	6522.30	6509.50	6509.47			$\nu_3 + 2\nu_5 + 3\nu_6, 3E$	6688.37	6689.09	6688.63		
$2\nu_5 + 4\nu_6, 1E$	6647.89	6692.77	6694.03			$\nu_4 + 2\nu_5 + 2\nu_6, 2A_1$	6864.69	6884.17	6884.52		
$\nu_3 + 2\nu_4 + \nu_5, 1E$	6717.17	6701.18	6700.98			$\nu_2 + \nu_4 + 2\nu_5, 1E$	6901.81	6887.83	6888.08		
$3\nu_4, A_1$	6694.32	6702.84	6704.33			$\nu_1 + 4\nu_3, A_1$	6885.60	6893.79	6893.16		
$2\nu_5 + 4\nu_6, 1A_1$	6634.88	6702.87	6700.55			$2\nu_1 + \nu_6, E$	6891.63	6899.53	6899.19		
$\nu_2 + 2\nu_3 + 2\nu_5, A_1$	6726.49	6703.06	6702.34			$\nu_4 + 2\nu_5 + 2\nu_6, 3A_1$	6883.07	6900.65	6900.29		
$\nu_3 + 2\nu_5 + 3\nu_6, 1A_1$	6669.73	6703.35	6701.42			$2\nu_3 + 3\nu_5 + \nu_6, 1E$	6872.91	6905.94	6905.58		
$2\nu_5 + 4\nu_6, 2A_1$	6665.81	6703.36	6702.41			$\nu_2 + \nu_4 + 2\nu_5, 2E$	6923.54	6908.36	6909.72		
$2\nu_5 + 4\nu_6, 2E$	6656.49	6705.95	6704.02			$\nu_4 + 2\nu_5 + 2\nu_6, 6E$	6879.92	6914.94	6913.95		
$\nu_3 + 2\nu_5 + 3\nu_6, 2A_1$	6672.28	6711.81	6709.37			$\nu_2 + \nu_4 + 2\nu_5, A_1$	6923.30	6915.61	6915.56		

(continued)

Table 13. Continued.

Band	Centre [64]	Centre calc., I	Centre calc., II	Centre exp.	Ref.	Band	Centre [64]	Centre calc., I	Centre calc., II	Centre exp.	Ref.
1	2	3	4	5	6	1	2	3	4	5	6
$2\nu_5 + 4\nu_6, 3E$	6673.18	6718.60	6717.73			$2\nu_3 + 3\nu_5 + \nu_6, 2E$	6912.45	6919.79	6919.61		
$\nu_2 + 2\nu_3 + 2\nu_5, E$	6748.11	6721.60	6720.48			$\nu_3 + 3\nu_5 + 2\nu_6, 1E$	6903.05	6925.78	6923.35		
$2\nu_5 + 4\nu_6, 4E$	6686.90	6723.27	6720.82			$\nu_3 + 3\nu_5 + 2\nu_6, 2E$	6914.21	6945.87	6943.90		
$\nu_3 + 2\nu_4 + \nu_5, 2E$	6750.30	6733.31	6736.10			$3\nu_5 + 3\nu_6, 1A_1$	6910.96	6946.82	6946.28		
$\nu_3 + 2\nu_4 + \nu_5, A_1$	6750.06	6742.46	6743.06			$2\nu_3 + 3\nu_5 + \nu_6, 3E$	6917.97	6951.84	6949.98		
$2\nu_4 + \nu_5 + \nu_6, 1A_1$	6748.29	6744.21	6745.67			$\nu_3 + 3\nu_5 + 2\nu_6, 3E$	6953.75	6955.61	6955.09		
$2\nu_5 + 4\nu_6, 5E$	6701.14	6749.63	6746.50			$3\nu_5 + 3\nu_6, 1E$	6912.80	6958.31	6958.13		
$2\nu_4 + \nu_5 + \nu_6, 1E$	6750.13	6753.28	6753.89			$\nu_3 + 3\nu_5 + 2\nu_6, 1A_1$	6917.90	6961.68	6959.45		
$\nu_2 + \nu_3 + 2\nu_5 + \nu_6, 1E$	6764.56	6753.63	6752.12			$3\nu_5 + 3\nu_6, 2A_1$	6972.82	6965.12	6966.44		
$\nu_3 + 2\nu_5 + 3\nu_6, 4E$	6699.42	6757.69	6753.92			$3\nu_5 + 3\nu_6, 2E$	6935.13	6967.79	6966.09		
$\nu_2 + \nu_3 + 2\nu_5 + \nu_6, 2E$	6784.33	6762.30	6761.16			$2\nu_4 + 2\nu_5, 1A_1$	6987.41	6972.22	6972.40		
$\nu_1 + 3\nu_5, E$	6763.55	6763.48	6763.52			$\nu_2 + \nu_3 + 3\nu_5, E$	6990.54	6978.32	6977.05		
$3\nu_3 + 3\nu_5, E$	6061.04	6770.39	6770.04			$\nu_3 + 3\nu_5 + 2\nu_6, 2A_1$	6946.28	6985.47	6983.01		
$\nu_2 + 2\nu_5 + 2\nu_6, 1A_1$	6767.39	6772.86	6771.79			$3\nu_5 + 3\nu_6, 3E$	6940.65	6986.12	6985.35		
$2\nu_4 + \nu_5 + \nu_6, 2E$	6779.96	6773.93	6774.52			$2\nu_4 + 2\nu_5, 1E$	7009.02	6990.02	6989.91		
$2\nu_4 + \nu_5 + \nu_6, 3E$	6781.56	6775.44	6778.06			$\nu_1 + 3\nu_3 + \nu_6, E$	6974.17	6990.56	6988.89		
$\nu_2 + 2\nu_5 + 2\nu_6, 2A_1$	6798.32	6777.59	6777.71			$3\nu_5 + 3\nu_6, 4E$	6952.34	6993.40	6991.56		
$\nu_2 + 2\nu_5 + 2\nu_6, 1E$	6780.39	6780.03	6779.12			$\nu_2 + 3\nu_5 + \nu_6, A_1$	7012.67	7009.41	7008.69		
$2\nu_4 + \nu_5 + \nu_6, 2A_1$	6784.71	6781.02	6782.66			$2\nu_4 + 2\nu_5, 2E$	7020.42	7015.75	7018.17		
$\nu_2 + \nu_3 + 2\nu_5 + \nu_6, A_1$	6788.02	6785.19	6782.95			$\nu_2 + \nu_3 + 3\nu_5, A_1$	7033.76	7018.01	7016.28		
$2\nu_5 + 4\nu_6, 3A_1$	6715.88	6786.34	6783.18			$2\nu_4 + 2\nu_5, 2A_1$	7042.27	7020.52	7021.45		
$2\nu_4 + \nu_5 + \nu_6, 4E$	6782.63	6792.72	6793.49			$3\nu_5 + 3\nu_6, 5E$	6957.87	7021.09	7018.68		
$\nu_2 + 2\nu_5 + 2\nu_6, 2E$	6789.00	6793.76	6792.62			$\nu_2 + 3\nu_5 + \nu_6, 1E$	7014.51	7021.11	7019.83		
$2\nu_3 + \nu_4 + 2\nu_5, 1E$	6780.10	6795.65	6798.91			$\nu_3 + 3\nu_5 + 2\nu_6, 4E$	6964.81	7023.86	7020.03		
$3\nu_3 + 3\nu_5, A_1$	6848.91	6801.11	6801.54			$2\nu_4 + 2\nu_5, 3E$	7041.79	7034.86	7034.74		
$\nu_1 + 3\nu_5, A_1$	6806.78	6810.73	6810.31			$\nu_1 + 2\nu_3 + 2\nu_6, A_1$	7027.50	7037.37	7035.16		
$\nu_2 + 2\nu_5 + 2\nu_6, 3E$	6805.69	6824.37	6822.28			$\nu_2 + 3\nu_5 + \nu_6, 2E$	7054.05	7039.62	7039.29		
$\nu_3 + \nu_4 + 2\nu_5 + \nu_6, 1E$	6828.54	6827.11	6826.32			$2\nu_3 + 4\nu_5, A_1$	7083.92	7045.05	7046.54		
$2\nu_2 + 2\nu_5, A_1$	6819.55	6834.27	6835.16			$\nu_1 + 2\nu_3 + 2\nu_6, E$	7040.50	7050.12	7048.15		
$\nu_3 + \nu_4 + 2\nu_5 + \nu_6, 2E$	6849.64	6841.83	6841.44			$2\nu_3 + 4\nu_5, 1E$	7105.53	7054.85	7054.00		
$\nu_3 + \nu_4 + 2\nu_5 + \nu_6, 1A_1$	6829.99	6842.68	6844.76			$\nu_1 + 4\nu_6, A_1$	7054.46	7056.26	7055.31		
$2\nu_3 + \nu_4 + 2\nu_5, 2E$	6801.83	6842.89	6844.37			$\nu_1 + \nu_3 + 3\nu_6, E$	7058.60	7066.29	7064.46		
$2\nu_1 + \nu_3, A_1$	6841.94	6848.20	6848.33	6848.112	tw	$\nu_1 + 4\nu_6, 1E$	7067.46	7067.71	7066.68		
$\nu_3 + \nu_4 + 2\nu_5 + \nu_6, 2A_1$	6848.43	6851.55	6853.83			$3\nu_5 + 3\nu_6, 3A_1$	6989.40	7070.39	7066.74		
$\nu_4 + 2\nu_5 + 2\nu_6, 1E$	6843.19	6855.01	6855.47			$\nu_2 + 3\nu_5 + \nu_6, 3E$	7059.58	7074.70	7072.72		
$2\nu_2 + 2\nu_5, E$	6841.16	6855.22	6856.03			$\nu_4 + 3\nu_5 + \nu_6, 1E$	7097.70	7085.32	7084.81		
$\nu_3 + \nu_4 + 2\nu_5 + \nu_6, 3E$	6851.87	6857.24	6858.09			$\nu_1 + \nu_3 + 3\nu_6, A_1$	7084.61	7088.99	7087.06		
$\nu_4 + 2\nu_5 + 2\nu_6, 2E$	6864.93	6861.63	6862.10			$\nu_4 + 3\nu_5 + \nu_6, 2E$	7099.04	7090.53	7090.10		
$\nu_4 + 2\nu_5 + 2\nu_6, 3E$	6857.66	6863.12	6865.98			$\nu_3 + \nu_4 + 3\nu_5, 1E$	7065.08	7093.47	7095.46		
$\nu_4 + 2\nu_5 + 2\nu_6, 1A_1$	6854.74	6864.55	6865.01			$\nu_1 + 4\nu_6, 2E$	7106.47	7101.76	7100.43		
$\nu_4 + 2\nu_5 + 2\nu_6, 4E$	6872.79	6868.05	6868.80			$\nu_3 + \nu_4 + 3\nu_5, 2E$	7108.18	7105.12	7104.12		
$\nu_3 + \nu_4 + 2\nu_5 + \nu_6, 4E$	6853.57	6868.19	6868.94			$\nu_4 + 3\nu_5 + \nu_6, 1A_1$	7099.42	7107.12	7106.53		
$2\nu_3 + 3\nu_5 + \nu_6, A_1$	6871.07	6869.12	6864.91			$\nu_4 + 3\nu_5 + \nu_6, 3E$	7101.00	7108.05	7109.54		
$2\nu_3 + \nu_4 + 2\nu_5, A_1$	6801.59	6873.35	6873.73			$2\nu_1 + \nu_5, E$	7105.89	7115.98	7116.07	7115.499	tw
$\nu_4 + 2\nu_5 + 2\nu_6, 5E$	6875.46	6873.73	6874.88			$\nu_1 + \nu_2 + 2\nu_3, A_1$	7138.23	7116.19	7115.54		
$\nu_3 + \nu_4 + 3\nu_5, A_1$	7065.20	7118.46	7119.50			$\nu_1 + \nu_3 + \nu_5 + 2\nu_6, A_1$	7327.94	7354.58	7352.70		
$\nu_4 + 3\nu_5 + \nu_6, 4E$	7139.20	7122.32	7124.79			$\nu_1 + \nu_5 + 3\nu_6, 2E$	7352.43	7358.34	7357.22		
$\nu_4 + 3\nu_5 + \nu_6, 2A_1$	7140.30	7128.89	7128.78			$\nu_3 + 5\nu_5, 1E$	7351.34	7371.21	7370.73		
$\nu_3 + \nu_4 + 3\nu_5, 3E$	7108.54	7136.54	7137.21			$\nu_3 + 5\nu_5, A_1$	7394.57	7378.78	7379.81		
$\nu_4 + 3\nu_5 + \nu_6, 3A_1$	7146.19	7152.67	7153.00			$\nu_1 + \nu_5 + 3\nu_6, 3E$	7357.95	7386.49	7384.59		
$\nu_3 + 4\nu_5 + \nu_6, 1E$	7135.21	7165.91	7164.76			$\nu_4 + 4\nu_5, 3E$	7403.97	7393.84	7392.18		
$\nu_1 + \nu_2 + \nu_3 + \nu_6, E$	7183.55	7167.53	7166.51			$5\nu_5 + \nu_6, 1A_1$	7386.70	7402.86	7401.31		
$\nu_4 + 3\nu_5 + \nu_6, 5E$	7144.37	7167.82	7166.43			$\nu_1 + \nu_2 + \nu_3 + \nu_5, E$	7407.25	7404.72	7403.96		
$\nu_3 + 4\nu_5 + \nu_6, 2E$	7154.98	7174.20	7173.40			$\nu_4 + 4\nu_5, 2A_1$	7404.45	7411.60	7411.11		
$\nu_1 + 3\nu_3 + \nu_5, E$	7201.22	7176.84	7175.17			$5\nu_5 + \nu_6, 1E$	7388.54	7414.55	7412.46		

(continued)

Table 13. Continued.

Band	Centre [64]	Centre calc., I	Centre calc., II	Centre exp.	Ref.	Band	Centre [64]	Centre calc., I	Centre calc., II	Centre exp.	Ref.
1	2	3	4	5	6	1	2	3	4	5	6
$v_1 + v_2 + 2v_6, A_1$	7193.63	7185.66	7184.59			$v_1 + v_2 + v_5 + v_6, A_1$	7436.64	7429.54	7429.26		
$2v_3 + 4v_5, 2E$	7170.37	7187.99	7187.20			$5v_5 + v_6, 2E$	7428.08	7433.06	7431.91		
$4v_5 + 2v_6, 1A_1$	7151.26	7190.46	7189.06			$v_1 + v_2 + v_5 + v_6, E$	7438.48	7440.93	7440.08		
$v_1 + v_2 + 2v_6, E$	7206.64	7193.98	7192.92			$v_1 + v_4 + v_5 + v_6, 1E$	7532.41	7460.96	7458.89		
$4v_5 + 2v_6, 2A_1$	7182.19	7196.46	7196.19			$v_1 + v_4 + v_5 + v_6, 2E$	7533.75	7465.63	7465.06		
$v_3 + 4v_5 + v_6, 1A_1$	7158.66	7197.44	7195.62			$5v_5 + v_6, 3E$	7433.61	7468.15	7465.35		
$4v_5 + 2v_6, 1E$	7172.87	7198.90	7197.60			$v_1 + 2v_3 + 2v_5, A_1$	7484.43	7472.42	7468.78		
$4v_5 + 2v_6, 2E$	7164.26	7211.38	7209.90			$v_3 + 5v_5, 2E$	7481.02	7486.13	7483.73		
$v_2 + 4v_5, A_1$	7222.16	7216.29	7215.05			$v_1 + 2v_4, A_1$	7441.81	7488.55	7492.32		
$v_3 + 4v_5 + v_6, 2A_1$	7217.97	7221.27	7220.10			$v_1 + 2v_4, E$	7474.82	7496.95	7501.02		
$4v_5 + 2v_6, 3E$	7189.56	7235.92	7236.52			$5v_5 + v_6, 4E$	7512.69	7505.17	7504.26		
$v_2 + 4v_5, 1E$	7243.77	7237.24	7235.92			$v_1 + 2v_3 + 2v_5, E$	7506.04	7505.48	7501.02		
$v_1 + 2v_3 + v_4, E$	7202.58	7238.42	7239.25			$v_1 + v_3 + v_4 + v_5, A_1$	7492.66	7532.61	7533.10		
$4v_5 + 2v_6, 4E$	7237.70	7243.25	7240.76			$v_1 + v_4 + v_5 + v_6, A_1$	7534.14	7541.73	7539.77		
$v_1 + v_3 + v_4 + v_6, E$	7258.27	7246.82	7246.89			$v_1 + v_4 + v_5 + v_6, 3E$	7535.71	7541.96	7541.38		
$v_1 + 2v_3 + v_5 + v_6, A_1$	7273.86	7248.07	7247.39			$v_1 + v_3 + v_4 + v_5, E$	7492.54	7547.30	7547.59		
$v_3 + 4v_5 + v_6, 3E$	7225.34	7266.52	7263.13			$5v_5 + v_6, 2A_1$	7521.90	7563.64	7559.98		
$v_1 + 2v_2, A_1$	7252.46	7269.59	7270.48			$v_1 + v_3 + 2v_5 + v_6, 1E$	7542.97	7575.40	7574.57		
$4v_5 + 2v_6, 5E$	7243.34	7274.15	7272.43			$v_1 + v_3 + 2v_5 + v_6, 2E$	7562.74	7581.64	7580.85		
$v_1 + v_4 + 2v_6, 1E$	7280.18	7282.42	7280.62			$6v_5, 1A_1$	7586.36	7584.30	7581.81		
$v_1 + v_4 + 2v_6, 2E$	7294.64	7285.96	7283.83			$v_1 + 2v_5 + 2v_6, 1A_1$	7566.28	7600.38	7598.02		
$v_4 + 4v_5, 1E$	7317.76	7289.68	7287.84			$v_1 + 2v_5 + 2v_6, 2A_1$	7597.21	7600.94	7598.56		
$v_1 + v_3 + v_4 + v_6, A_1$	7259.73	7291.92	7291.64			$v_1 + v_3 + 2v_5 + v_6, A_1$	7566.43	7602.23	7600.10		
$v_1 + v_4 + 2v_6, A_1$	7291.73	7292.61	7291.06			$v_1 + 2v_5 + 2v_6, 1E$	7579.28	7603.06	7600.49		
$v_1 + 2v_3 + v_5 + v_6, E$	7275.70	7299.61	7299.04			$6v_5, 1E$	7607.97	7605.25	7602.36		
$v_2 + 4v_5, 2E$	7308.61	7300.09	7298.54			$v_1 + 2v_5 + 2v_6, 2E$	7587.89	7614.68	7613.22		
$v_4 + 4v_5, 1A_1$	7339.25	7322.33	7320.78			$v_1 + 2v_5 + 2v_6, 3E$	7604.58	7643.77	7641.86		
$v_4 + 4v_5, 2E$	7339.49	7326.12	7327.90			$v_1 + v_2 + 2v_5, A_1$	7643.85	7645.81	7645.49		
$4v_5 + 2v_6, 3A_1$	7258.08	7329.49	7325.67			$v_1 + v_2 + 2v_5, E$	7665.47	7666.60	7666.19		
$v_1 + v_3 + v_5 + 2v_6, 1E$	7313.10	7330.56	7329.12			$6v_5, 2E$	7672.80	7668.10	7665.30		
$v_1 + v_3 + v_5 + 2v_6, 2E$	7324.26	7340.95	7339.25			$v_1 + v_3 + 3v_5, E$	7756.84	7676.29	7671.87		
$v_1 + v_2 + v_4, E$	7345.46	7346.55	7345.20			$v_1 + v_4 + 2v_5, A_1$	7771.69	7762.08	7759.88		
$v_1 + v_5 + 3v_6, 1E$	7330.10	7347.43	7347.07			$v_1 + v_4 + 2v_5, 1E$	7750.20	7768.93	7769.11		
$v_1 + v_5 + 3v_6, A_1$	7328.26	7348.64	7347.71			$6v_5, 2A_1$	7780.86	7772.85	7769.67		
$v_1 + 3v_5 + v_6, A_1$	7799.45	7795.04	7794.42			$2v_1 + v_2, A_1$	7994.72	8004.98	8004.79		
$v_1 + v_4 + 2v_5, 2E$	7771.93	7802.74	7802.26			$v_1 + 4v_5, 1E$	8018.44	8021.56	8019.35		
$2v_1 + 2v_3, A_1$	7814.12	7823.21	7822.89			$v_1 + 4v_5, 2E$	8083.28	8083.67	8082.56		
$v_1 + 3v_5 + v_6, 1E$	7801.29	7823.40	7822.38			$2v_1 + v_3 + v_5, E$	8091.50	8088.39	8087.11		
$v_1 + v_3 + 3v_5, A_1$	7800.06	7835.76	7834.29			$2v_1 + v_4, E$	8111.80	8137.87	8136.45		
$v_1 + 3v_5 + v_6, 2E$	7840.83	7841.85	7841.72			$2v_1 + v_5 + v_6, A_1$	8141.36	8149.64	8149.39		
$v_1 + 3v_5 + v_6, 3E$	7846.35	7876.74	7874.98			$2v_1 + v_5 + v_6, E$	8143.21	8161.44	8159.37		
$2v_1 + v_3 + v_6, E$	7879.91	7880.87	7880.44			$2v_1 + 2v_5, A_1$	8336.47	8347.05	8346.88	8346.919	tw
$2v_1 + 2v_6, A_1$	7910.47	7921.17	7920.15			$2v_1 + 2v_5, E$	8358.08	8368.65	8367.05		
$2v_1 + 2v_6, E$	7923.48	7928.59	7927.66			$3v_1, A_1$	8605.28	8622.89	8622.78	8623.349	tw
$v_1 + 4v_5, A_1$	7996.83	7999.40	7999.17								

Note: <sup>a</sup>See footnote to Table 12.numbers  $l_\lambda$ :

and

$$q_\lambda^+ |v_\lambda \ l_\lambda\rangle = \left\{ \frac{v-l}{2} \right\}^{1/2} |v_\lambda - 1 \ l_\lambda + 1\rangle - \left\{ \frac{v+l+2}{2} \right\}^{1/2} |v_\lambda + 1 \ l_\lambda + 1\rangle \quad (33)$$

$$q_\lambda^- |v_\lambda \ l_\lambda\rangle = - \left\{ \frac{v+l}{2} \right\}^{1/2} |v_\lambda - 1 \ l_\lambda - 1\rangle - \left\{ \frac{v-l+2}{2} \right\}^{1/2} |v_\lambda + 1 \ l_\lambda - 1\rangle \quad (34)$$

Table 14.  $F_{ij}$  parameters of the methane molecule.

Parameter	Present work, I	Present work, II	[64]	[32]
$F_{11}/\text{aJ \AA}^{-2}$	5.47384 <sup>a</sup>	5.47384 <sup>a</sup>	5.47384	5.47384 <sup>a</sup>
$F_{22}/\text{aJ}$	0.574225(638)	0.574203(613)	0.57770	0.578602
$F_{33}/\text{aJ \AA}^{-2}$	5.374354(744)	5.400781(731)	5.37696	5.387874
$F_{34}/\text{aJ \AA}^{-1}$	-0.16080 (983)	-0.21057 <sup>a</sup>	-0.21057	-0.21057 <sup>a</sup>
$F_{44}/\text{aJ}$	0.531674(539)	0.532938(506)	0.53225	0.533740
$N^b$	124	124		
$n^b$	64	63		
$d_{\text{rms}}/\text{cm}^{-1}$	0.73	0.75		

Notes:<sup>a</sup>Constrained to the value from [64].

<sup>b</sup> $N$  is the number of experimental band centres;  $n$  is the number of fitted parameters.

As a result of our analysis of experimental band centres a set of 64 parameters was obtained which are presented in column 2 of Table 14 and columns 2 and 5 of Table 15. Values in parenthesis are  $1\sigma$  statistical confidence intervals. Columns 4 and 5 of Table 14 give, for comparison, the values of quadratic  $F_{ij}$  parameters obtained from *ab initio* calculations, [64], and from the fit of experimental band centres of the  $\text{CH}_2\text{D}_2$  molecule, [32], respectively. One finds reasonable agreement between all sets of parameters.

The parameters obtained reproduce the experimental band centres used in the fit with the  $d_{\text{rms}} = 0.73 \text{ cm}^{-1}$ . In order to illustrate the accuracy of the results derived, column 3 of Tables 12 and 13 give the values of the band centres calculated with our parameters from Tables 14 and 15. One finds a good agreement between the experimental and calculated band centres. The columns 2 of Tables 12 and 13 present, for comparison, the values of the same band centres calculated with the parameters from [64].

As can be seen from Table 14, the values of the parameters  $F_{22}$ ,  $F_{33}$ , and  $F_{44}$  obtained from the fit are close to the values of the corresponding parameters from [64] and [9]. On the other hand, larger differences arise for the values of the  $F_{34}$  parameter. To understand the origin of this inconsistency, we repeated the fit with a fixed value of the parameter  $F_{34}$ . The results of this second fit are very close to the results of the first fit (see column 3 of Table 14, columns 3 and 6 of Table 15, and column 4 of Tables 12 and 13). The  $d_{\text{rms}}$  increases only a little, to  $0.75 \text{ cm}^{-1}$ . Comparison of results of the first and the second fit shows, that the fit to just the frequencies in our experimental data is not able to determine the parameter  $F_{34}$ .

## 6. Discussion and conclusion

Using the strategy of the direct assignment of the  $J=0$  states of excited vibrational levels [29,32,65] we have

thus been able to identify and precisely determine a large number of pure vibrational state energies for  $\text{CH}_3\text{D}$  extending to about  $6300 \text{ cm}^{-1}$  and for  $\text{CHD}_3$  extending up to  $8700 \text{ cm}^{-1}$ . Essential to such an analysis are very high resolution spectra with reduced Doppler width taken at low temperatures of about 80 K and allowing for assignment of the low  $J$  transitions in these spectra. Besides applications in atmospheric and planetary science (particularly for the isotopomer  $\text{CH}_3\text{D}$ ) these results open a window towards the complete nine-dimensional quantum dynamics of intramolecular vibrational motion and redistribution in the fundamental methane molecule. The present results are of sufficient accuracy to serve as benchmarks for further experimental and theoretical studies.

As one application of the present results we might compare with the results on the spectrum and femtosecond intramolecular vibrational redistribution by the strong Fermi-resonance within the CH-chromophore in  $\text{CHD}_3$  [7,20,21,33,34,66]. Table 16 provides such a comparison for the lower polyads designated by the symbol  $N_j$ , where  $N$  is the polyad quantum number ( $N = v_1 + v_5/2$  in the normal mode basis) and  $j$  gives a state index increasing with decreasing energy within each polyad. The polyads with  $A_1$  symmetry have integer  $N$ , whereas polyads with  $E$  symmetry have half-odd integer  $N$ . One recognises a good agreement of the experimental level positions where overlap exists in Table 16. The differences between experiment and the effective hamiltonian fit as well as the three-dimensional vibrational variational calculations of [20] using 180 basis functions for the CH chromophore's stretching and bending levels remain modest and are of the expected magnitude for such model fits. This provides one confirmation for the validity of the time dependent wavepacket dynamics obtained from the variational calculations in the CH-chromophore subspace [19,33,34]. Table 16 indicates the obvious need to

Table 15. Vibrational spectroscopic parameters of the CH<sub>3</sub>D and CHD<sub>3</sub> molecules (in cm<sup>-1</sup>).

	CH <sub>3</sub> D				CHD <sub>3</sub>		
1	2	3	4	[64]	5	6	7
Parameter	Present work, I	Present work, II			Present work, I	Present work, II	[64]
$\omega_1$	3072.6833 <sup>a</sup>	3073.6784 <sup>a</sup>	3071.4	3133.8793 <sup>a</sup>	3136.1717 <sup>a</sup>	3130.5	
$\omega_2$	2289.9925 <sup>a</sup>	2288.7415 <sup>a</sup>	2285.2	2192.8606 <sup>a</sup>	2192.3649 <sup>a</sup>	2191.3	
$\omega_3$	1339.8435 <sup>a</sup>	1340.7082 <sup>a</sup>	1339.8	1026.1678 <sup>a</sup>	1026.0830 <sup>a</sup>	1025.4	
$\omega_4$	3160.6238 <sup>a</sup>	3163.8824 <sup>a</sup>	3156.8	2343.7880 <sup>a</sup>	2342.3602 <sup>a</sup>	2337.0	
$\omega_5$	1504.4874 <sup>a</sup>	1504.3008 <sup>a</sup>	1508.1	1318.6017 <sup>a</sup>	1319.0257 <sup>a</sup>	1321.4	
$\omega_6$	1188.8961 <sup>a</sup>	1188.2985 <sup>a</sup>	1188.1	1054.2383 <sup>a</sup>	1054.9672 <sup>a</sup>	1055.5	
$x_{11}$	-4.0633(818)	-5.3214(855)	-17.197	-58.7895(452)	-58.9936(486)	-59.221	
$x_{12}$	-2.9308(787)	-2.5552(753)	-1.878	-2.4050(615)	-2.9045(640)	-2.204	
$x_{13}$	5.6371(651)	488461(664)	-0.981	-9.0383(489)	-9.1934(502)	-9.731	
$x_{14}$	-99.5704(782)	-99.0218(766)	-72.771	2.7796(381)	2.3367(363)	2.184	
$x_{15}$	-9.5368(521)	-9.1793(542)	-19.016	-21.2261(337)	-21.3667(396)	-21.111	
$x_{16}$	-7.4372(527)	-7.2330(570)	-5.612	-0.7920(333)	-1.4056(347)	-0.309	
$x_{22}$	-28.0925(886)	-27.9443(898)	-31.167	0.7911(316)	1.1391(307)	-8.826	
$x_{23}$	-7.3640(473)	-7.3118(433)	-6.739	3.1231(796)	3.0935(757)	15.727	
$x_{24}$	-7.8757(779)	-7.7295(758)	1.639	-42.9968(658)	-42.7271(649)	-37.352	
$x_{25}$	-3.6385(505)	-3.5220(550)	-3.331	-5.1721(857)	-5.2201(826)	-4.017	
$x_{26}$	-17.8095(565)	-17.5869(550)	-22.266	-2.3816(904)	-2.4885(875)	4.674	
$x_{33}$	-7.6676(813)	-7.7593(809)	-6.802	-6.1956(351)	-6.1883(368)	-7.230	
$x_{34}$	-10.3564(459)	-10.5173(490)	-9.440	-7.0455(441)	-6.9765(464)	-8.449	
$x_{35}$	-2.8660(632)	-2.9084(618)	-2.033	-2.9438(832)	-2.7954(798)	-1.029	
$x_{36}$	-3.0865(617)	-3.0729(622)	-1.091	3.5503(873)	3.4450(824)	1.638	
$x_{44}$	-31.8247(753)	-32.4024(774)	-31.611	-16.6579(791)	-16.3487(761)	-18.601	
$x_{45}$	-8.1681(558)	-8.3727(578)	-14.611	-8.4413(424)	-8.4541(409)	-7.195	
$x_{46}$	-9.3785(841)	-9.3041(850)	-7.686	-11.2718(978)	-11.0441(975)	-8.402	
$x_{55}$	-4.4819(536)	-4.4168(547)	-1.874	-4.5233(368)	-4.5516(401)	-4.604	
$x_{56}$	-5.1763(831)	-5.0898(800)	-4.068	5.1780(380)	4.9188(415)	0.055	
$x_{66}$	0.261 <sup>b</sup>	0.261 <sup>b</sup>	0.261	-5.2427(860)	-5.3057(865)	-5.500	
$y_{666}$	-0.2239(789)	-0.2166(807)					
$g_{44}$	27.0956(326)	28.5389(352)	12.636	8.5470(662)	8.5598(640)	8.252	
$g_{45}$	-7.0826(727)	-7.0618(759)	-1.721	3.6205(449)	3.5837(422)	-0.060	
$g_{46}$	3.1700(852)	3.1598(873)	-0.230	1.1200(874)	1.1429(854)	-0.729	
$g_{55}$	2.4586(317)	2.3804(385)	0.384	5.1145(384)	5.0951(373)	5.403	
$g_{56}$	-4.6803(674)	-4.6841(713)	-5.056	6.1304(751)	5.8940(730)	0.921	
$g_{66}$	1.4987(830)	1.5158(789)	0.645	2.8833(910)	2.8714(889)	3.251	
$k_{155}$	-56.3671(349)	-56.6885(342)		30.0 <sup>c</sup>	30.0 <sup>c</sup>		
$k_{345}$				-70.8100(638)	-70.6261(671)		
$F_{11,44}$	-70.1382(896)	-74.8129(912)					
$F_{33,56}$	15.7181(785)	15.3674(714)					
$F_{33,66}$				-18.0922(812)	-17.9093(824)		
$F_{1,333}$				8.2431(786)	8.1787(757)		

Notes:<sup>a</sup>Was not fitted, but calculated on the basis of the  $F_{ij}$  parameters given in columns 2 and 3 of Table 14.

<sup>b</sup>Was constrained to the value from [64].

<sup>c</sup>Was constrained to the value from [20], obtained including intensity information.

extend the present analyses to higher excitations, with currently available data from our cold samples extending to about 12,000 cm<sup>-1</sup>. Indeed, our analysis of 1988 extended to about 19,000 cm<sup>-1</sup> using also further results from the literature [67]–[74] (see also [4–9,19,33,66,75,76]).

While the present analysis confirms the results on the quantum dynamics in the three-dimensional subspace of the CH-chromophore, our current analyses

extend well beyond this by including excitations of all vibrations in the full nine-dimensional coordinate space of normal modes. They thus will allow analyses of intramolecular vibrational redistribution to non-CH chromophore modes, which is generally expected on longer time scales than the 100 fs times for intrachromophore redistribution.

Table 16 illustrates a further important aspect. The approximate zero order assignments of the vibrational

Table 16. Results for CH-chromophore polyad states in  $\text{CHD}_3$  (all term values  $\tilde{\nu}/\text{cm}^{-1}$ ).

$N_j$	Exp. from Table 13, this work	Calc. I from table 13, this work	Theory $\tilde{\nu}_{var}$ Exp. ref. [20] ref. [20]
(1/2) <sub>1</sub>	1292.500	1292.12	1292.499
1 <sub>2</sub>	2564.676	2564.63	2564.67
1 <sub>1</sub>	2992.786	2992.73	2992.75
(3/2) <sub>2</sub>	3838.040	3838.48	3839.96
(3/2) <sub>1</sub>	4261.662	4261.91	4262.1
2 <sub>3</sub>	—	5092.73	—
2 <sub>2</sub>	5515.603	5514.98	5515.7
2 <sub>1</sub>	5865.004	5865.64	5864.98
(5/2) <sub>3</sub>	—	—	6346.88
(5/2) <sub>2</sub>	—	—	6766.40
(5/2) <sub>1</sub>	7115.499	—	7115.48
3 <sub>4</sub>	—	7584.30	—
3 <sub>3</sub>	—	7999.40	8005.4
3 <sub>2</sub>	8346.919	8347.05	8347.1
3 <sub>1</sub>	8623.349	8622.89	8623.32
			8624.19

levels as given in columns 1 of Tables 12 and 13 have, of course, only a very rough, qualitative meaning. Only the symmetry assignments and band centre wavenumbers have a real significance. Similarly, the parameters of the effective hamiltonians used in the fits (Tables 14 and 15) have significance only in the framework of a given effective fit and should not be considered to be simply related to the parameters of the potential hypersurface (see discussion in [20,77]–[79]). Finally, the effective Hamiltonian used may not necessarily lead to very accurate level predictions, if far removed from the fitted range. This deserves a further test.

An aspect not analysed here in detail concerns the absorption intensities and dipole function related among other things to the important question of the dipole moment direction in  $\text{CH}_3\text{D}$  and  $\text{CD}_3\text{H}$  [4,80]. Analyses of our current results will provide further important experimental information on the multidimensional dipole function in these isotopomers [6,9,19]. The relation to the quantum dynamics in excited electronic states of methane [17] and in the limit of electronic excitation the Rydberg states and the cations of methane isotopomers [81] deserves mention as well as the use of understanding the true nature of the multidimensional coupled vibrational states in methane isotopomers reacting with reactive atoms [12]–[15]. Particularly for the isotopomer  $\text{CH}_3\text{D}$  our accurate experimental results and their analysis should prove useful in understanding features in planetary atmospheres including the moon Titan [82].

## Acknowledgements

Our work is supported financially by ETH Zürich and the Schweizerischer Nationalfonds. Part of the work benefited from the joint PICS grant of CNRS (France) and RFBR (Russia), 4221N0000211752a and from the Russian Science and Innovations Federal Agency under contract No. 02.740.11.0238. We gratefully acknowledge discussions with Tucker Carrington, Veronika Horká Zelenková, Roberto Marquardt, Hans Martin Niederer, and Georg Seyfang. We enjoyed many years of fruitful scientific exchange and friendship with Richard N. Zare to whom this paper is thus justly dedicated.

## References

- [1] J.H. van't Hoff, *Vorlesungen über theoretische und physikalische Chemie* (Vieweg, Braunschweig, 1898).
- [2] L. Pauling, *The Nature of the Chemical Bond*, 2nd ed. (Oxford University Press, London, 1940).
- [3] R.N. Zare, *Angular Momentum: Understanding Spatial Aspects in Chemistry and Physics* (Wiley, New York, 1988).
- [4] H. Hollenstein, R. Marquardt, M. Quack and M.A. Suhm, *J. Chem. Phys.* **101** (5), 3588 (1994).
- [5] H. Hollenstein, R. Marquardt, M. Quack and M.A. Suhm, *Ber. Bunsenges. Phys. Chem.* **99** (3), 275 (1995).
- [6] R. Marquardt and M. Quack, *J. Chem. Phys.* **109** (24), 10628 (1998).
- [7] S.D. Peyerimhoff, M. Lewerenz and M. Quack, *Chem. Phys. Lett.* **109** (6), 563 (1984).
- [8] D.W. Schwenke, *Spectrochim. Acta A* **58** (4), 849 (2002).
- [9] R. Marquardt and M. Quack, *J. Phys. Chem. A* **108** (15), 3166 (2004).
- [10] M. Quack and J. Troe, *Ber. Bunsen-Ges. Phys. Chem.* **81**, 329 (1977).
- [11] M. Quack, *J. Phys. Chem.* **83** (1), 150 (1979).
- [12] J.P. Camden, H.A. Bechtel, D.J.A. Brown and R.N. Zare, *J. Chem. Phys.* **124** (3), 034311 (2006).
- [13] W.F. Hu, G. Lendvay, D. Troya, G.C. Schatz, J.P. Camden, H.A. Bechtel, D.J.A. Brown, M.R. Martin and R.N. Zare, *J. Phys. Chem. A* **110** (9), 3017 (2006).
- [14] J.P. Camden, H.A. Bechtel, D.J.A. Brown, M.R. Martin, R.N. Zare, W.F. Hu, G. Lendvay, D. Troya and G.C. Schatz, *J. Am. Chem. Soc.* **127** (34), 11898 (2005).
- [15] J.P. Camden, W.F. Hu, H.A. Bechtel, D.J.A. Brown, M.R. Martin, R.N. Zare, G. Lendvay, D. Troya and G.C. Schatz, *J. Phys. Chem. A* **110** (2), 677 (2006).
- [16] M. Quack, *Angew. Chem. Int. Ed. (Engl.)* **28** (5), 571 (1989).
- [17] M.J.M. Pepper, I. Shavitt, P.v. Ragué Schleyer, M.N. Glukhovtsev, R. Janoschek and M. Quack, *J. Comput. Chem.* **16** (2), 207 (1995).
- [18] A. Bakasov, T.K. Ha and M. Quack, *J. Chem. Phys.* **109** (17), 7263 (1998).

- [19] R. Marquardt, M. Quack and I. Thanopulos, *J. Phys. Chem. A* **104** (26), 6129 (2000).
- [20] M. Lewerenz and M. Quack, *J. Chem. Phys.* **88** (9), 5408 (1988).
- [21] T. Carrington, L. Halonen and M. Quack, *Chem. Phys. Lett.* **140** (5), 512 (1987).
- [22] X.G. Wang and T. Carrington, *J. Chem. Phys.* **118** (14), 6260 (2003).
- [23] X.G. Wang and T. Carrington, *J. Chem. Phys.* **119** (1), 94 (2003).
- [24] X.G. Wang and T. Carrington, *J. Chem. Phys.* **119** (1), 101 (2003).
- [25] H.G. Yu, *J. Chem. Phys.* **121** (13), 6334 (2004).
- [26] S. Albert, S. Bauerecker, V. Boudon, L.R. Brown, J.-P. Champion, M. Loëte, A. Nikitin and M. Quack, *Chem. Phys.* **356** (1–3), 131 (2009).
- [27] O.N. Ulenikov, E.S. Bekhtereva, S. Albert, S. Bauerecker, H.M. Niederer, M. Quack, in preparation.
- [28] H.M. Niederer, S. Albert, S. Bauerecker, V. Boudon, J.P. Champion and M. Quack, *Chimia* **62** (4), 273 (2008).
- [29] M. Hippler and M. Quack, *J. Chem. Phys.* **116** (14), 6045 (2002).
- [30] O.N. Ulenikov, E.S. Bekhtereva, S.V. Grebneva, H. Hollenstein and M. Quack, *Phys. Chem. Chem. Phys.* **7** (6), 1142 (2005).
- [31] O.N. Ulenikov, E.S. Bekhtereva, S.V. Grebneva, H. Hollenstein and M. Quack, *Mol. Phys.* **104**, 3371 (2006).
- [32] O.N. Ulenikov, E.S. Bekhtereva, S. Albert, S. Bauerecker, H. Hollenstein and M. Quack, *J. Phys. Chem. A* **113** (10), 2218 (2009).
- [33] R. Marquardt and M. Quack, *J. Chem. Phys.* **95** (7), 4854 (1991).
- [34] R. Marquardt and M. Quack, in *Encyclopedia of Chemical Physics and Physical Chemistry, Vol. 1 (Fundamentals)*, edited by J.H. Moore and N. Spencer (IOP, Bristol, 2001), pp. 897–936.
- [35] H.R. Dübä and M. Quack, *J. Chem. Phys.* **81** (9), 3779 (1984).
- [36] J. Segall, R.N. Zare, H.R. Dübä, M. Lewerenz and M. Quack, *J. Chem. Phys.* **86** (2), 634 (1987).
- [37] A. Amrein, M. Quack and U. Schmitt, *J. Phys. Chem.* **92** (19), 5455 (1988).
- [38] O.N. Ulenikov, E.S. Bekhtereva, A.S. Bulavenkova, S. Bauerecker, H. Hollenstein and M. Quack, in *Proceedings Nineteenth Colloquium on High Resolution Molecular Spectroscopy, Salamanca, Spain, 11–16 September 2005*, edited by D. Bermejo, J.L. Doménech, and M.A. Moreno (Sociedad Española de Óptica, Salamanca, 2005), paper N10.
- [39] E.S. Bekhtereva, O.N. Ulenikov, E.A. Sinitzin, S. Albert, S. Bauerecker, H. Hollenstein and M. Quack, in *Proceedings of the 20th Colloquium on High-Resolution Molecular Spectroscopy*, edited by V. Boudon (Université de Dijon, Dijon, 2007), paper J 30, p. 268.
- [40] A.V. Nikitin, J.P. Champion and L.R. Brown, *J. Mol. Spectrosc.* **240** (1), 14 (2006).
- [41] S. Albert, K.K. Albert and M. Quack, in *Trends in Optics and Photonics (TOPS)* (Optical Society of America, Washington, DC, 2003), Vol. 84, pp. 177–180.
- [42] S. Albert and M. Quack, *Chem. Phys. Chem.* **8** (9), 1271 (2007).
- [43] S. Albert, S. Bauerecker, M. Quack and A. Steinlin, *Mol. Phys.* **105** (5), 541 (2007).
- [44] S. Bauerecker, M. Taraschewski, C. Weitkamp and H.K. Cammenga, *Rev. Sci. Instrum.* **72** (10), 3946 (2001).
- [45] S. Bauerecker, *Phys. Rev. Lett.* **94** (3), 033404 (2005).
- [46] S. Bauerecker, F. Taucher, C. Weitkamp, W. Michaelis and H.K. Cammenga, *J. Mol. Struct.* **348**, 237 (1995).
- [47] A.G. Maki and J.S. Wells, *NIST Spec. Publ.* 821 (1991).
- [48] L.S. Rothman, D. Jacquemart, A. Barbe, D.C. Benner, M. Birk, L.R. Brown, M.R. Carleer, C. Chackerian, K. Chance, L.H. Coudert, V. Dana, V.M. Devi, J.M. Flaud, R.R. Gamache, A. Goldman, J.M. Hartmann, K.W. Jucks, A.G. Maki, J.Y. Mandin, S.T. Massie, J. Orphal, A. Perrin, C.P. Rinsland, M.A.H. Smith, J. Tennyson, R.N. Tolchenov, R.A. Toth, J. Vander Auwera, P. Varanasi and G. Wagner, *J. Quant. Spectrosc. Radiat. Transfer* **96** (2), 139 (2005).
- [49] M. Quack, *Mol. Phys.* **34** (2), 477 (1977).
- [50] M. Quack, in *Symmetries and Properties of Non-rigid Molecules: A Comprehensive Survey*, edited by J. Maruani and J. Serre, in series Studies in Physical and Theoretical Chemistry, Vol. 23 (Elsevier, Amsterdam, 1983) pp. 355–378.
- [51] E.B. Wilson, J.C. Decius and P.C. Cross, *Molecular Vibrations the Theory of Infrared and Raman Vibrational Spectra* (McGraw-Hill, New York, 1955).
- [52] H.C. Longuet-Higgins, *Mol. Phys.* **6** (5), 445 (1963).
- [53] E.R. Cohen, T. Cvitas, J.G. Frey, B. Holmström, K. Kuchitsu, R. Marquardt, I. Mills, F. Pavese, M. Quack, J. Stohner, H.L. Strauss, M. Takami and A.J. Thor, *Quantities, Units and Symbols in Physical Chemistry*, 3rd ed., second corrected printing (IUPAC and Royal Society of Chemistry, RSC Publishing, Cambridge, 2008).
- [54] O.N. Ulenikov, G.A. Onopenko, N.E. Tyabaeva, J. Schroderus and S. Alanko, *J. Mol. Spectrosc.* **200** (1), 1 (2000).
- [55] O.N. Ulenikov, G.A. Onopenko, N.E. Tyabaeva, S. Alanko, M. Koivusaari and R. Anttila, *J. Mol. Spectrosc.* **186** (2), 293 (1997).
- [56] O.N. Ulenikov, G.A. Onopenko, N.E. Tyabaeva, J. Schroderus, S. Alanko and M. Koivusaari, *J. Mol. Struct.* **517–518**, 25 (2000).
- [57] E.P. Wigner, *Quantum Theory of Angular Momentum* (Academic Press, New York, 1965).
- [58] V.N. Saveliev and O.N. Ulenikov, *J. Phys. B – At. Mol. Opt. Phys.* **20** (1), 67 (1987).
- [59] Y.S. Makushin, O.N. Ulenikov and A.E. Cheglokov, *Symmetry and Its Applications to the Problems of*

- Molecular Vibration–Rotation Spectroscopy, Parts I and II* (in Russian) (Tomsk State University Press, Tomsk, 1990).
- [60] D.A. Varshalovitch, A.N. Moskalev and V.K. Khersonsky, *Quantum Theory of Angular Momentum* (Nauka, Leningrad, 1975).
  - [61] U. Fano and G. Racah, *Irreducible Tensorial Sets* (Academic Press, New York, 1959).
  - [62] O.N. Ulenikov, G.A. Onopenko, N.E. Tyabaeva, J. Schroderus and S. Alanko, *J. Mol. Spectrosc.* **193** (2), 249 (1999).
  - [63] O.N. Ulenikov, G.A. Onopenko, N.E. Tyabaeva, S. Alanko, M. Koivusaari and R. Anttila, *J. Mol. Spectrosc.* **186** (2), 230 (1997).
  - [64] T.J. Lee, J.M.L. Martin and P.R. Taylor, *J. Chem. Phys.* **102** (1), 254 (1995).
  - [65] M. Quack, *Chimia* **57** (4), 147 (2003).
  - [66] T.K. Ha, M. Lewerenz, R. Marquardt and M. Quack, *J. Chem. Phys.* **93** (10), 7097 (1990).
  - [67] L.F.H. Bovey, *J. Chem. Phys.* **21** (5), 830 (1953).
  - [68] J.K. Wilmhurst and H.J. Bernstein, *Can. J. Chem. – Rev. Can. Chim.* **35** (3), 226 (1957).
  - [69] T.A. Wiggins, E.R. Shull, J.M. Bennett and D.H. Rank, *J. Chem. Phys.* **21** (11), 1940 (1953).
  - [70] G.J. Scherer, K.K. Lehmann and W. Klemperer, *J. Chem. Phys.* **81** (12), 5319 (1984).
  - [71] G.A. Voth, R.A. Marcus and A.H. Zewail, *J. Chem. Phys.* **81** (12), 5494 (1984).
  - [72] J.W. Perry, D.J. Moll, A. Kuppermann and A.H. Zewail, *J. Chem. Phys.* **82** (3), 1195 (1985).
  - [73] A. Campargue and F. Stoeckel, *J. Chem. Phys.* **85** (3), 1220 (1986).
  - [74] A. Campargue, F. Stoeckel, M. Chenevier and H. Ben Kraiem, *J. Chem. Phys.* **87** (10), 5598 (1987).
  - [75] D. Permgorov, A. Campargue, M. Chenevier and H.B. Kraiem, *J. Mol. Spectrosc.* **170** (1), 10 (1995).
  - [76] C. Domingo, A. Delolmo, R. Escribano, D. Bermejo and J.M. Orza, *J. Chem. Phys.* **96** (2), 972 (1992).
  - [77] M. Quack, *Annu. Rev. Phys. Chem.* **41**, 839 (1990).
  - [78] A. Beil, D. Luckhaus, M. Quack and J. Stohner, *Bunsenges. Phys. Chem.* **101** (3), 311 (1997).
  - [79] D. Luckhaus and M. Quack, *Chem. Phys. Lett.* **205** (2–3), 277 (1993).
  - [80] R. Signorell, R. Marquardt, M. Quack and M.A. Suhm, *Mol. Phys.* **89** (1), 297 (1996).
  - [81] H.J. Wörner and F. Merkt, *Angew. Chem.-Int. Edit.* **48** (35), 6404 (2009).
  - [82] D.E. Jennings, P.N. Romani, G.L. Bjaraker, P.V. Sada, C.A. Nixon, A.W. Lunsford, R.J. Boyle, B.E. Hesman and G.H. McCabe, *J. Phys. Chem. A* **113** (42), 11101 (2009).
  - [83] O.N. Ulenikov, A.B. Malikova, S. Alanko, M. Koivusaari and R. Anttila, *J. Mol. Spectrosc.* **179**, 175 (1996).

### Appendix 1. Tables of line wavenumbers

The appendix contains tables of observed transition wavenumbers for more than 9000 lines for CH<sub>3</sub>D and CD<sub>3</sub>H with their preliminary assignments as used for the final assignment of transitions leading to the  $J=0$  levels of excited vibrational states. The Appendix can be viewed online. These tables contain as Table A the results for CH<sub>3</sub>D and as Table B the results for CHD<sub>3</sub>. These tables have nine columns with the following content:

- (I) Observed wavenumbers,  $\nu^{\text{exp.}}$  (in cm<sup>-1</sup>).
- (II, III) Quantum numbers of the upper ro-vibrational state,  $J'$ ,  $K'$ .
- (V, VI) Quantum numbers of the lower ro-vibrational state,  $J''$ ,  $K''$ .
- (IV, VII) Symmetry of the upper and lower ro-vibrational states, respectively. Index 0 corresponds to  $A_1$  symmetry; indices 1 and 2 correspond to  $A_2$  and  $E$ , respectively; index ‘a’ corresponds to a pair of degenerate  $A_1/A_2$  ro-vibrational states (not split under the conditions of our experiment).
- (VIII) Band.
- (IX) Symmetry of the vibrational state.